PDMS/PNIPAAM INTERPENETRATING POLYMER NETWORKS AS OPHTHALMIC BIOMATERIALS

PDMS/PNIPAAM INTERPENETRATING POLYMER NETWORKS AS OPHTHALMIC BIOMATERIALS

By

LINA LIU M. ENG.

A Thesis

Submitted to the School of Graduate Studies

in Partial Fulfilment of the Requirements

for the Degree

Master of Applied Science

McMaster University

MASTER OF APPLIED SCIENCE (2003) McMaster University

(Chemical Engineering) Hamilton, Ontario

TITLE: PDMS/PNIPAAM Interpenetrating Polymer Networks

as Ophthalmic Biomaterials

AUTHOR: Lina Liu, M. Eng. (Beijing University of Chemical Technology)

SUPERVISOR: Professor H. Sheardown

NUMBER OF PAGE: xvii, 149

ABSTRACT

Poly (dimethyl siloxane) (PDMS) has been widely used as a biomaterial in ophthalmic and other applications due to its good compatibility, high mechanical strength and excellent oxygen permeability and transparency. For use as an artificial cornea, contact lens and in other applications, modifications are necessary to improve glucose permeability and wettability for cell and tear protein and mucin interactions through modification with hydrophilic functional groups or polymers. Poly (N-isopropyl acrylamide) (PNIPAAM) is a biocompatible and hydrophilic polymer that has been extensively studied in controlled drug release applications due to its lower critical solution temperature (LCST) phenomenon. In this study, a composite interpenetrating polymer network (IPN) of PDMS and PNIPAAM was formed to generate material with reasonable oxygen and glucose permeability as well as improved wettability and mechanical properties compared to the PDMS and PNIPAAM homopolymers.

Semi-IPNs, with low water uptake and mechanical strength, were found not to be suitable as biomaterials. Vinyl terminated PDMS / PNIPAAM IPNs had reasonable water uptake and excellent tensile stress and strain, but low glucose permeability ($< 10^{-10}$ cm^2/s). Hydroxyl terminated PDMS/PNIPAAM IPNs (PDMS-OH IPN) were successfully synthesized with reasonable mechanical properties and significantly higher glucose permeability ($\sim 10^{-7}$ cm^2/s). Curing the PDMS-OH film with solvent was found to improve glucose transport.

The presence of PNIPAAM in the composite networks was confirmed by FT-IR and Differential Scanning Calorimetry (DSC). Transmission Electron Microscopy (TEM) images verified the structure of interpenetrating networks. Attenuated Total Reflectance Fourier Transform Infrared Spectroscopy (ATR-FTIR) and X-ray Photoelectron Spectroscopy (XPS) suggested that PNIPAAM was also present on the surface and this translated to increased roughness compared with the PDMS control as determined by AFM. The LCST phenomena still remained in the IPN, although the change was not as abrupt as with pure PNIPAAM. These results suggest that the copolymer may be useful as an ophthalmic biomaterial and for controlled drug release applications.

ACKNOWLEDGEMENTS

I would like express my sincere appreciation to my supervisor Dr. Heather Sheardown for giving me guidance on the research and thesis writing, motivating my independent thought and providing the resources to complete this thesis. She has always been understanding and has encouraged me during the last two years. She is the most impressive supervisor in all my previous work and study experience.

I also would like thank the other people who contributed to the completion of this thesis: Dr. John Brash for useful discussions and valuable suggestions in the group meetings; Dr. Shiping Zhu and Dr. Robert Pelton for providing access the research facilities; Rena Cornelius and Glenn McClung for their technical assistance. The help of these individuals is gratefully acknowledged. Thanks is also extended to the many graduate students and postdoctoral colleagues in Dr. Brash and Dr. Sheardown's group for their help and friendship, which allowed me to work in a very amicable environment over the last two years.

Finally, I am very thankful to my husband Jijun Duan for his support, understanding and love. His sacrifice during my graduate studies is gratefully appreciated and I hope to repay him in the future. I dedicate this thesis to my family: my husband, my daughter and my baby on the way.

TABLE OF CONTENTS

LIST OF FIGURES

LIST OF TABLES

LIST OF ABBREVIATIONS

AFM	Atomic Force Microscopy
AIBN	2,2-azobisisobutyronitrile
BisAAM	N,N-methylene bisacrylamide
DMAEMA	N,N-dimethylamino ethylmethacrylate
DMF	N,N-Dimethylformamide
DSC	Differential Scanning Calorimeter
EWC	Equilibrium Water Content
FTIR	Fourier Transform Infrared Spectroscopy
HTV	High temperature vulcanization
IPN	Interpenetrating Polymer Network
LCST	Low Critical Solution Temperature
EGDMA	Ethylene glycol dimethylacrylate
MAA	Methacrylic acid
Mn	Number average molecular weight
Mpa	Megapascal
MPC	2-methacryloyloxyethy phosphorylcholine
PDMAAM	Poly (N,N-dimethyl acrylamide)
PDMAEMA	Poly (N,N-dimethylamino ethylmethacrylate)
PDMS	Poly (dimethylsiloxane)
PDMS-OH	Hydroxyl teminated poly (dimethylsiloxane)
PDMS-OH IPN	Hydroxyl terminated poly (dimethylsiloxane)/poly(N-isopropylacrylamide) interpenetrating polymer network
PDMS-V	Vinyl terminated poly (dimethylsiloxane)
PDMS-V IPN	Vinyl terminated poly (dimethylsiloxane)/poly(N-isopropylacrylamide) Interpenetrating Polymer Network
PEO	Polyethylene oxide
PHEMA	Poly (hydroxyethyl methacrylate)

PIB	Poly (isobutylene)
PMA	Poly (methacrylic acid)
PMMA	Poly (methyl methacrylate)
PNIPAAM	Poly (N-isopropyl acrylamide)
PNVP	Poly (N-vinyl pyrrolidone)
PP	Polypropylene
PTFE	Poly (tetrafluoroethylene)
PVA	Poly(vinyl alcohol)
Ra	Arithmetic average of the absolute values of surface height
R-IR	Reflectance Infrared Spectroscopy
Rms	Root mean square average of height from the mean data plane
RTV	Room temperature vulcanization
SEM	Scanning Electron Microscopy
Tc	Critical temperature
TEM	Transmission Electron Microscopy
TEOS	Tetra ethyl orthosilicate
Tg	Glass transition temperature
THF	Tetrahydrofruan
XPS	X-ray Photoelectron Spectroscopy

1. INTRODUCTION

Poly (dimethylsiloxane) (PDMS) has been widely used in biomedical applications. The biocompatibility of PDMS has been thoroughly studied and a wide range of modifications have been investigated (Belanger and Marois, 2001; Abbasi et al., 2001). It is particularly attractive as an ophthalmic biomaterial and has been used as both a contact lens (Lopez-Alemany et al., 2002; Lai and Valint, 1996) and as the polymer substrate for an artificial cornea (Hsuie et al., 1993; Aucoin et al., 2002; Merrett et al., in press) due to its good ophthalmic compatibility, high oxygen permeability, transparency and mechanical properties. However, low water and small nutrient such as glucose permeability severely limit its potential use, since glucose and small ion permeability have been suggested to be important factors to success of artificial cornea and high quality contact lens (Xie et al., 1999; Mester et al., 1978). Glucose from the tears and the aqueous humor plays an important role on cell metabolism, providing nutrients and energy for corneal cells. Therefore, enhancing the glucose and other small molecule permeability of the polymers to be used as ophthalmic biomaterials could improve cellular compatibility of the material. In contact lens applications, glucose permeation is essential for extended wear, improving ophthalmic health in the wearer.

Unlike PDMS, hydrogels have high water content and are highly glucose permeable. Hydrogels including poly (hydroxyethyl methacrylate) (PHEMA) and poly (N-vinyl pyrrolidone) (NVP) and their copolymers with poly (methyl

methacrylate) (MMA) and poly (methacrylic acid) (MA) are currently widely used as ophthalmic materials (Chirila et al., 1998). However, due to their high water content, these materials have relatively poor mechanical properties. Several groups have investigated the glucose and other small molecule transport through these hydrogels or introduced these hydrophilic polymers as guests into hydrophobic polymers to improve a variety of properties including glucose permeability for hydrophobic polymer matrices (Shtanko et al., 2000; Liou and Wang, 1995; Burczak et al., 1994a,b; Nonaka, 1997). Generally, it is been found that water and water soluble substances have significant diffusion rates through hydrogel membranes. For example, the diffusion coefficient of water through HEMA hydrogels used for soft contact lenses has been reported to be approximately 10^{-7} cm^2/s (Hoch et al., 2003). In these systems, glucose and small molecule diffusion is thought to occur through the water containing hydrogel regions (Ling, 1972; Ling, 1988). These investigations suggest that introducing hydrophilic polymer domains is an effective method of improving the permeability of hydrophobic matrices to small molecules such as glucose. The glucose transport is thought to be predominately controlled by the hydrogel domain size, the interconnectivity of the domains, the size of capillary water channel and water content of the matrix. These factors must therefore be considered when designing glucose permeable membranes.

PNIPAAM, novel biocompatible polymer which attracted extensive study interest on drug delivery applications due to its low critical solution temperature

(LCST) phenomenon (Liang et al., 2000), is of particular interest in this work due to reported ophthalmic compatibility. PNIPAAM is a good candidate guest polymer for modifying the hydrophilicity and altering the glucose permeability of PDMS for a number of reasons. In hydrogel form, the polymer has excellent permeability to water soluble substances (Chandy and Sharma, 1992; Baker, 1995) and in copolymer form, even in a water swollen state it has been suggested to have reasonable mechanical properties (Kazunori, 1996). Furthermore, N-isopropylacrylamide-based polymers are known to allow cell growth, both on their surface and, more importantly, when the cells are completely encapsulated (Stile et al., 1999). PNIPAAM is a temperature sensitive polymer with lower critical solution temperature (LCST) at 32.0°C (Panda et al., 2000). This temperature can be altered by copolymerization with other hydrophilic monomers. However, this LCST phenomenon may be useful in drug delivery applications for example.

The hydrophobic, non-polar PDMS and hydrophilic, polar PNIPAAM are highly incompatible polymers and are difficult to mix by simple blending. Even with block or graft copolymerization, an obvious sea-island domain style (Sperling, 1997) is expected, resulting in a non-continuous hydrogel domain that does not form channels through which water soluble molecules can penetrate. However, if the mixing is accomplished by the formation of networks of the two crosslinked polymers, the severe phase separation maybe kinetically controlled or prevented by permanent interlocking of entangled polymer chains (Lipatov 1990).

In the current work, polymer networks of PDMS and PNIPAAM were formed. The resultant polymer membranes were found to have reasonable oxygen and glucose permeability as well as improved wettability and mechanical properties compared to the PDMS and PNIPAAM homopolymers. Characterization of the modified PDMS/PNIPAAM copolymer materials suggest that they may be useful as ophthalmic biomaterials and controlled drug release applications.

2. LITERATURE REVIEW

2.1 Interpenetrating Polymer Networks

Interpenetrating polymer networks (IPN's) are defined as "combinations of two or more polymers in network form, at least one such polymer being polymerized and /or crosslinked in the immediate presence of the other(s)" (Sperling, 1981). In an IPN, neither phase can be extracted because of the permanent interlock and entanglement of the polymer chains intensified by crosslinking. Due to differences in structure, IPNs can be divided into semi-IPN (or pesudo-IPN) and full IPN (or true IPN) (Sperling, 1997). Semi-IPNs are based on combination of a crosslinked polymer (a thermoset network) and an unreactive thermoplastic linear polymer. The coexisting structures are stabilized by physical cross-links or strong and permanent entanglements caused by the existence of the network in the thermoplastic phase. Generally the thermoset provides temperature resistance, chemical resistance or other properties which can be intensified by continuous phase and crosslinking, while the thermoplastic phase can improve toughness and other mechanical properties. Full IPNs are composed of two or more thermosetting polymer networks which are chemically crosslinked. The formation of a full IPN can be an effective way to mix two normally incompatible polymers. In both semi- and full-IPN's, the domain sizes are smaller and there is better mixing compared with a general polymer blend.

2.1.1 Interpenetrating Polymer Network Preparation

Preparation methods for interpenetrating networks are classified as sequential IPN, simultaneous IPN, gradient IPN, latex IPN as well as thermoplastic IPN (Klempner et al., 1994). Preparation methods most related to biomaterials, including sequential IPN, simultaneous IPN and gradient IPN are described here.

In a sequential IPN, one of the monomers (host) is initially polymerized and crosslinked to form the network. The host is then swollen in the second monomer, its crosslinker and initiator (guest). Polymerization of the guest monomer results in *in situ* network formation. Silicone rubber is a common host polymer for sequential IPN formation.

Simultaneous IPNs are prepared by thoroughly mixing the monomers or prepolymers, crosslinkers and initiator(s) for both the guest and host. The polymerizations and crosslinking reactions are carried out simultaneously. It is assumed that the two polymerizations do not interfere with each other. Figure 2.1 depicts the process of sequential and simultaneous IPN formation (Sperling, 1994).

In a gradient IPN, there are different compositions or crosslinking densities of the two IPN components in different locations on a macroscopic level. For gradient IPN preparation by chain polymerization, polymer one is swollen with monomer two, mixed and polymerized before the system equilibrates and diffusion creates a uniform solution. For gradient IPN preparation by step polymerization, the guest monomer is initially swollen into the bead made of the host polymer, while a second component of

the condensation of the guest monomer is added to the outside later. Thus, in this type of system, the concentration of the guest polymer is a function of distance from the surface. These systems are useful for controlled release of drugs for example (Mueller and Heiber, 1982).

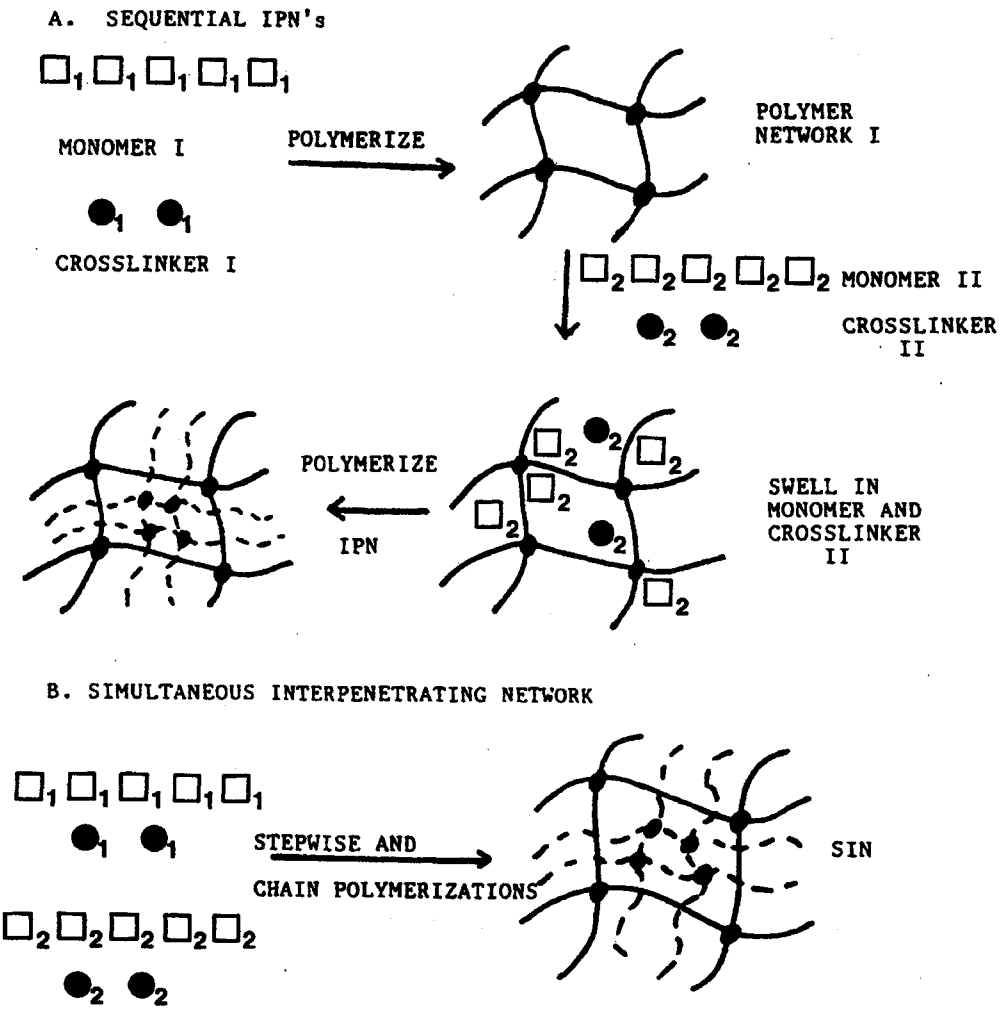

Fig.2.1: Basic synthesis methods for IPNs. A,Sequential IPNs; B, simultaneous IPNs (Sperling, 1994).

2.1.2 Advantages of the Interpenetrating Polymer Networks

IPNs exhibit several advantageous characteristics in comparison to polymer blends, graft and block polymers. Two networks interweaving to form more continuous phases, although not always completely continuous, can provide optimized properties and a greater extent of mixing. In fact, IPN formation is the only way of intimately combining crosslinked polymers, and can effectively combine two incompatible polymers with less phase separation.

Although the most IPNs synthesized to date do not interpenetrate on a molecular level and therefore phase separation of polymers occurs, the broader interfacial area assures that better mixing morphology occurs. This characteristic can be confirmed by glass transition behavior and electron micro-images of true IPN, semi-IPN and linear blends. The existence of two glass transition temperatures (Tg) suggest heterophase presence. Generally the Tgs of a true IPN shift more toward the range of the original Tgs than for linear blends and semi-IPNs, indicative of phase mixing by interpenetration, most likely at the phase boundaries (Frisch and Klempner, 1982). Transmission electron microscopy (TEM) images show an unclear and broader boundary area of two phases or two continuous phase formation images, consistent with the Tg results.

IPN formation can result in the presence of smaller domains relative to other physical blends. This is particularly true for the case of IPN formation with two compatible polymers (Klein, 1986). The decrease in the phase separation that results

corresponds with modification in mechanical and other properties of networks due to chain interlocking and interpenetration. This domain size can be adjusted by decreasing Mc, the average molecular weight between two neighbouring crosslinks, of either polymer in the IPN. This can be achieved by increasing the content of crosslinking agent (Donatelli et al., 1976) in reaction mixture or using shorter prepolymers. Another technique used to mediate the domain size is the introduction of a charged prepolymer which reduces the energy required for blending and interpenetration (Klein, 1986). In a polyurethane / epoxy / acrylic IPN system for example, the charged prepolymers produce much smaller domains, resulting in a tensile strength of 5180 psi compared 4450 psi for non charged prepolymer (Klein, 1986). Generally, IPNs with domain sizes in the range of 50-100 nm have potential for application as tough and high impact materials. IPN's with domains on the order of 10 to 50nm are useful as vibration damping materials (Sperling, 1986).

However, when a polymeric material is modified by another polymer, the improvement in a target property is typically offset by impairment of one or more other properties. In the case of interpenetrating polymer networks, the continuity of the domains, the interpenetrating effect and the permanent entanglement inhibiting phase separation may actually result in a synergistic effect for property improvement. Interpenetration may provide endurance, as well as environmental temperature and solvent resistance by stabilization of the integrity of structure, properties that are particularly useful in biomaterials intended for long term implantation.

2.1.3 Phase Separation and Dual Phase Continuity in Sequential IPNs

During IPN formation, both nucleation or growth and spinodal decomposition kinetics of phase separation occur (Lipatov, 1990; An, 1989). Micro-phase separation of the system occurs during synthesis of simultaneous and sequential IPNs, as a result of the increasing thermodynamic incompatibility between cross-linked chains in the network (Binder and Frisch, 1984). Nucleation and growth kinetics tend to generate spherical and nodule domains of the second phase within the first formed matrix. Spinodal decomposition interrupts nucleation, tending to cut the spherical domains into small elliptic shape domains. These changes may be promoted by crosslinking, resulting in the formation of small and continuous domains.

IPN formation undergoes four distinct stages of morphology development (Sperling, 1997). Initially, the monomer (2) is dissolved in the host resulting in the formation of a clear homogeneous mixture. As polymerization proceeds, phase separation governed by nucleation and gelation occurs. The domain size increases and the system may become cloudy. As polymerization and crosslinking proceed, the induced spinodal decomposition process results in the formation of a connective cylindrical structure. Ultimately, the system tends to have a stable even morphology because the gelation reduces diffusion limiting further reaction. If however, phase separation occurs before gelation, the domains tend to be larger. If gelation occurs before crosslinking, smaller, more continuous domains result. The latter is the case with sequential IPN formation, as the initially formed network assures that gelation

occurs prior to interpenetration. The domains in a sequential IPN are always finely divided and continuous domains through whole matrix are formed as described in Figure 2.2.

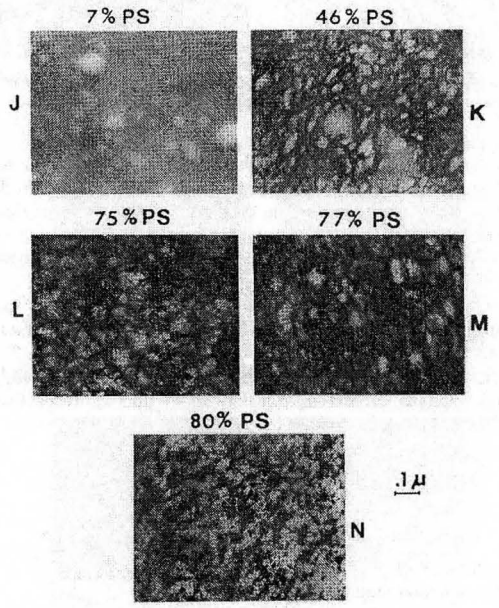

Figure 2.2: TEM of polymerizing polybutadiene-polystrene (PIB/PS) IPN, as the PS is being polymerized. Osmium tetroxide stains the PIB. As the PS is formed, first spheres and then cylinders form, which indicates a change from nucleation and growth to spinodal decomposition kinetics (Klempner et al., 1994).

The domain size of a sequential IPN can be modeled mathematically by Equation (2-1) derived by Donatelli et al. (1977) and Equation (2-2), derived by Yeo et al. (1983). The domain diameter of the guest polymer D_2 is determined by interfacial tension γ, the absolute temperature T (K), the concentration of effective network chain ν_1, ν_2 and volume fraction V_1, V_2 of networks.

$$D_2 = \frac{2\gamma V_2}{RTV_1 v_1 \left[{}^{1}\!/_{v_1^{2/3}} - \frac{1}{2} \right]} \qquad (2\text{-}1)$$

$$D_2 = \frac{4\gamma}{RT(A v_1 + B v_2)} \qquad (2\text{-}2)$$

$$A = \frac{1}{2}\left({}^{1}\!/_{v_2} \right)\left(3V_1^{1/3} - 3V_1^{4/3} - V_1 \ln V_1 \right)$$

$$B = \frac{1}{2}\left(\ln V_2 - 3V_2^{2/3} + 3 \right)$$

For a sequential IPN, the first formed polymer of the network tends to be the continuous phase for any composition. At intermediate and higher concentrations, both of the polymers in the network tend to be continuous (dual phase continuity). For highly immiscible systems, 50-100 nm microheterogeneous systems can be formed. On the other hand, if the two polymers are more compatible, domains on the order of 10-50 nm are commonly formed. Dual phase continuity and domain size are also strongly infected by crosslinking density.

2.1.4 Continuity of Phases of IPN and Mass Transport

The continuity of the phases, relative domain size and regions of guest polymer in the IPN are important determinants of mass transfer properties of the network. IPNs have been used in gas separation and drug delivery due to the fact that these properties can be controlled (Jan and Luca, 2000; Muratore, 2000). In

addition to these properties, the surface morphology significantly influences mass transfer as well as other properties including biocompatibility. Turner and Cheng (2000) and Zhang and Peppas (2002) found that the phase at the interface is different from the bulk for sequential IPNs, believed to be due to the evaporation of the monomer during formation of the host network or differences in the distribution of the guest monomer at the host substrate interface during synthesis. Peppas et al. developed PMAA/PNIPAAM pH and temperature sensitive IPN hydrogel membranes for separation or drug delivery. A dense, less permeable skin layer was clearly evident on cryogenic SEM images (Zhang and Peppas, 2002). Turner and Cheng (2000) attempted to alter the surface properties of a PDMS/PMAA IPN by polymerizing the guest monomer immersed in a monomer swollen host network. This was shown to improve the homogeneity of both the surface and the bulk. Furthermore, networks prepared this way showed increased permeability to small molecules.

2.1.5 IPN and Transparency of Materials

Because the domain size for IPN's generally ranges from 10 to 200nm, it is possible to obtain transparent materials using this technique. The transparency of materials is directly related to the size of nodule domain and the difference in the index of refraction of the two polymer phases (Haaf et al., 1981). It has been suggested (Heim et al., 1993) that a nodule size less than 1 μm, results in high impact

strength transparent PMMA/PU IPN casting sheets. Boeleau and Wang (2000) believed that the transparency of their poly siloxane based IPNs consisting of polymers with very different refractive indices was resulted at least in part by partial interpenetration of the polymers and the small domain sizes. Ree et al. (1998) concluded that transparency of semi-IPNs was controlled by phase separation on a sub micron scale. This phase separation was achieved by solvent assisted mixing and demixing controlled by a composition quenching process which was thought to result from solvent removal. During solvent evaporation, a ternary solution may be instantaneously driven into the spinodal decomposition region leading to phase separation. The demixing process is believed to be controlled predominately by the competition between spinodal decomposition and compositional quenching governed by continuous solvent evaporation (Ree et al., 1998).

2.1.6 Application of Interpenetrating Polymer Networks as Biomaterials

Initially, the impetus for the development of IPN's was the improvement of mechanical properties and energy absorption (Pandit, 1994; Sperling, 1994). Materials such as PDMS/polystyrene (PS), PS/polyethylene (PE) polyurethane (PU) / PS and PU/allynoyola resin IPNs were prepared with increased mechanical and tensile strength relative to the base polymers (Ree, et al., 1998; Borsig, et al., 1993; Tenhu and Vaahtera, 1991; Chiang et al., 1995). More recently, interpenetrating networks have been widely used in biomaterials applications. Most siloxane based interpenetrating networks are prepared for biomaterials applications (Leoncio et al.,

1991; Mark, 1990). A wide range of siloxane IPNs have been explored for such medical applications as skin, bone, and lung tissue replacements as well as intra-aortic balloon pumps (Arkles, 1983). The typical siloxane IPN applied in biomedical applications is a siloxane polyurethane IPN coplymer. The siloxane component provides biocompatibility and oxygen permeability, while the PU component adds tensile strength and excellent fatigue endurance to inhibit environment and stress cracking (Honda, 1975). Additional siloxane based IPNs used as biomaterials and in related applications include a silicone/aromatic polyester/PU IPN designed as extrusion grade materials for medical use (Arkles, 1983), gradient IPN composed of polyHEMA and polyurethane for water soluble drug delivery (Mueller and Heiber, 1982) and a number of siloxane hydrogel interpenetrating polymer networks designed for biomolecule separation (Miyata et al., 1996) or controlled drug release applications (Shin et al., 2002; Kim et al., 2001). Abbasi et al. (2002) developed PDMS/polyHEMA IPNs to modify surface and bulk properties or PDMS for biomedical applications.

In addition, several researchers are developing IPNs for gas or small molecule separation. A PU/PS IPN was developed for N_2 and O_2 gas transport and selection (Lee et al., 1992; 1991). A semi-permeable semi-IPN composed of PNVP/PU has been developed for glucose and other biomolecule permeation. PAA/PVA semi-IPNs and IPNs were synthesized as membranes with improved mechanical properties for water/ethanol separation through the continuous PAA hydrogel matrix (Ruckenstein and Liang, 1996).

The hydrophobic, nonpolar nature of PDMS and the hydrophilic, polar nature of PNIPAAM renders these polymers highly incompatible and therefore difficult to mix by general blending. Even using block or graft copolymerization, the sea-island domain style would be expected to occur. The continuous hydrogel domains formed using these techniques are suitable for forming channels for the permeation of water soluble molecules. However, if the mixing was accomplished by forming an interpenetrating network of the two crosslinked polymers, the phase separation maybe kinetically controlled or prevented by permanent interlocking of entangled polymer chains, suggesting that IPN formation may be a suitable method for improving the glucose permeability of PDMS.

2.2.Poly (Dimethylsiloxane) (PDMS) as a Biomaterial

2.2.1 PDMS Chemistry

PDMS is the simplest silicone with the structure shown in Figure 2.3. A variety of groups including vinyl, hydrogen, silanol etc. can replace the methyl groups especially the terminal methyl groups for further reaction and curing or crosslinking the polymer to form a network.

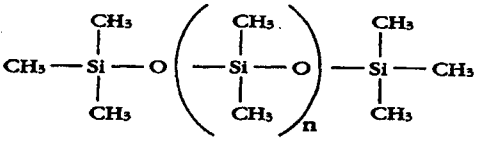

Fig. 2.3: Chemical structure of poly(dimethylsiloxane)

At 25°C, the refractive index of PDMS ranges from 1.397 to 1.404. In most forms, PDMS is very transparent in the air. Typically, the viscosity of the base PDMS polymers range from 1000 to 60,000cst, although its viscosity can be lower than 100 cst. The viscosity of PDMS is as function of degree of polymerization or molecular weight. When the molecular weight of the polymer is greater than 2500, a linear relationship, known as Barry's equation (2-3), exists between these parameters as shown in Figure 2.4.

$$\log \mu_{cst} = 1.00 + 0.0123M^{0.5} \qquad (2\text{-}3)$$

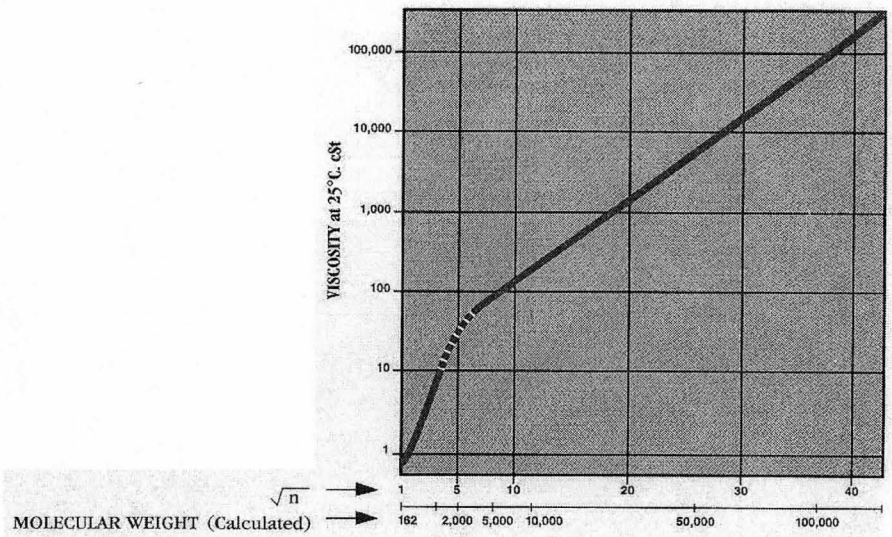

Fig.2.4: Viscosity of PDMS as a function of degree of polymerization "n" or molecular weight. The straight portion of the slope corresponds to Barry's relationship on molecular weight greater than 2,500 (From Gelest Inc. brochure)

The mechanical properties of unfilled PDMS elastomer are extremely poor. However the addition of reinforcing fillers including hexamethyldisilazane, divinyltetramethyldisilazane and cylic and short linear silioxane-treated fused silica

can effectively increase the modulus, tensile and tear strength and abrasion resistance. If transparency must be maintained, a reinforcing resin with vinyl Si-O_4 structure shown has been suggested for improvement of rigidity.

Si-O_4 : 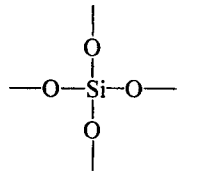

2.2.2. Curing Methods

Due to the variety of functional groups available, curing mechanisms are highly versatile. The most commonly used PDMS prepolymers are vinyl and hydroxyl terminated, which are cured by the four fundamental processes described below.

(1) High temperature vulcanization (HTV), used for vinyl or methyl terminated PDMS using peroxide as activator as shown in Scheme (2-1) is consistent with conventional rubber crosslinking methods. The most widely used peroxide activators include dibenzoyl peroxide, dicumylperoxide, bis (dichlorobenzoyl)peroxide. Curing is performed at temperatures between 140 and 160°C and is initiated by a free radical mechanism.

Scheme (2-1):

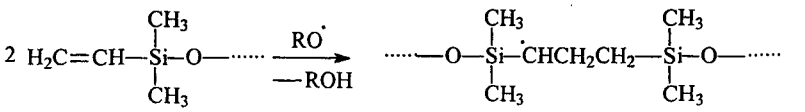

(2) Vinyl addition is induced by a Pt based catalyst system. This method involves the reaction between methylhydrosiloxane-dimethylsiloxane copolymer with methyl hydrosiloxane through the addition of silicone hydride to vinyl-substituted silane. The

catalyst is usually dissolved in alcohol, xylene, divinyl siloxane or cylic vinyl siloxanes. Commercially, the curing kit is prepared in two parts, consisting of the platinum catalyst at level of 5~10 ppm and a hydride functional siloxane. The reaction is depicted in the following reaction scheme (2-2).

Scheme (2-2):

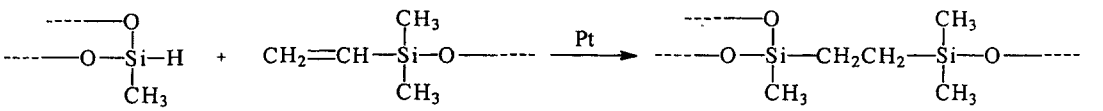

(3) Room temperature vulcanization (RTV) involves a condensation reaction between silanols and a moisture sensitive silane crosslinker. The silanol functionalized PDMS is reacted with an excess of a multifunctional silane such as TEOS. However other crosslinkers with silica andacetoxy, or enoxy, nxime, alkoxy and amine bond can also be used to form PDMS with terminal groups that are susceptible to hydrolysis. Upon exposure to moisture, the crosslinking occurs readily, resulting in the formation of a cured gel as depicted in Scheme 2-3.

Scheme 2-3:

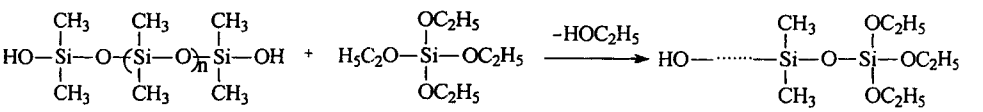

(4) Hydride and silanol condensation involves a metal salt catalyzed condensation reaction between hydride Si-H and silanol Si-OH groups resulting in a foamed

structure caused by the formation of H_2 as a byproduct of the reaction as depicted in scheme (2-4).

Scheme (2-4):

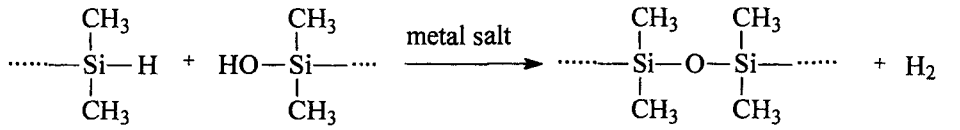

2.2.3 PDMS as a Biomaterial

In the past three decades, PDMS has been applied widely applied in biomaterials and bioengineering because of its relatively good biocompatibility (Abbasi et al., 2001; Szycher, 1994). It was selected along with low density polyethylene (LDPE) as one of the primary reference materials and a discriminatory tool for validation of standardized and novel materials in assessment of biocompatibility of new developed materials and medical devices in 1984 (Belanger, 2001). The biocompatibility of PDMS including complement activation, inflammatory response and in vivo tissue reaction generated by contact with PDMS has been investigated extensively (Sevastianov et al., 1984; Ertel et al., 1994; Belanger et al., 2000). In most studies, PDMS shows reasonable blood compatibility, and low toxicity to cell growth. However, longer term vivo studies showed it to induce a mild inflammatory response on subcutaneous foreign body reaction.

Therefore, because of its excellent stability and oxygen permeability, good mechanical properties and biocompatibility, PDMS in both gel and elastomeric form

as well many copolymers of PDMS have been used in fabrication of such medical devices as blood pumps, cardiac pacemakers, orthopedic pads, mammary prostheses, oxygenators, contact lenes, artificial skin, finger joints, and drug delivery systems (Arkles, 1983; Abbsi, 2001). Furthermore, PDMS/PU IPN materials have been used in blood pumps, as intra-aortic balloons and other related devices (Honda et al., 1975a,b). The materials were shown to have high fatigue strength, as well as toughness, flexibility and low levels of interaction with plasma proteins. Similarly, interpenetrating polymer networks of PDMS and PHEMA have also been proposed as potential materials for biomedical applications (Falcetta et al., 1975; Abbasi. 2002 a,b). PDMS/polycarbonate copolymers with high mechanical strength and high oxygen and water permeability have been designed for blood oxygenation and dialysis (Nelson, 1962; Boileau et al., 1998) and microelectrode applications (Montalvo, 1975). Artificial skin can fabricated with cured top layer of PDMS that in addition to providing mechanical support for new skin growth (Schulz et al., 2000) prevents fluid loss and bacterial infiltration.

Due to its transparency and high oxygen permeability, PDMS has been particularly widely used as an ophthalmic biomaterial. Copolymers of PDMS with hydrophilic comonomers including (hydroxyethyl methacrylate) have been used in the synthesis of extended wear contact lens materials. Siloxane based materials have also been widely studied as the base polymers in artificial cornea applications (Ruedemann, 1974; Hsiue et al., 1993a,b; Lee et al., 1996; Aucoin et al., 2002; Merrett et al., in press).

2.3 PNIPAAM in Biomaterials and Drug Delivery Applications

PNIPAAM, depicted structurally in Figure 2.5, exhibits a phase transition lower critical solution temperature (LCST) at 31.5 °C (Zhang and Zhou, 2001; Wu and Sassi, 1996a,b). This phase transition causes conformation and property changes including solubility, volume, hydrogel pore size, swelling ratio and permeability as depicted in Figure 2.6, and has resulted in considerable research interest in this polymer. Biomedical applications of this polymer including controlled drug delivery (Suzuki et al., 2001; Kono et al., 1999; Hoffman et al., 1986), separation of water soluble molecules (Liang et al., 1999; Hoffman, 2002; Jeong et al., 2002), enzyme immobilization (Sun et al., 1999; Park and Hoffman, 1990; Chen et al., 1997), protein dewatering (Knodo et al., 1994; Stayton et al., 1995) and as a cell culture substrate (Shapiro and Cohen, 1997; Kwon et al., 2002). However, the poor mechanical properties of this polymer, resulting from its high water content, severely limit its potential for use as a biomaterial.

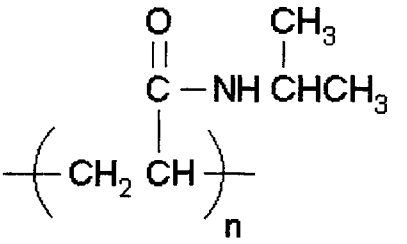

Fig. 2.5: Chemical structure of PNIPAAM

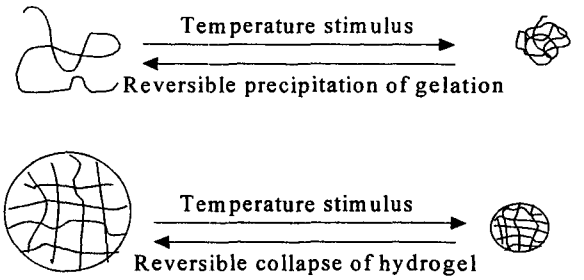

Fig. 2.6: The conformational changes of PNIPAAM undergoing LCST

Many studies of PNIPAAM have focused on its LCST behavior (Bae et al., 1990; Hiroshi et al., 1990; Feil et al., 1993). It is commonly agreed that this LCST behavior is caused by a balance between hydrophilic and hydrophobic interactions of polymer chains at different temperatures (Hiroshi et al., 1990). Based on the structure of PNIPAAM, it is clear that significant hydrogen bonding will occur between hydrophilic groups in side chains with N, O elements. The polymer chains also exhibit hydrophobic character. The balance between these two interactions is believed to be dominated by changes in temperature. At temperatures below the LCST, hydrogen bonding between hydrophilic groups in the polymer chains and water molecules is strong and the water molecules form a cage-like structure around the hydrophobic polymer chains. This leads to good solubility of polymer chains in water and a high degree of swelling of the network in an aqueous environment. However, when the temperature is at or above the LCST, the water structure is destroyed and hydrophobic interactions become dominant, so that the water entrapped within polymers will be squeezed or expelled out. The PNIPAAM chains associate and phase transition occurs as the linear polymer precipitates and the pores collapse.

2.3.1 Modification of the LCST of PNIPAAM

PNIPAAM is most extensively investigated among the temperature sensitive polymers because it demonstrates more abrupt changes in phase transition and the transition temperature is within a suitable range (Brazel and Peppas, 1995). Zhang and Zhou et al. (1999a,b) have used different synthesis techniques or incorporation of other chemicals to prepare fast response PNIPAAM based thermosensitive polymers for better control of drug release and for separation of biomolecules. Panda et al. (2000) investigated synthesis a NIPAMM hydrogel by electron beam and gamma irradiation to produce a much faster swelling/deswelling rate. It has also been found that the LCST of PNIPAAM can be changed or tailored by incorporating other comonomers (Yoshioka, et al., 1994) or with the addition of cosolvents (Winnik et al., 1992), salts (Louai et al., 1991) or surfactants (Schild and Tirrell, 1991) to the polymer water solution. Yoshioka et al. (1994) suggested when copolymerized with a more hydrophilic comonomer such as acrylamide or PEG, the LCST of PNIPAAM coplymer may be higher than pure PNIPAAM. This research also indicated that, in addition to comonomer content, the sequence length of the blocks in the copolymer is the dominant factor in LCST tailoring. The loss of LCST phenomenon in these polymers was comfirmed by disappearance of the endothermal phase transition peak by DSC. The LCST of PNIPAAM-co-AAC is also influenced by pH and the presence of polyelectrolyte solutes, decreased by inter or intramolecular hydrogen bonding between amide and carboxylic acid groups (Yoo et al., 1997; 1998).

2.3.2 Preparation Methods for PNIPAAM Based Polymers

Because the high swelling ratio of PNIPAAM results in polymers of low mechanical strength, PNIPAAM is most often used in combination with or as a modification to other polymers. A variety of PNIPAAM based copolymer hydrogels or surfaces modified by PNIPAAM have been prepared.

2.3.2.1 PNIPAAM Surface Grafting

Li et al. (1999) used pre-irradiation to graft PNIPAAM to the surface of silicone rubber for controlled protein adhesion to surfaces in response to different temperatures. Graft yields of up to 70% were obtained depending on the dose of radiation used. Liang et al. (2000) prepared PNIPAAM hydrogels grafted on silicon wafers as cell culture substrates. The resultant surfaces were found to be very hydrophilic below 25°C, with contact angles that were approximately 0°. However, at temperatures above 40°C, the surfaces were extremely hydrophobic with contact angles of 92°. PNIPAAM grafted silica substrates have been used as column packing materials for chromatography (Kanazawa et al., 1997). Modified PS substrates have been used for cell culture (Okano et al., 1995; Ito et al., 1997). Cells were attached and proliferated on the PNIPAAM modified surface at temperatures above the LCST, while the cells were easily to be detached from the substrate without damage by decreasing the temperature to below the LCST. PNIPAAM grafting modified porous membranes was used to control liquid transportation and separation

(Liang et al., 1999). Ethylene vinyl acetate (EVA) grafted with PNIPAAM has been used to improve PNIPAAM mechanical properties for immobilization and extraction applications (Pu et al., 1996).

2.3.2.2 PNIPAAM Copolymers

Copolymers of NIPAAM and sodium vinylsulfonate or sodium acrylamide were prepared by free radical polymerization to develop the materials which were sensitive to temperature and the charge of the surrounding medium. These polymers have been used to concentrate dilute enzyme and protein solutions and to exclude molecules by size and charge (Vasheghani-Farahani et al., 1992). Zhou et al. (1998) synthesized acrylamidolactamine-based PNIPAAM copolymers. Incorporation of the lactose moieties was found to improve the biocompatibility and the PNIPAAM was expected to provide with thermally sensitive properties for biomaterial applications.

2.3.2.3 PNIPAAM Containing IPNs and Semi-IPNs

Zhang and Peppas (2000) combined pH sensitive PMAA and temperature sensitive PNIPAAM to form a UV initiated sequential IPN. These networks were observed to demonstrate significant size exclusion behavior with different model drugs permeating the IPN membrane. Membrane permeabilities were found to be sensitive to both temperature and pH. Kim et al. (2000) developed similar temperature and pH sensitive IPNs using PNIPAAM and chitosan. However, the use of chitosan

with an amine group resulted in membranes with an inverse pH response compared with the PMAA based membranes. Semi-IPNs of polyacrylamide and linear PNIPAAM (Muniz and Geuskens, 2000) as well as alginate and linear PNIPAAM (Guilherme et al., 2002) have been prepared for studies of drug permeability for controlled release.

Semi-IPNs containing linear PNIPAAM can be synthesized by dissolving the PNIPAAM polymer into a solution of monomer and crosslinking to form the network prior to polymerization (Lowe et al., 1998). Semi-IPN hydrogels combining chitosan with linear PNIPAAM has been exploited in such applications as temperature controlled optical switches or modulators (Wang et al., 2000). To reinforce the PNIPAAM hydrogel, a temperature dependent polyacrylamide/PNIPAAM semi-IPN has been synthesized (Muniz, 2000).

2.3.3 Transport Properties of PNIPAAM

The permeability of water and water soluble substances through hydrogels such as PNIPAAM is governed by water content or swelling ratio in hydrogel since the water filled region acts as a permeation channel (Guilherme et al., 2002). In addition to being affected by the specific polymer used, the permeability is therefore related to the crosslinking density of the polymer. In PNIPAAM, this swelling ratio is also greatly affected by ambient temperature. For example, Muniz et al. (2000) reported that the permeability of poly acrylic acid (PAA) / linear PNIPAAM

semi-IPNs to water soluble Orange II dye increased at temperatures below 32°C, because shrinkage of the PNIPAAM below the LCST resulted in increased pore volume, facilitating water and water soluble molecule diffusion.

For PNIPAAM hydrogels used to surface modify a porous bulk polymer, the permeation mechanism becomes more complicated. Kim et al. (2002) reported that the grafting of a PNIPAAM hydrogel on the inner surfaces of a porous poly(propylene) matrix enhanced hydrophilicity and water affinity, leading to higher water permeability. The permeability was found to increase with increased graft yield and to respond to temperature changes. At temperatures above the LCST, where the PNIPAAM becomes increasingly hydrophobic due to the dissociation of structured water, the water permeability was found to decrease. Inversely at lower temperatures below the LCST, the permeability was dramatically enhanced.

A more detailed discussion of the permeability of PE grafted PNIPAAM porous membranes is provided by Peng and Cheng (1998). As shown in Figure 2.7, the permeability of the membranes was found to increase with increased graft yield, ultimately reaching a maximum value. However, depending on the graft yield, the mechanism of permeation was found to be different. At low graft yield, the permeability was found to be governed by pore grafting of PNIPAAM, with the swollen and expanded PNIPAAM acting to block the pores. When the temperature was increased above 32°C in this case, the collapse of the PNIPAAM gel resulted in more open pores with increased permeability. At high graft yields, the permeability

was found to be controlled by thickness or density of the grafted PNIPAAM chains. Higher yields resulted in polymers that absorbed more water. In this case, the permeability was higher at temperatures below the LCST, while at higher temperatures, the shrinking of the PNIPAAM and compaction of the gel decreased water and small molecule diffusion.

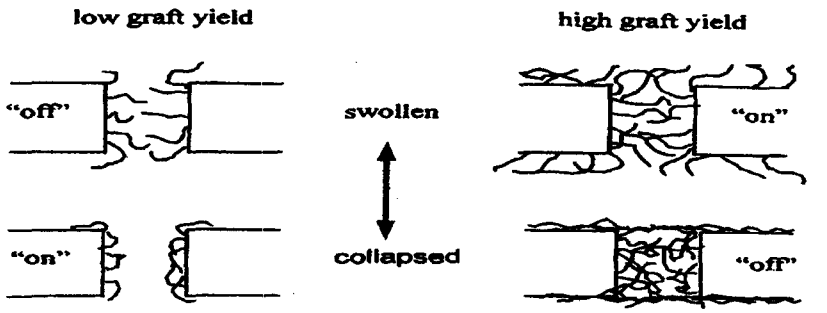

Fig.2.7: Explanation of dual-response mechanism (Peng and Cheng, 1998)

2.3.4 PNIPAAM for Drug Delivery

The thermosensitive characteristics of PNIPAAM have been widely applied to the delivery of drugs. The thermal regulation of the swelling ratio and resulting conformation change of PNIPAAM and its copolymer hydrogels have made it possible to use PNIPAAM in the design of drug delivery systems that incorporate an "on-off" concept induced by the LCST.

PNIPAAM has been used as a polymeric coating for compression-coated soluble or insoluble tablets to give site specific and sustained release (Eeckman et al.,

2002). In this model, environmental temperatures less than LCST result in high permeability and relatively fast drug release. Inversely, at temperatures higher than the LCST, the PNIPAAM becomes a collapsed gel with a concomitant decrease in the permeability. Since it has been shown that the LCST of PNIPAAM can be easily modified by the addition salt or surfactant or their presence in the surrounding environment (Schild and Tirrell, 1992 and 1990), thought to be due to changes in the normal hydrogen bonding in the water in the presence of these electrolytes, altering the response temperature is relatively easy. This has been exploited for the development of controlled drug delivery systems for drug release in the GI tract and colon using the salt concentration as an on/off switch. Different salt and surfactant types including Na_2SO_4 NaCl, NaOH , CH_3COONa, lauric acid sodium salt and galacturonic acid sodium salt for example were incorporated into the PNIPAAM coating to lower the LCST under aqueous conditions (Eeckman et al., 2002). The mechanism of drug release from the thermosensitive coatings in the presence of salt is depicted in Figure 2.8.

When the tablets are immersed in water with a temperature greater than 27°C, the saline micro-environment and LCST of the polymer gel prevents or delays drug release. Depending on the environment, the salt concentration in the coating will decrease as it is released. The PNIPAAM polymer remains insoluble and less swollen until salt concentration decreases to a level that is too low to maintain the LCST below the temperature of the surrounding medium. At this time, drug release

increases significantly. Therefore, the release of the drug experiences a lag relative to immersion in the surrounding biological medium.

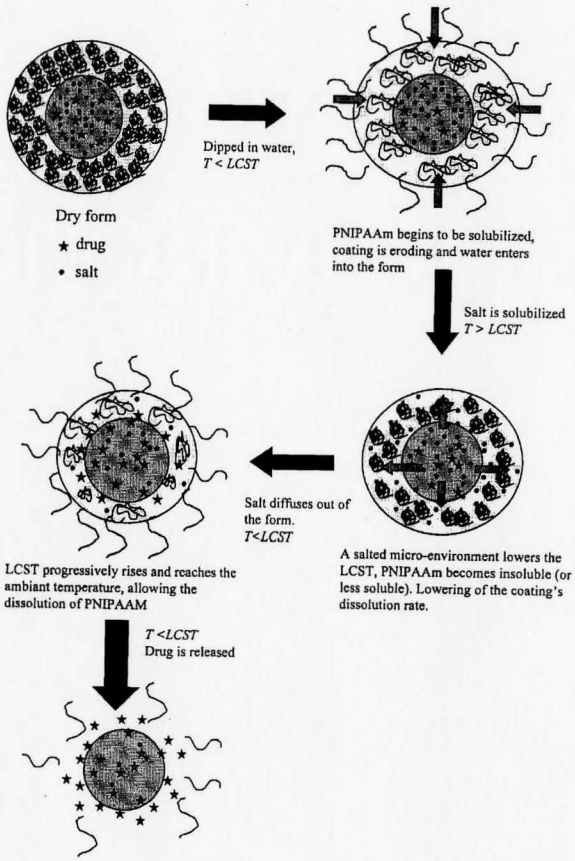

Fig. 2.8: Mechanism of drug release from thermosensitive polymers in the presence of salt (Eeckman et al., 2002)

PNIPAAM gels can be loaded in an inorganic connective porous matrix, including porous silica (Suzuki et al., 2001) or hydroxyapatite ceramics (Shin et al., 2002) to form hybrid gel as water-soluble drug loaded vehicles. Under these conditions, the PNIPAAM performed as an "on-off" switch for drug release. At temperatures higher than the LCST, the PNIPAAM gel loaded in the pores shrinks and

providing a more open channel for drug permeation and a faster rate of drug release. However, at temperatures below the LCST, the swollen gel fills the pore, resulting in no release in the case of a non-soluble silica matrix and significantly slower release for the more hydrophilic hydroxapatite. In latter case, at a temperature of 40°C, a slow, but almost constant drug release rate was noted while no release was observed at a temperature of 10°C. This drug release vehicle provided sustained delivery of hydrophobic drugs over a period of approximately one month. However, the case of more hydrophilic drug, temperatures increase above the LCST resulted in an increase in the rate of release as the drug is pushed out of the gel by the contraction process.

Pure PNIPAAM hydrogels are not suitable as drug delivery vehicles because of the very fast release and the low loading possible in the highly swollen gels. Therefore, various methods of improving drug release properties from PNIPAAM gels while retaining the LCST characteristics have been attempted. Peptide and protein drug delivery systems were developed using PNIPAAM modified with a polyethylene glycol (PEG) hydrogel of various molecular weights ranging from 2000 to 6000 Da as a pore forming agent (Zhou and Li, 2003). Pore size was controlled by the PEG molecular weight. In these systems, the protein molecules remained in bulk solution within the large aqueous pore. It was shown that this can reduce protein inactivation during storage and improve the release characteristics using this macro-porous hydrogel.

Hsiue et al. (2002, 2003) designed PNIPAAM-g-PHEMA and PNIPAAM thermosensitive systems for delivery of the drug H-epinephine as an eye drop for glaucoma therapy. The eye drops were clear solutions when stored at room temperature. In contact with the cornea, which has a surface temperature between 34 and 35°C, a sol-gel phase transition occurred resulted in the formation of a gel film on the corneal surface and release of drug to the eye. Similarly, a PNIPAAM nano gel particle drug loaded ophthalmic drop system was developed (Feil et al., 1993). The result showed that when the eye drop was placed on the surface of the cornea, the drug was initially squeezed from the polymer gel particles due to the phase transition forming a bulk film on the outer layer of the gel. However, this dense skin layer on the surface of the gel inhibited further release and resulting in a prolonged period of drug delivery. The NIPAAM homopolymer also became rigid and uncomfortable in contact with cornea and there was significant loss of the gel particles due to their nano-size. To solve these problems, a release system containing linear polymer and gel particles of PNIPAAM-g-PHEMA along with the entrapped drug was developed. The PHEMA was grafted to the PNIPAAM backbone to enhance flexibility and biocompatibility. Sustained release was observed for up to 26 hours with this system, significantly more than that with the pure PNIPAAM gel particle eye drop with a delivery period of 8 hours.

Block copolymers of PNIPAAM and hydrophobic cholic acid (CA) were used to form amphiphilic self-assembled polymer micelles as hydrophobic drug vehicles

(Kim et al., 2000). CA was coupled to amine terminated PNIPAAM using N,N-dicyclohexylcarbodiimide. In an aqueous environment, the polymer self-assembled to form micelles consisting of an inner hydrophobic core which can contain drug and a hydrophilic outer layer which can respond to changes in external temperature. At temperatures greater than the LCST of the micelle, the conformation of the outer layer changes to a collapsed state and rate of drug release decreases. At environmental temperature is below the LCST, an expanded outer layer facilitates faster release of the drug. Using these principles, the micelle can be used to deliver drugs site specifically with a release rate controlled by the temperature of target site.

2.4 Artificial Cornea

Millions of patients worldwide suffer from variety of corneal disorders including inflammation, dystrophies, degenerative diseases and traumatic disorder (Robert, 1993; Maudgal, 1985; Guyton, 1996). Cornea blindness is a leading cause of blindness, second only to cataracts. While highly treatable through replacement of the diseased or damaged tissue with donor tissue, with success rates on the order of 85%, many of these patients, in spite of treatment, or as a result of the lack of available treatment will lose normal vision. Replacement of the diseased tissue with a suitable corneal prosthesis could potentially restore vision for these patients.

2.4.1 Corneal Anatomy and Physiology

2.4.1.1 The Structure and Function of the Cornea

The cornea, depicted in Figure 2.9, has a thickness of approximately 600μm. The central area is a little thinner than at the periphery. The cornea consists of five avascular tissue layers: the epithelium, Bowman's layer, stroma, Descemet's membrane, and the endothelium (Klyce, 1998). On the anterior surface, the tear film maintains a smooth epithelial surface essential for vision. The tight junctions between the cells of the epithelial layer maintain a protective barrier, preventing invasion by toxins and microbes as well as preventing corneal dehydration. The nerve endings present in the epithelial layer are important for limiting traumatic damage. Bowman's layer, composed primarily of the cell adhesion protein laminin, is the scaffold for the epithelium, separating the epithelial and stromal layers. The stroma, accounting for as much as 90% of the thickness of cornea, performs its primary optical function and contributes to metabolism. It is almost acellular, composed primarily of Type I collagen, chondroitin sulfate and keratin sulfate with a low density of stromal fibroblasts. Descemet's layer is a basement membrane of endothelium composed of fine collagenous filaments. The endothelium acts as a regulating membrane, maintaining the hydration of the stroma essential for vision, and balancing the water content for metabolism under normal physiological conditions.

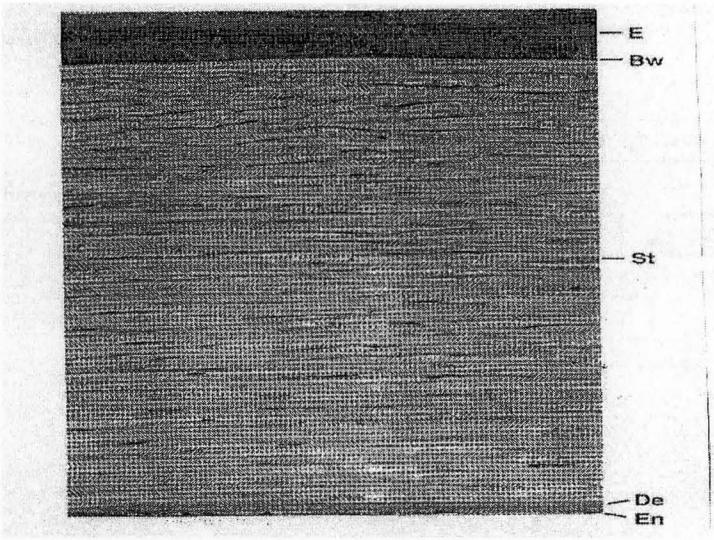

Fig.2.9: The layered cornea structure consisting of the epithelium (E), Bowman's layer (Bw), stroma (St), Descemet's membrane(De), and the endothelium(En) (From Klyce, 1998)

The eye has a lens system much like that of a camera composed of different refractive elements including the cornea, aqueous humor, lens and the vitreous humor. The transparent cornea is the first and most important refractive element of the eye. The refractive power of the eye is measured in term of diopters, with one diopter of refractive power of a convex lens being equal to one meter divided by the focal length of the lens. The eye has a total refractive power of approximately 59 diopters when the lens is accommodated for distant vision. Of this, the curvature of anterior surface of cornea accounts for as much as 40 diopters in total or up to 70% of the refractive power of the eye.

Besides the refractive function, the cornea performs a barrier function, and can absorb most ultraviolet radiation, preventing it from reaching and damaging the inner

ocular structures. Corneal strength, elasticity and thickness, primarily due to the stromal layer, allow for a mechanically tough barrier that withstands the intraocular pressure and protects eye from slight mechanical damage. The cellular component of the cornea maintains a chemically impermeable barrier between the eye and the environment, protecting it from chemical insults and the invasion of microbes and pathogens. Due to the avascular nature of the cornea, the ability to permit oxygen permeation from the atmosphere via the anterior corneal surface is necessary. Additional nutritional requirements from the aqueous humor via the posterior corneal surface for metabolism are also maintained.

2.4.1.2 Glucose and Oxygen Permeability and Metabolism

Much of the energy necessary for the metabolic processes of the cornea is derived from the catabolism of glucose (Klyce, 1998). Approximately 105 $\mu g/cm^2/h$ of glucose is consumed by corneal metabolic processes, the source of which is primarily permeation from the aqueous humor. Only a small fraction of the glucose consumed enters the cornea from the limbus and tears. Corneal catabolism of glucose yields energy in the form of ATP by oxygen-dependent Krebs cycle and by anaerobic glycolysis. The hexose monophosphate shunt uses a fraction of available glucose for cell synthetic activities.

Normally, the glucose content of the cornea derived from the aqueous humor is balanced by the loss of corneal lactate. However, if the corneal oxygen supply is

insufficient for a variety of reasons, the entry of pyruvate into the Krebs cycle is reduced, anaerobic glycosis is intensified and the rate of lactate production increases. This results in an excessive concentration of lactate, resulting in epithelial edema which alters the cellular refractive index. Increased metabolic lactate production may also alter endothelial morphology and function. Therefore, it is important that the glucose and oxygen transport processes of the native cornea be maintained. The normal metabolism of corneal cell also requires a constant supply of amino acids vitamins and other constituents diffused from the aqueous humor. If these nutrition are significantly reduced over a long time, anterior corneal necrosis can occur.

2.4.2 Requirements for Artificial Materials and Current Artificial Cornea Models

The complicated structure of the cornea allows it to perform various functions. Clearly, imitating all of these properties in an artificial cornea is impossible. There has been considerable research on the development of a substitute that can maintain basic optical and metabolic functions. Basic requirements for artificial corneal materials include transparency, and biocompatibility. To fulfill both native cornea functions and for surgical convenience however, additional properties are desired. Adequate strength for suturing and for resisting internal intraocular pressures is necessary. Furthermore, related to biocompatibility, maintenance of an epithelial layer over prosthetic anterior surface would provide a wettable renewable layer with

the ability to interact with the tears for visual clarity. A watertight junction at the interface between the material and the native tissue would inhibit infection and epithelial down-growth, as well as withstanding intraocular pressure. Optimally, an artificial cornea would heal with the host cornea to obtain this property. Finally, permeability to oxygen and glucose as well as other nutrients is necessary to satisfy the needs of corneal metabolism and catabolism. The presence of corneal cells necessitates the glucose permeability. Oxygen permeation is required regardless for the maintenance of the health of the internal ocular structures.

2.4.3 Current Artificial Cornea Models

There are many groups working on development of keratoprostheses with a porous skirt as shown in Table 2.1. Various kinds of polymeric materials including PMMA, PDMS, PU, PTFE and hydrogel of PHEMA, PVP PVA have been used in the artificial cornea models developed to date. Most current designs follow a core and skirt model: a central optical core is surrounded by a porous skirt that allows for the ingrowth of stromal cells to maintain the device in the eye (Chirila et al., 1998).

Trinkaus-Randall and coworkers (1991) used a model consisting of a central core made of a poly(vinyl alcohol-co-vinyl acetate) copolymer. The core was joined to a skirt made from polybutylene / polypropylene (80/20) blend with contiguous pores with sizes ranging from 10-100μm. This model was retained in rabbit eyes for periods between 3 weeks and 3 months (Trinkaus-Randall et al., 1993). However, because of the incompatibility of the core and skirt materials, mechanical problems at

the interface between the two materials was noted. In order to improve the hydrophilic properties of the core, complicated chemical treatment was necessary after attachment to the skirt.

Porous PTFE is the most extensively used skirt material for artificial corneas based on its biocompatibility and availability. Legeais et al. (1992) proposed an artificial cornea model consisting of a cylindrical PMMA or poly siloxane core and a porous PTFE skirt (Legeais et al., 1995; Renard et al., 1996). Four month retention times with few complications were observed with this model.

With the purpose to retaining the cornea permanently, Chirila's group (1994a,b; 1995) designed an artificial cornea model using hydrophilic PHEMA. The core was made of a PHEMA hydrogel; the skirt was fabricated from a crosslinked PHEMA sponge to facilitate cell adhesion and growth. By using the same polymer for the core and the skirt, incompatibilities due to differences in chemical structure and physical properties were avoided. The connection of skirt and core was performed using a gradient IPN method (Chirila et al., 1994c). The porosity of sponge, controlled by water content during polymerization was varied to give pores between 20 and 30 μm in size. 80% of full thickness implants were retained for 12-20 months in rabbits without complications. The main shortcoming of this model is the poor mechanical properties of the PHEMA hydrogel and sponge which present significant problems related to suturing and to withstanding intraocular pressure. Attempts to improve these properties have had some success, but mechanical properties are significantly lower than those of the native cornea.

Table 2.1: Core-porous skirt artificial cornea model study situation and their performance

Group	Core	Skirt	Connection	Biological performance
Caldwell	PU elastomer	Six pronged skirt, mesh or sponge PTFE, 15- 90μm.	PU polymerization within circular cavity surround by PTFE penetrating	Retaining time: Cat: >1 year Human: >1 year
Coldwell	PU	PU	Molding	Retaining time: 8 in 28 patient: 3 years
Legeais	PMMA cylindrical	PTFE D=18-80μm	Clamping by titanium ring	1. fibrilorientation 2. rabbit: >4 months 3. patient:70% patient vision improvement 4. biocompatibility study to cornea
Legeais	Polysiloxane	Porous PTFE	Cure SR in penetrating PTFE core	1.plasma treatment surface to help cell adhesion 2.retaining time: 11 rabbits: >3 months; 5 people: >3 months
Trinkaus-Randall	poly(vinyl alcohol-co-vinyl acetate)	polybutylene/ polypropylene blend	Acetone as solvent glue	1. 3 months retaining in rabbit 2. More step treatment for improvement of core hydrophilic properties 3. need preseeded with epithelial cells
Ikada	Polysiloxane	Nonwoven PU fabric, 90% pores covered, D=50μm .	Unknown glue	1. massive cell invasion 2. tissue growth into skirt 3.Retaining time: 8 rabbits: > 4 weeks
Ikada	PU	PU	Unknown	1. massive cell invasion 2. 7 rabbits trials: retaining time > 2 months
Dohlman	PMMA	Porous PE D=8μm	Unknown	10 rabbits: > 6 months and no complication
Chirila	PHEMA homogenous hydrogel	PHEMA porous sponge d>10μm	Gradient IPN method to connects core and skirt	1. 25 rabbit trial: 80% trials 12~22 months 2. 30 rabbits trial: 2 weeks~6 months and no complication

2.4.4 Silicone Rubber for an Artificial Cornea

Polysiloxanes, primarily due to their high oxygen permeability, have been widely examined as ophthalmic biomaterials. Silicon based hydrogels have been developed and used as extended wear contact lenses (Huise et al., 1993a; Tanaka et al., 1979). In addition to oxygen permeability, these materials are transparent, provide a barrier for water permeation and have good biocompatibility (Dumbleton, 2003; Lai et al., 1993). However, the high hydrophobicity of these materials makes it necessary to modify the surface for improving the wettability.

Dohlman (1983) developed transparent silicone rubber artificial corneal endothelium applied the posterior surface of cornea to act as endothelium to prevent water permeation and edema. In some cases, these membranes were shown to work well for periods of 2 years or longer. Ruedemann et al. (1974), using various designs, showed with extensive trials in both animals and human, that a silicone rubber based cornea was maintained for more than 2 years in 12 of 27 eyes. Two were maintained for 7 years. However there were complications in most of the trials that impacted the visual rehabilitation.

Hsuie and Chang et al. (1993a,b, 1996, 1998) developed a novel silicone rubber heterobifuctional membrane for corneal use by plasma induced grafting. The anterior surface of the membrane was grafted with a small amount of hydroxyethyl methacrylate (HEMA) to promote corneal epithelial cell adhesion. The posterior surface was modified by grafting 2-methacryloyloxyethy phosphorylcholine (MPC) of

bisamino polyethylene oxide (PEO). This was shown to suppress the growth of corneal epithelial cells and it was postulated that this could inhibit corneal epithelial downgrowth. In vitro protein adsorption studies showed that protein adsorption on the poly(MPC) grafted silicone was reduced to 36% of that on the control samples.

Sheardown et al. have also used PDMS for artificial cornea applications. Modification of PDMS surfaces by combinations of cell adhesion and synergistic peptides was shown to facilitate the attachment of corneal epithelial cells in vitro (Aucoin et al., 2002). Surface modification with growth factors, specifically TGF-b2 has also been studied to improve and manipulate cell interactions with these materials (Merrett et al., 2003 (in press)).

2.5 Hypothesis and Objectives of Present Research

In all previous studies, using a variety of materials both polymeric and natural, there has been little if any attention to the glucose and oxygen permeation properties which are essential for maintaining a healthy interface between the materials and the native tissue. Although PDMS has been previously demonstrated to have with good ophthalmic compatibility, excellent oxygen permeability and other properties suitable for use in artificial cornea applications, its hydrophobic nature negatively affects other properties including cell adhesion and glucose permeation, both of which are important for success. The objective of this work is therefore to improve permeability of small molecules through the introduction of a hydrophilic connective domain in the

PDMS matrix. Water diffusion channels will be generated which allow the permeation of small water soluble molecules such as glucose without adversely affecting oxygen permeation or material properties. Specifically it is hypothesized that:

- The introduction of a hydrophilic polymer into the bulk PDMS will both increase the wettibility and generate channels for water and small molecule permeation.
- Based on the high swelling ratio and reported ophthalmic compatibility of PNIPAAM hydrogels, they should be effective at improving the bulk hydrophilicity of PDMS and ultimately its cellular interactions. Furthermore, the LCST properties can be exploited for generating copolymers with thermal sensitivity for both drug delivery and or tissue engineering applications.
- Interconnected water channels resulting from the introduction of the hydrophilic polymers can be obtained by interpenetrating network formation. Although the domain sizes may be very small, adequate glucose permeation can be obtained while maintaining the barrier functions associated with the PDMS.
- The bulk mechanical properties of the PDMS will not be adversely affected by the formation of the IPNs
- PDMS continuity in the network will be maintained, allowing for sufficient oxygen permeation in the networks.

The synthesis of semi-IPNs and IPNs of PDMS/PNIPAAM using different

types of PDMS and procedures are described in this work. Studies of polymerization kinetics, bulk and surface characterization and glucose permeation are described. Specific objectives include:

- Combination of hydrophilic PNIPAAM with different type of PDMS in different procedures using an IPN method to form a continuous hydrogel phase for glucose permeation. Network formation is confirmed by chemical and physical methods.
- Characterization of the bulk morphology of the membranes.
- Measurement of the surface properties of the membranes using various techniques.
- Measurement of glucose permeation in the various network polymers synthesized.
- Examination of the thermal sensitivity of these network materials.

3. EXPERIMENTAL

3.1 Interpenetrating Network (IPN) and Semi-IPN Preparation

3.1.1 IPN Preparation and Purification

PDMS/PNIPAAM semi-interpenetrating networks and sequential interpenetrating networks were prepared and tested as potential new biomaterials with glucose permeability for ophthalmic applications. Sequential IPN preparation involves two steps: PDMS film preparation and IPN synthesis. All chemical reagents and solvents used in these experiments are shown in Appendix A.

3.1.1.1 PDMS Film Preparation and Purification

Both vinyl and hydroxyl terminated poly(dimethylsiloxane) elastomer kits were used for the preparation of the PDMS host polymers. Hydroxyl terminated PDMS films however have a less hydrophobic surface and can be more easily cured in the presence of solvent. PDMS prepolymers of lower viscosity (2000 - 5000 cst) were selected for this work as it resulted in a more transparent film. Furthermore, using this viscosity, it was possible to avoid the degassing step to remove air bubbles from the film.

The vinyl terminated PDMS prepolymer kit Sylgard 184 was used to prepare PDMS film according to the manufacturer. The propolymer and curing agent kit were mixed in 10:1 ratio by weight and poured into a polystyrene petri dish. The films were cured at room temperature for 24 hrs, at 65°C for 4hrs or at 100°C for 1 hour. Film thickness was controlled by manipulating the volume of the prepolymer / curing agent mixture and surface area of the petri dish. The resultant films were soft and transparent.

Unreacted prepolymer and crosslinker were extracted in tetrahydrofruan (THF) for 24 hours by Soxhlet extraction or rinsed in THF for 48 hours with changing fresh solvent every 10 hours and the films were dried completely overnight followed by 2-4 hours under vacuum.

Hydroxyl terminated PDMS films were prepared in a similar manner. However, in order to prepare looser PDMS networks for the introduction of more PNIPAAM, hydroxyl terminated PDMS was also cured in the presence of solvent. This procedure can decrease the physical crosslinking caused by PDMS prepolymer chain entanglement, increasing the molecular weight between crosslinks. This more open host polymer network allows for both the incorporation of more PNIPAAM in the network as well as greater connectivity of the PNIPAAM phase which will result in higher permeability of low molecular weight nutrients and a higher molecular weight cutoff for these compounds.

Hydroxyl terminated PDMS films were also prepared from a kit containing the PDMS prepolymer (2000cst), a crosslinker (tetraethyl orthosilicate, TEOS) and catalyst (Tin(II)-2-ethylhexanote) mixed in a 100:10:3 (wt/wt/wt) ratio. All components of the whole kit were dissolved in toluene at weight fractions varying from 0% solvent to 87% solvent and then slowly pipetted onto water in a vial. The vial was sealed to prevent solvent evaporation. The solvent allowed for the formation of a more open host polymer network while it is believed that the water increased the surface hydrophilicity of the resultant PDMS film. Film curing was complete after approximately three days at room

temperature and the films were purified in the same manner as the PDMS vinyl films. The film preparation procedure is depicted in Figure 3.1.

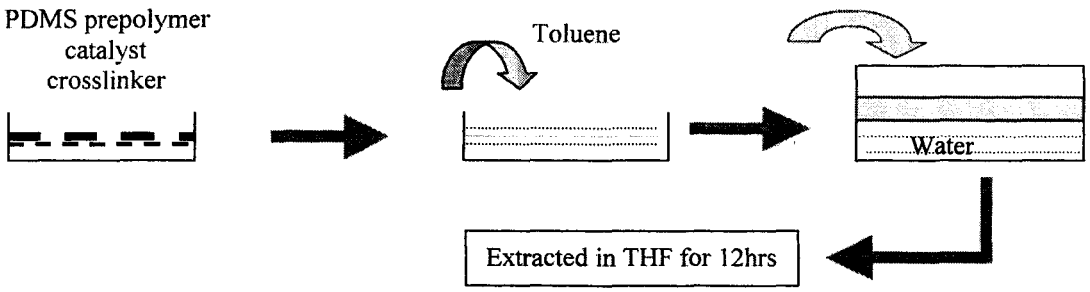

Fig. 3.1: Procedure for the formation of hydroxyl terminated PDMS films cast on water and cured with solvent

3.1.1.2 PDMS/PNIPAAM IPN Synthesis

NIPAAm monomer was purified by recrystalization in hexane. 20 g of NIPAAM monomer, as purchased (97%), with inhibitor and other impurity was dissloved in 20 ml of toluene. The mixture was heated slightly until all of the NIPAAM monomer had dissolved. To this, 10 ml hexane was added to recrystalize NIPAAM. The NIPAAM / toluene / hexane was placed on ice bath until the monomer was fully recrystallized (approximately 4 hours). The crystal was filtered and rinsed with excessive hexane until a yellowish substance was washed out. The purified NIPAAm crystal was transferred to a covered container and purged with nitrogen for a period of 8 hours prior to storage. The crosslinkers (EGDMA) and bisacrylamide (BisAAm) as well as the photo initiator xanthone were used as purchased.

The concentration of monomer, crosslinker and initiator are defined based on the following equations:

$$\text{Monomer of concentration} = \frac{\text{weight of NIPAAm monomer}}{\text{weight of monomer solution}} \times 100\% \qquad (3\text{-}1)$$

$$\text{Initiator weight fraction} = \frac{\text{weight of initiator}}{\text{weight of monomer}} \times 100\% \qquad (3\text{-}2)$$

$$\text{Crosslinker mole fraction} = \frac{\text{moles of crosslinker}}{\text{moles of monomer}} \times 100\% \qquad (3\text{-}3)$$

The concentration of monomer was changed from 10% to 60%. Different NIPAAM concentrations were used to synthesize the IPN film with varying PNIPAAM content. Initiator weight fractions were ranged from 1.0% to 2.5% and crosslinker mole fractions were changed from 0% to 3.0% respectively based on NIPAAM for polymerization kinetics study.

UV initiated free radical polymerization of NIPAAm was performed for preparation of PDMS/PNIPAAM IPN film. NIPAAm monomer, crosslinker and initiator were dissolved in tetrahydrofruan (THF) to prepare reaction solution. The PDMS film was immersed in the NIPAAm reaction solution and the system was purged with nitrogen for 30 minutes to remove oxygen from the reaction system. Swelling of the PDMS film in the NIPAAm mixture was continued for 4 to 9 hours to investigate the effect of soaking on varying PNIPAAM content. An 8W UV lamp emitting 312 or 365 nm UV light was mounted in front of the vial containing NIPAAm reaction solution and PDMS film. The distance from the lamp to the vial ranged from one to four cm. After 12 hours of initiation and reaction, the IPN film was seperated from the bulk PNIPAAM. The resultant IPN

film was purified by extraction with in THF for 48 hours with a four changes of solvent to remove unreacted monomer. The IPN synthesis procedure is described in Figure 3.2.

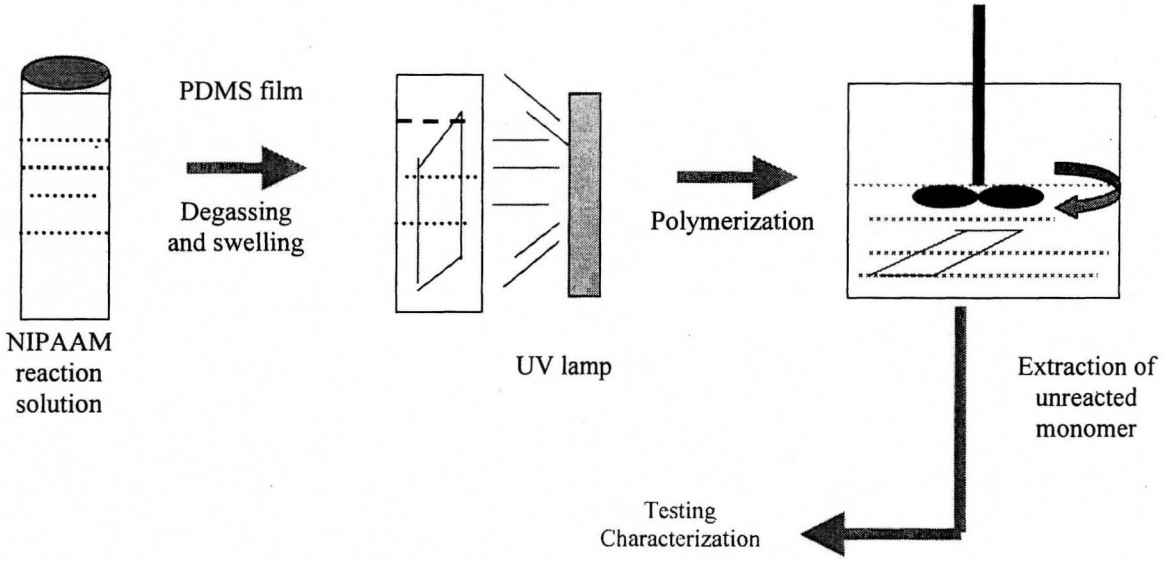

Fig. 3.2: Flowing chart showing the synthesis procedure for sequential PDMS/PNIPAAM IPNs

In addition to varying the swelling time, different concentrations of monomer were used to control the amount PNIPAAM in networks formed. The films were dried and weighed to determine the approximate PNIPAAM content in the IPN. Depending on the concentration of monomer and PDMS film used in IPN preparation, the weight increase after IPN formation, defined as:

$$\text{PNIPAAm wt\%} = \frac{\text{weight of the IPN film - weight of the PDMS film}}{\text{weight of the PDMS film}} \times 100\% \quad (3\text{-}4)$$

was between 0 and 50%.

3.1.2 Semi-IPN Synthesis

Linear PNIPAAM polymers and vinyl terminated PDMS elastomers were selected to synthesize semi-IPNs. PNIPAAM was dissolved in THF at a concentration of 0.45% to 4.5% (weight percentage) and 4 mL of this solution was added to the PDMS curing kit. Solvent evaporation and PDMS curing occurred simultaneously. After 48 hours at room temperature, a translucent semi-IPN film had formed. This film was rinsed in THF extensively and was dried in fumehood and under vacuum.

3.2 Bulk Characterization

3.2.1 Fourier Transform Infrared Spectroscopy (FTIR)

Fourier-transfer Infrared Spectroscopy (FTIR) was used to confirm the presence of the PNIPAAM in the IPN. Since the films were insoluble in organic solvents and as prepared, were too thick to obtain a clear FTIR signal, the networks were frozen in liquid nitrogen and ground into a powder. The IPN power was subsequently mixed with KBr as 1:4 (weight) and was molded into a thin piece using a compression die for testing. Samples were examined by FTIR at room temperature.

3.2.2 Differential Scanning Calorimeter (DSC)

TA 2910 MDSC Differential Scanning Calorimeter was used for the measurement of thermal properties of the networks formed. The presence of the glass transition temperature (Tg) of PNIPAAM provided further confirmation of the existence of the polymer in the network. In addition, the existence of the LCST endothermal peaks in the

PDMS/PNIPAAM IPN was detected by DSC. For Tg determination, the temperature was increased from –20°C to 250°C at a rate of 15°C/min. All the samples were initially subjected to a -20°C to 250°C increase. Tg measurements were then made by decreasing the temperature. In this way it was ensured that all samples had the same thermal history. For LCST measurements, the scanning temperature range was 0°C to 60°C with a heating rate of 1°C /min. Samples were fully swollen in distilled water at 5°C for 12 hours prior to testing. The reference cell and sample cells were filled with 15 μl of distilled water during measurement. All tests were performed in a nitrogen atomosphere with a 30 cc/min nitrogen purge.

3.2.3 Transmission Electron Microscopy (TEM) and Scanning Electron Microscopy (SEM) Measurements

SEM and TEM were used to investigate phase formation and domain size of the IPNs. Samples for SEM were frozen in liquid nitrogen and fractured in order to view the cross-section. The cross-sections were sputter coated with gold for 30 seconds prior to analysis.

For TEM analysis, 2 mm × 3 mm cross-sections of samples were embedded in Spurr's expoxy resin and resin was polymerized overnight at 60°C. 100 nm ultrathin sections were cut using a Reichert Ultracut E. Ultramicrotome and placed on 200 mesh fornvar carbon coated nichel grids. Sections were viewed and photographed using JEOL 1200EX electron microscope with 80kv electron beam.

3.2.4 Tensile Strength Testing

The mechanical properties of the networks formed were measured at room temperature using Instron Series XI Automated Material Testing System with a 50 N load cell and a crosshead speed 50 mm/min. The samples were cut into 6 cm × 0.4 cm strips and tensile maximum stress and strain were examined in both the dry and water swollen states. The dry samples were placed in a drying oven at 60°C for 12 hours prior to testing. Water swollen samples were swollen in distilled deionized water for 24 hours at room temperature prior to testing. To protect the samples from damage due to clamping, the tops of the strips were wrapped with paper tape. Tensile stress and strain at the break point are defined by Equation (3-5) and (3-6).

$$\text{Tensile Stress}(MPa) = \frac{\text{Force at break point (N)}}{\text{Cross - sectional area (mm}^2\text{)}} \tag{3-5}$$

$$\text{Tensile Strain (\%)} = \frac{\text{Sample length at break (cm)}}{\text{Initial sample length (cm)}} \times 100\% \tag{3-6}$$

3.3 Surface Characterization

Various surface analysis methods including water contact angles, Attenuated Total Reflection FTIR (ATR-FTIR), X-Ray Photoelectron Spectroscopy and Atomic Force Microscopy were used to characterize the chemical and morphological characteristics of the network polymers synthesized.

3.3.1 Water Contact Angle Measurements

Sessile drop advancing and receding water contact angles were measured to evaluate the relative hydrophilicity and hydrophobicity of various network surfaces prepared including the PDMS control. Samples were fixed on glass slides using double sided tape. Milli Q water with drop volume of approximate 20 μL was used for contact angle measurement. Contact angles of both the air and water sides of film were measured to determine whether there were differences in the surface hydrophilicity.

3.3.2 X-Ray Photoelectron Spectroscopy (XPS)

XPS was used to determine quantitative elemental information about the surfaces. Testing was performed at Surface Interface Ontario at the University of Toronto using a Leybold Max200 X-Ray Photo Electron Spectrometer. Prior to XPS analysis, samples were extensively rinsed in THF for 24 hours and dried under vacuum for 2 hours. Low and high resolusion XPS measurements were made at takeoff angles of 90^{o} and 20^{o} to obtain compositional profile at different depths. The air and water sides of the samples

were examined. Data analysis was performed using SPECS software. Peaks were referenced to C-C at 285.0 eV.

3.3.3 Atomic Force Microscopy (AFM)

Surface roughness and topographical information were obtained using Atomic Force Microscopy (AFM) at the Brockhouse Institute for Material Research at McMaster University. The data and images were processed using Digital Instrument Nanoscope 3 in tapping mode. PDMS vinyl and hydroxyl terminated PDMS/PNIPAAM IPN surfaces and PDMS controls in the dry state were examined. Attempts were also made to obtain images of the samples in the wet state, but the water swollen nature of the samples made it difficult to obtain high quality images. Phase measurements also were made in order to detect the phase seperation between the PNIPAAM and PDMS phases on the sample surface. A scan size of 10μm × 10μm was used for height images and 1μm × 1μm for phase images.

3.3.4 Attenuated Total Reflectance- Fourier Transform Infrared Spectroscopy

Attenuated Total Reflectance Fourier Transform Infrared Spectroscopy (ATR-FTIR) is used to obtain chemical information from a broad region near the surface at a penetration depth of between 1 and 5 μm. An infrared spectrum provides vibration information for atomic and molecular units. Information related to the chemical elements and groups in NIPAAm confirms the existence of the PNIPAAM at or near the surface.

3.4 Equilibrium Water Content (EWC) Measurement

The water content of the IPNs synthesized was measured to characterize changes in the hydrophilicity of IPN film. The dry IPN film was weighed and immersed in deionized water and shaken slightly for a period of 24 hours to achieve an equilibrium swollen state. Following removal from the water, the film was wicked with filter paper to remove free water on the surface of the sample. Based on the difference between the swollen weight and the dry weight, the water uptake could be determined as:

$$\text{Water Uptake}(\%) = \frac{m_s - m_d}{m_d} \times 100\% \qquad (3\text{-}7)$$

where m_s is the mass of the swollen sample (g) and m_d is the mass of the dry sample. Equilibrium water content measurements were made at temperatures ranging from 5 to 40°C to examine the effect of the LCST phenomenon.

3.5 Glucose Permeation

3.5.1 Permeability Coefficient and Permeation Device

The glucose permeability of the membranes was measured using a standard two chamber diffusion device as shown in Figure 3.3. Films were punched into 2.5 cm or 1.5 cm diameter disks and swollen in water for 12 hours prior to mounting in the permeation apparatus. The receptor and donor cells were connected with the membrane and the system was tested for approximately 12 hours to ensure that leakage did not occur. For the permeation experiment, the donor chamber was filled with a 0.1g/ml solution of glucose in deionized water solution and the receptor cell was filled with an equal volume

of water. The receptor chamber was sampled by periodic removal of a known volume of the permeant and replacement of the solution with fresh water. Permeation measurements were carried out at room temperature and at increased temperatures of between 24°C and 37°C to determine the effect of the LCST on the glucose permeability.

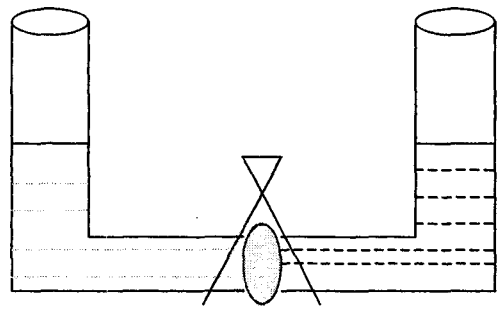

Fig. 3-3: The diagram of permeation device

The glucose concentration of the sample solution was analyzed using the glucose assay kit GAHK20 (see Appendix B) and the accumulated concentration was corrected for permeability calculation. From the slope of a plot of $\ln(1-2C_t/C_0)$ versus permeation time, where C_t is the concentration of glucose in the receptor at time t and C_0 is the initial concentration of glucose on the donor side, the permeability of the membrane can be determined from Equation (3-8). Full details of the derivation can be found in Appendix C. Appendix D shows an example of glucose permeability coefficient calculation.

$$P = \frac{k \cdot V \cdot D}{2A} \qquad (3\text{-}8)$$

where:

P: permeability coefficient of material membrane (cm^2/s)

D: the thickness of dry membrane (cm)

V: volume of solution in each side (ml)

k: the slope of the plot

A: membrane area (cm^2)

4. VINYLTERMINATED PDMS/ PNIPAAM SEMI-IPNs AND IPNs

4.1 PDMS / PNIPAAM Semi-IPNs

4.1.1 Preparation of PDMS-V / PNIPAAM Semi-IPNs

PDMS/PNIPAAM semi-IPNs were prepared by curing vinyl-terminated PDMS (PDMS-V) in solution with linear PNIPAAM. PDMS and PNIPAAM are two inherently immmiscible polymers; PNIPAAM is rigid and hydrophilic while PDMS-V is flexible and hydrophobic. Therefore, the preparation of a PDMS-V /PNIPAAM semi-IPN requires a mutual solvent that allows for the polymers to be combined into a homogeneous solution with an appreciable concentration (Ree et al., 1998). Based on solubility data (Grulke, 1999) and solubility testing, THF was found to be the best solvent. The PNIPAAM content of these gels was determined to be between 0.45% and 4.5% based on the weight of PDMS prepolymer. In all cases the concentration of the PNIPAAM was 20% by weight in THF. The resultant films were generally translucent. Transparent films could be obtained by curing at a higher temperature with sealing to decrease the evaporation of solvent and with a lower PNIPAAM content. In this case, the presence of the solvent facilitates the penetration of the PNIPAAM polymer chains into the PDMS matrix. The curing process, more rapid as a result of the elevated temperature, was complete prior to the quenching of phase separation by the solvent.

4.1.2 Equilibrium Water Content

Figure 4.1 shows the equilibrium water content as a function of PNIPAAM content of the semi-IPNs. There was no clear trend in the water uptake as the PNIPAAM content of the semi-IPN was varied up to 5%. In all cases, the data fall between 0.5% and 1.0% water in the polymers at equilibrium. This result suggests that in the semi-IPNs, the PNIPAAM did not form a connective phase, providing continuous channels for water diffusion. Instead, the relatively low and highly variable water uptake in these polymers resulted from the absorption of water by PNIPAAM domains close to the surface.

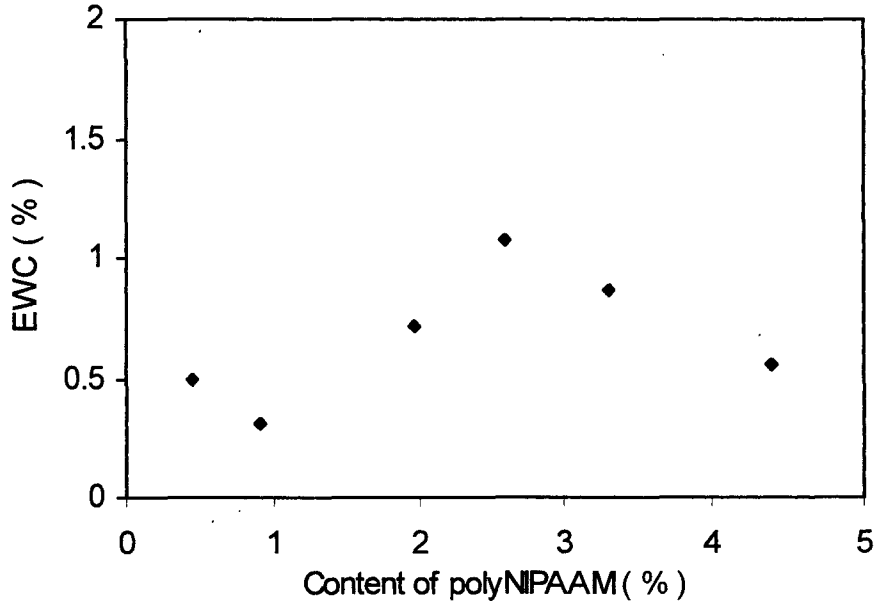

Fig. 4.1: Equilibrium water content of PDMS-V/PNIPAAM semi-IPNs. Samples were swollen in water for 24 hours to achieve equibrium state before the test. The plot showed low water uptake of semi-IPNs.

4.1.3 Mechanical Properties

The change in the mechanical properties of the PDMS-V / PNIPAAM semi-IPN's was investigated through tensile strength testing. Figure 4.2 demonstrates the significant tensile stress decrease of semi-IPN relative to the PDMS-V control. While the control had a stress at maximum load equal to 6.6 MPa, the semi-IPN samples had stresses of less than 3.5 MPa in all cases. A trend was noted in the data, with an increase in the tensile stress of the semi-IPN samples with increasing PNIPAAM content up to approximately 2%. Above 2% PNIPAAM, a sharp decrease in the tensile stress was noted. Due to the relatively small number of samples examined, it is unclear whether this trend is simply an artifact. However, it is reasonable to postulate that the decrease in the tensile stress with increasing PNIPAAM content in the IPNs may be due to the incompatibility of the two polymers. While a homogeneous solution of the polymers in THF was initially present, PDMS crosslinking and the evaporation of the solvent may have resulted in phase separation during semi-IPN formation, thereby affecting the mechanical integrity of the polymer network. As the PNIPAAM content of the semi-IPN is increased, the phase separation becomes more significant. In fact, PNIPAAM particles can be observed visually at PNIPAAM contents of greater than 5% in the semi-IPN system.

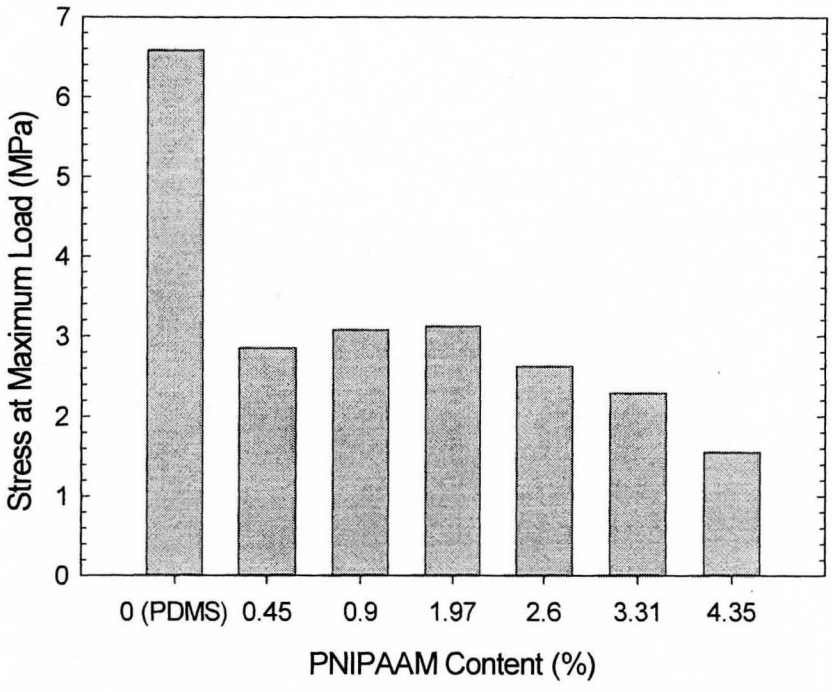

Fig. 4.2: Tensile stress at maximum load of PDMS-V/PNIPAAM semi-IPNs. Samples were dried in oven at 60°C for 12 hours prior to testing. Crosshead speed used for tensile test was 50 mm/min. Note the decrease of stress after PDMS incorporated with PNIPAAM by semi-IPN method.

4.1.4 Contact Angles

Depending on the PNIPAAM content, the contact angles of the semi-IPNs ranged from 90° to 95°, a very slight decrease relative to the PDMS-V control at 103°. Therefore, the wettibility improvement of these polymers was very limited.

4.1.5 Conclusions: PDMS-V / PNIPAAM Semi-IPN's

Clearly, from these results, reasonable glucose permeability of these polymers was not achievable. Membranes with PNIPAAM contents greater than 5% were not

obtained. The polymers showed significant phase separation and showed very little water uptake and virtually no improvement in wettability.

4.2 PDMS-Vinyl/PNIPAAM IPNs

The sequential IPN method was used to generate interpenetrating networks consisting of a vinyl terminated PDMS host and a PNIPAAM guest polymer. The PNIPAAM content of the IPNs was varied by varying the time that the PDMS host polymers were swelled in the NIPAAM reaction solution and by varying the NIPAAM reaction solution concentration. It was expected that this method would result in polymer networks with high levels of interpenetration and interlock resulting in a more continuous PNIPAAM phase that would permit the diffusion of water and low molecular weight permeants such as glucose through the polymer membranes.

4.2.1 Chemical Characterization of PDMS-vinyl/PNIPAAM IPN

4.2.1.1 FT-IR Determination NIPAAM in Composite

FT-IR spectra of pure PDMS and pure PNIPAAM are shown in Figures 4.3 and 4.4. The typical peaks corresponding to PDMS include a broad peak at 1110-1000 cm^{-1} resulting from the Si-O-Si bonds, the antisymmetric deformation vibration of CH_3 at 1450 cm^{-1} as well as antisymmetric stretching vibration of CH_3 at 2970 cm^{-1}. The spectra for the PNIPAAM also include peaks associated with the CH_3 group as well as an N-H stretching vibration at 3310 cm^{-1} and a broad range peak at 3200-3600 cm^{-1}. Typical amide bonds also can be found consisting C=O stretching vibration near 1640 cm^{-1} and

N-H vibration near 1546 cm^{-1}. The double bond near 1370 cm^{-1} belongs to the C-N and N-H in PNIPAAM. The group of peaks between 1370 and 1650 cm^{-1} form the fingerprint for a chemical substance containing acryl amide. Figure 4.5 shows spectra of PDMS-V/PNIPAAM IPNs containing 44.6 and 21.7% PNIPAAM. Both FT-IR spectra are similar, showing identical peaks to PNIPAAM. However, the spectrum of the 44.6% IPN shows stronger peaks in the fingerprint area as expected accompanying the higher amount of PNIPAAM in the IPN sample determined by weight measurements, confirming these results.

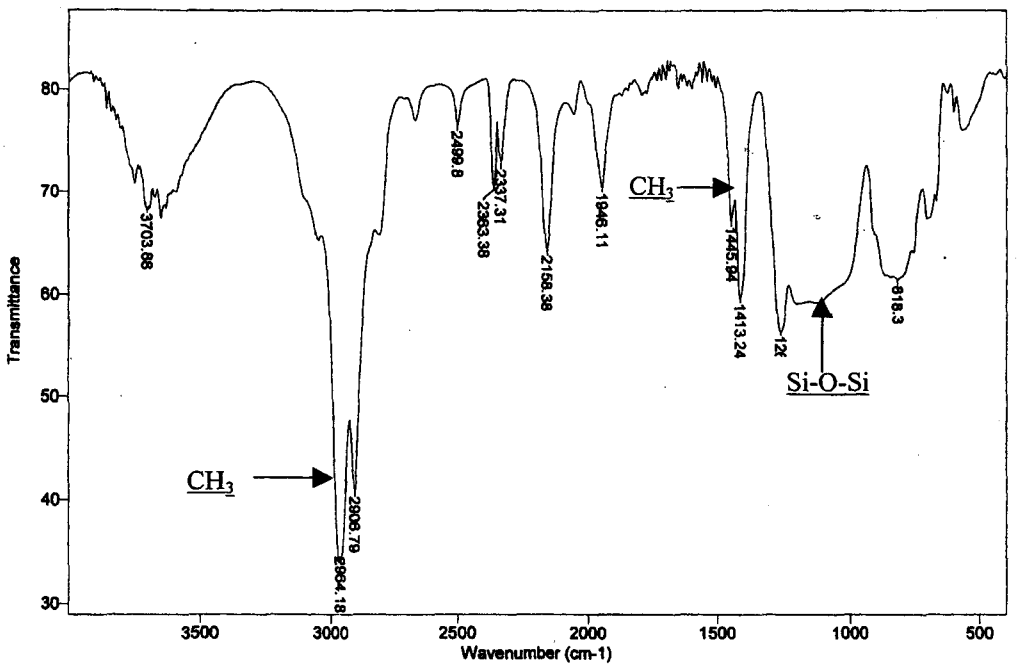

Fig. 4.3: FT-IR spectrum of pure PDMS

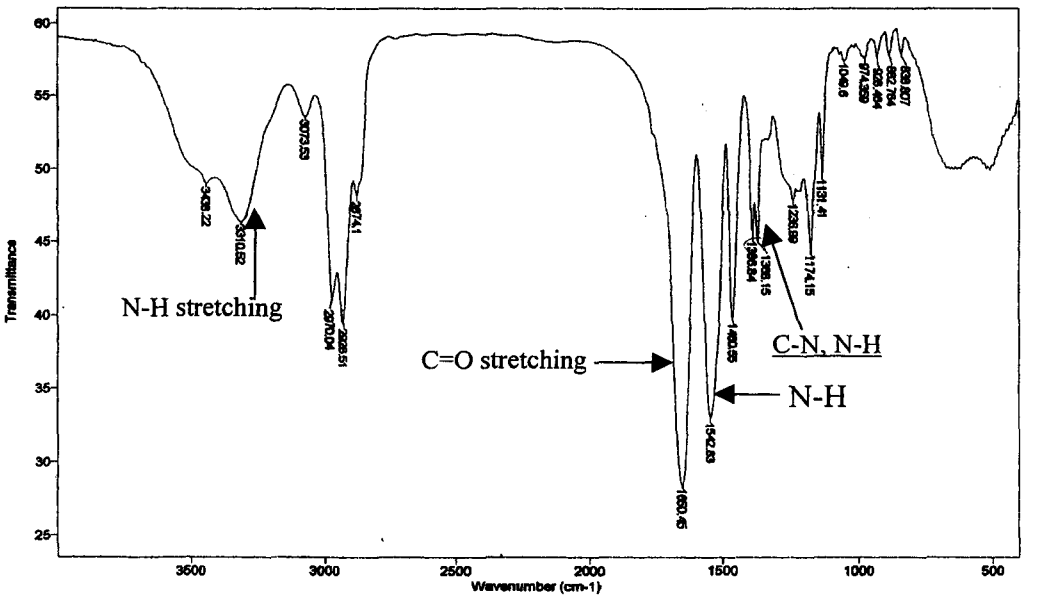

Fig. 4.4: FT-IR Spectrum of pure PNIPAAM

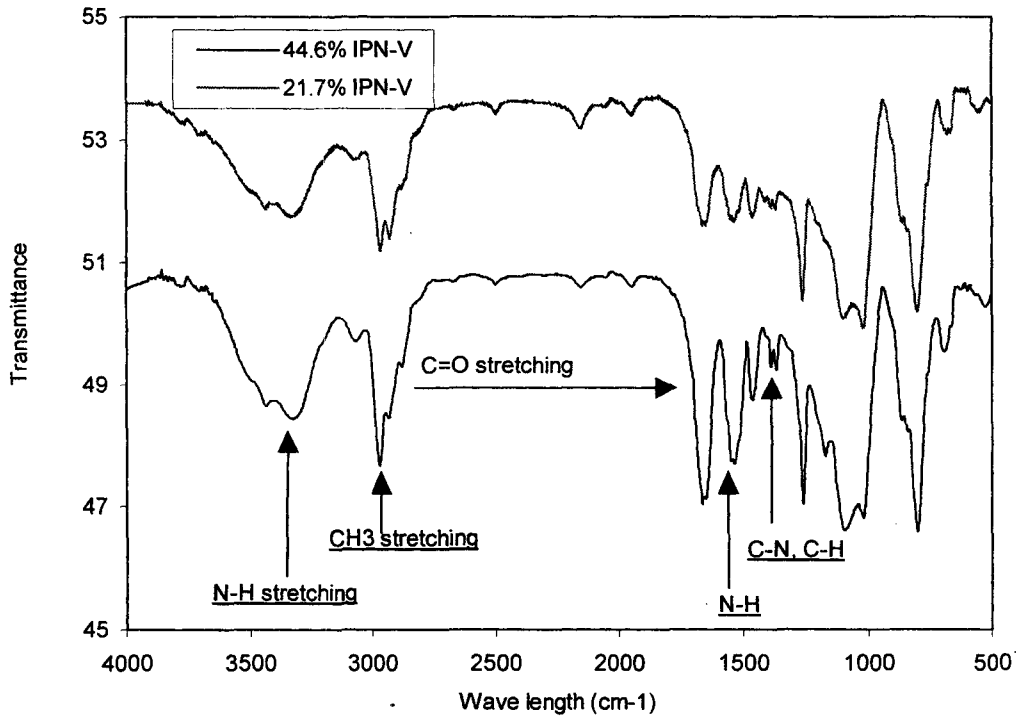

Fig. 4.5: FT-IR Spectrum of PDMS-V IPNs. Typical PDMS peaks 1110~1000cm^{-1} were covered by peaks of PNIPAAM. Compared with the spectrum for PDMS, new peaks associated with PNIPAAM at 3310, 1370 and 1640 showed up and are correspond with the amount of PNIPAAM in the networks.

4.2.1.2 DSC Analysis of IPNs

The glass transition, Tg, was determined by differential scanning calorimetry (DSC) and can be used as further confirmation of the presence of the PNIPAAM in the network polymer samples. Figure 4.6 shows the DSC curves for the various PDMS-V/PNIPAAM IPNs as well as for pure PDMS at temperatures between 75 and 225°C. Within this range, curves of pure PDMS do not show an enthalpic transition as expected. The glass transition temperature of pure PDMS has been reported to be –114 °C (Miyata et al., 1996). However, all of the IPN samples with PNIPAAM contents ranging between 20 and 50% weight showed clear Tgs at approximately 140°C. This corresponds well to the reported Tg for PNIPAAM and demonstrates that the network polymers contain increasing amounts of PNIPAAM. Linear PNIPAAM has been reported to have a Tg between 85 and 130°C depending on the molecular weight (Otake et al., 1990). A Tg of 135°C has been reported for crosslinked PNIPAAM (Ricardo et al., 1998). The slightly higher Tgs found in the current study are likely the result of either a higher crosslinking density in the PNIPAAM in this study or the lower mobility of the guest polymer because of the constraints on the chains in the interlocked networks. Regardless, the Tg shift induced by the effect of PDMS networks was not significant. Frisch et al. (1982) reported that the Tgs of PS/PA IPNs shifted by 5 to 10°C because of interpenetration and mixing at the phase boundary. This obvious shifted in the Tg was not noted with the PDMS/PNIPAAM IPNs in the current study, likely because the two polymers in the IPN performed more independently because they are less compatible.

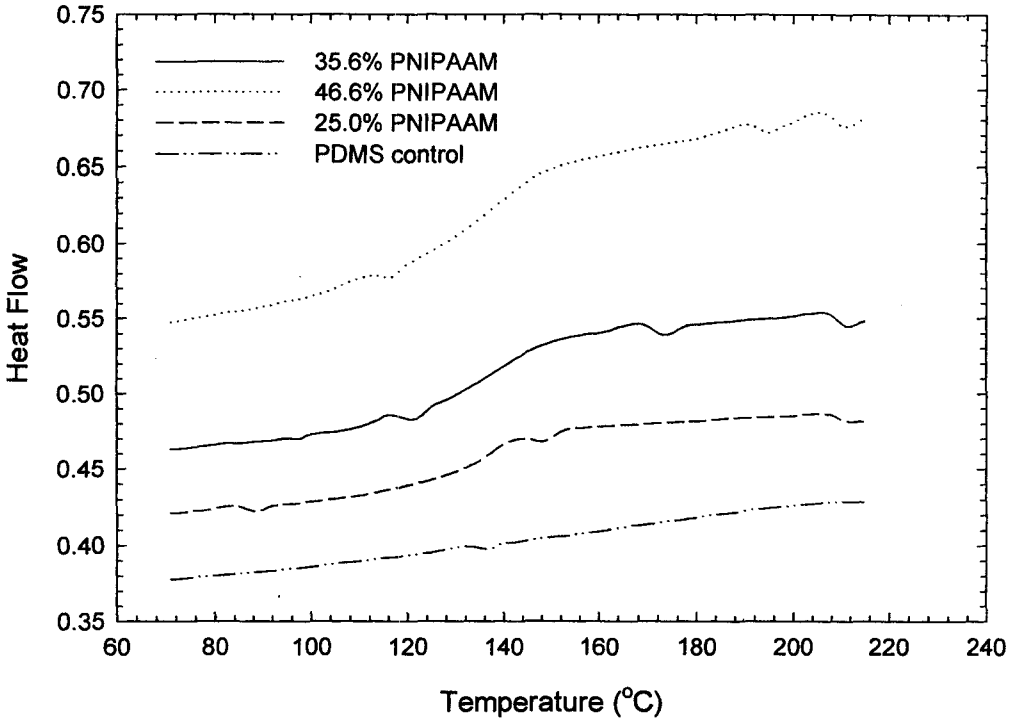

Fig. 4.6: DSC curves for PDMS-vinyl/PNIPAAM IPNs, showing the Tg of the PNIPAAM in the network. The presence of the Tg for PNIPAAM in the IPNs provides evidence for the existence of PNIPAAM in PDMS matrix. The Tg shift from reported literature values was not significant. Enthalpic transitions correspond to the amount of PNIPAAM in the IPNs.

4.2.2 Effect of Polymerization Conditions on PNIPAAM Content of IPNs

Glucose permeability and equilibrium water content the PDMS/PNIPAAM network polymers were expected to be highly dependent on PNIPAAM content, as well as the domain size and phase continuity of PNIPAAM, with the PNIPAAM content being the dominant factor. In order to optimize the PNIPAAM content in the IPN, several polymerization parameters including crosslinkers, initiators, and reaction conditions were examined.

4.2.2.1 Effect of NIPAAM Concentration

The IPNs were formed by immersion of the purified PDMS films in a solution of NIPAAM, initiator and crosslinker and the reaction was initiated by UV radiation. As shown in Figure 4.7, the PNIPAAM content of the resultant IPN was strongly dependent on the concentration of NIPAAM in the guest solution, with higher NIPAAM solution concentrations resulting in films with higher PNIPAAM contents. The solubility of the NIPAAM monomer in THF limited this concentration to approximately 40% (wt), which resulted in an PDMS-V IPN containing ~20% PNIPAAM in the cases which PDMS was swollen in the NIPAAM solution for a period of four hours and the NIPAAM was polymerized 4 cm from the UV lamp. Based on these results, the concentration of NIPAAM monomer was used to control the PNIPAAM content of the IPNs.

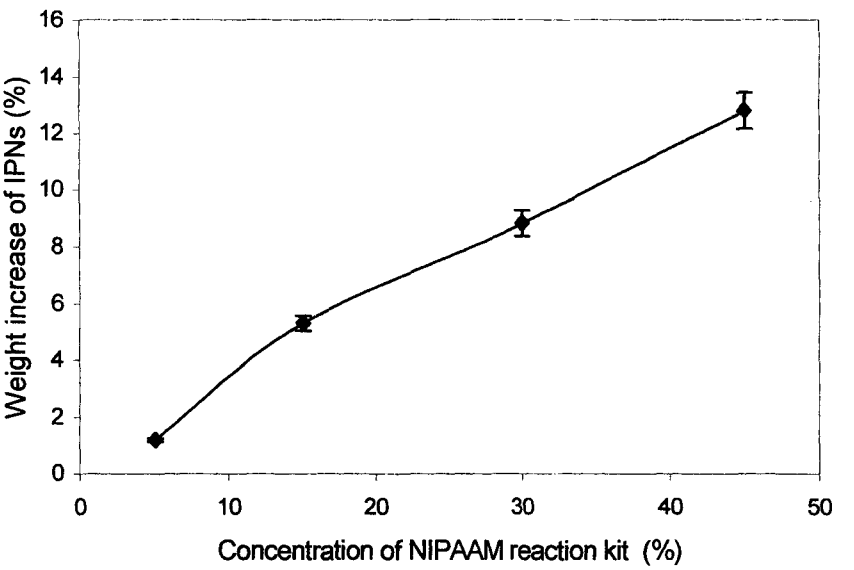

Figure 4.7: The concentration effect of reaction on PNIPAAM% of IPNs.
(Swelling time: 4 hours; Distance to 365nm UV lamp: 4 cm; Crosslinker: BisAAm)

4.2.2.2 Crosslinker Effect on PNIPAAM Content of IPNs

Bisacrylamide (BisAAM) and ethylene glycol dimethacrylate (EGDMA) were selected as the crosslinkers for the PNIPAAM in this work. The solubility of BisAAM in THF limited the NIPAAM reaction solution concentration based on a 2% (mol) crosslinker ratio of monomer. In order to achieve higher NIPAAM concentrations and subsequently higher PNIPAAM content in the IPNs, EGDMA was chosen as crosslinker for this system. As can be seen in Figure 4.8, higher monomer concentrations (60%) based on 2.0% mol of crosslinker EGDMA could be achieved. However, within a reasonable range of concentrations, the effect of the crosslinker on the networks was relatively small in spite of the relatively high THF solution of EGDMA relative to BisAAM, likely due to the low polymerization reactivity ratio of EGDMA .

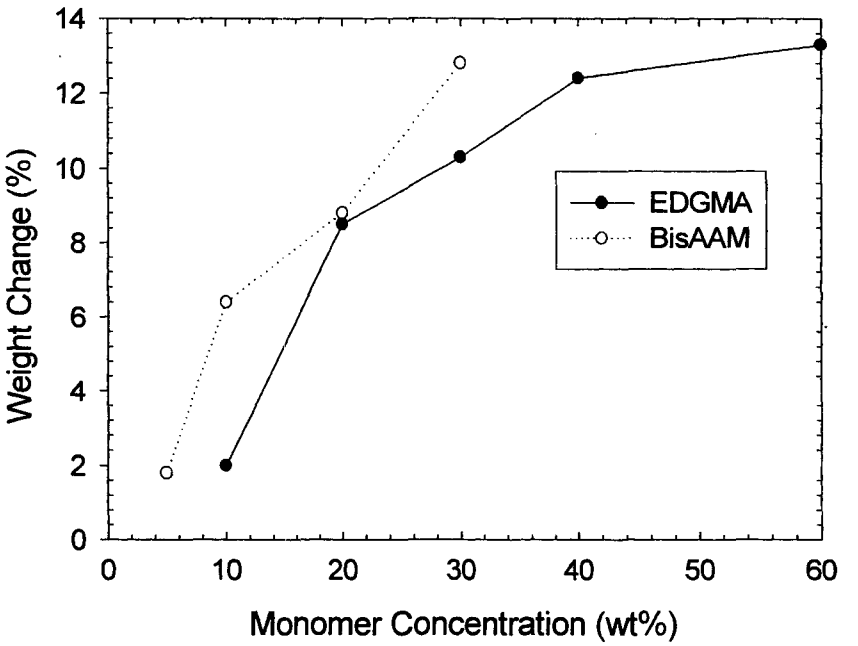

Fig. 4.8: Comparison of the effect of different crosslinker on the amount of PNIPAAM incorporated into the network polymers. In all cases, the crosslinker concentrations were 2.0% (mol, based on monomer). The reactions were performed after 4 hours of swelling in the reaction solution at a distance of 4 cm from the UV lamp 4 cm.

Higher concentrations of crosslinker were found to result in IPNs with higher PNIPAAM contents as shown in Figure 4.9 for BisAAM. Clearly, if the amount and type of crosslinker used was not adequate, more linear polymer would be formed with less crosslinking and less incorporation into the PDMS host. As the BisAAM concentration was increased to 3%, an increase in the PNIPAAM content was noted. At concentrations above 3%, it is thought that the higher amount of crosslinker actually hindered the reaction and network formation, hence resulting a lower PNIPAAM content.

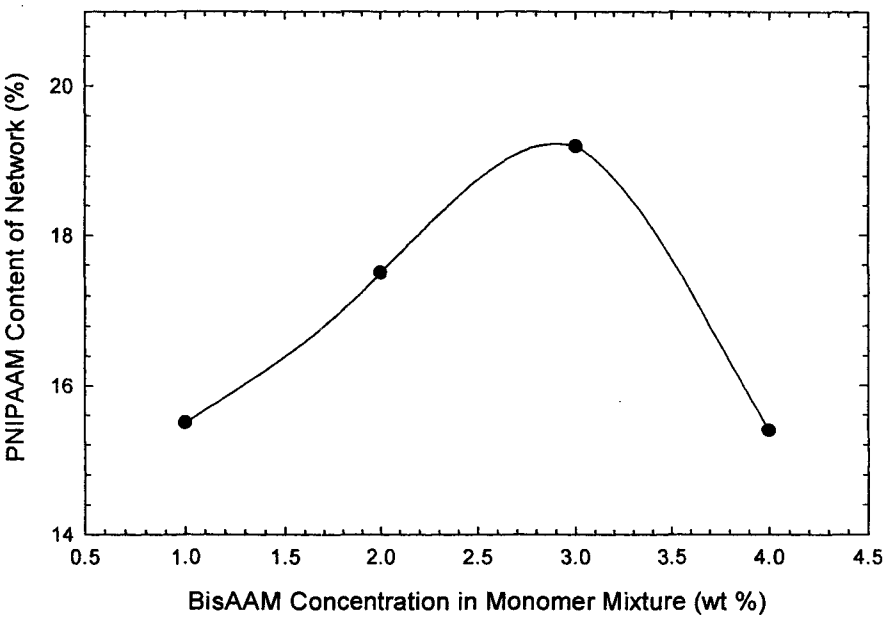

Fig. 4.9: Effect of crosslinker concentration on PNIPAAM content in IPNs (Monomer concentration: 30% wt; initiator: 2.0% wt of monomer; swelling time: 4 hours; Distance to 365nm UV lamp: 4 cm).

4.2.2.3 Initiator Concentration Effect on PNIPAAM Content

While AIBN and xanthone can be used as UV sensitive initiators for the NIPAAM, xanthone was selected in the current work because AIBN is also thermal initiator for free radical polymerization. Figure 4.10 shows that the initiator concentration had a small effect on PNIPAAM content of the IPNs. High initiator concentrations allowed for more NIPAAM polymerization and increased network formation. However, it is believed that initiator concentrations greater than 3 mole % resulted in the formation of short polymer chains that could be easily removed from the network films by solvent extraction.

4.2.2.4 Additional Factors Influencing IPN Formation

The thickness of PDMS film, the time the host polymers were soaked in the NIPAAM mixture and the distance from the reaction vessel to the UV lamp were found to dramatically influence the PNIPAAM content of the network polymers. Thickness of the membranes was difficult to control, but generally thinner (<0.6 mm) PDMS host polymer membranes were found to result in superior networks, likely due to diffusion limitations in the thicker polymers. In the current work, a 9 hour swelling time in the NIPAAM monomer mixture was used. The reaction vessel was placed 1.5 cm from the UV lamp for optimal network formation. Under these conditions, the highest PNIPAAM content of the network that could be achieved was approximately 50%.

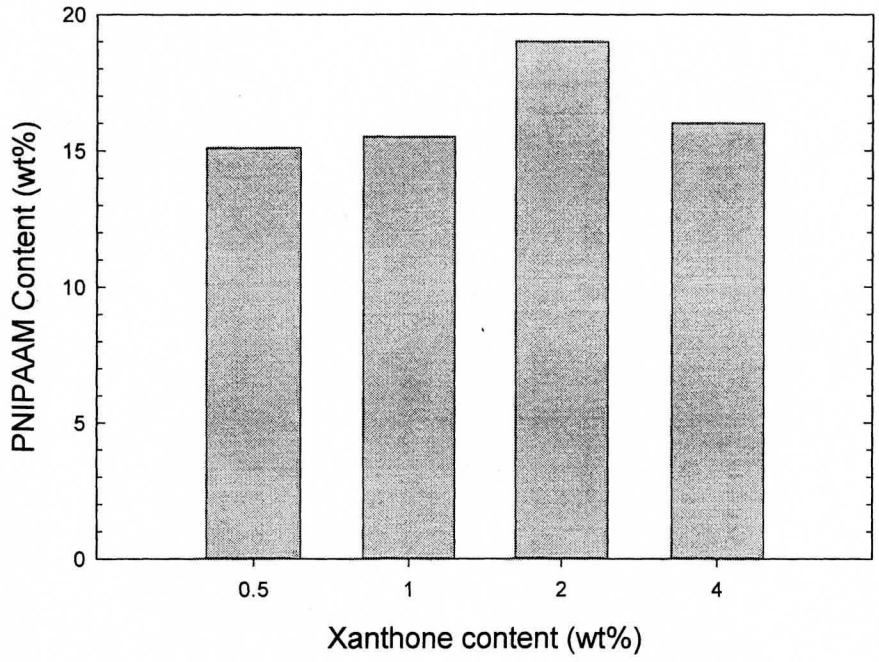

Fig. 4.10: Effect of initiator concentration on PNIPAAM content
(monomer concentration: 30% wt; crosslinker: 3% BisAAM / mol of monomer; Swelling time: 4 hours; Distance to 365 UV lamp:4 cm)

4.2.3 Bulk Characterization of PDMS-V/PNIPAAM IPNs

4.2.3.1 Transmission Electron Microscopy

Transmission Electron Microscopy has been suggested to be an important method for confirming IPN formation (Sperling, 1997). TEM can provide 10 nm to 1 μm resolution which covers the general IPN domain size. SEM resolution ranges in micrometer level which is not sufficient to provide phase information of IPNs. The TEM image of the PDMS-V control, shown in Figure 4.11, shows only one phase. In contrast, images of the IPNs with varying PNIPAAM contents, shown in Figure 4.12, clearly show two phases. The white area was identified as PDMS based on the image of pure PDMS

and the darker spots are thought to represent the PNIPAAM domains. Although some phase separation can be observed, the domain sizes are very small in these images. The width of PNIPAAM channels is only about 10 to 20 nm and the channels do not appear to be highly connective within the PDMS matrix. This may be due to the very dense network structure of pre-formed PDMS host film. All of the images showed cooperation of PNIPAAM through the PDMS matrix, but the interpenetration of two phases at the boundary was very limited. This result was in accord with the DSC result which showed that the Tgs of the network polymers had not shifted significantly relative to thehomopolymers.

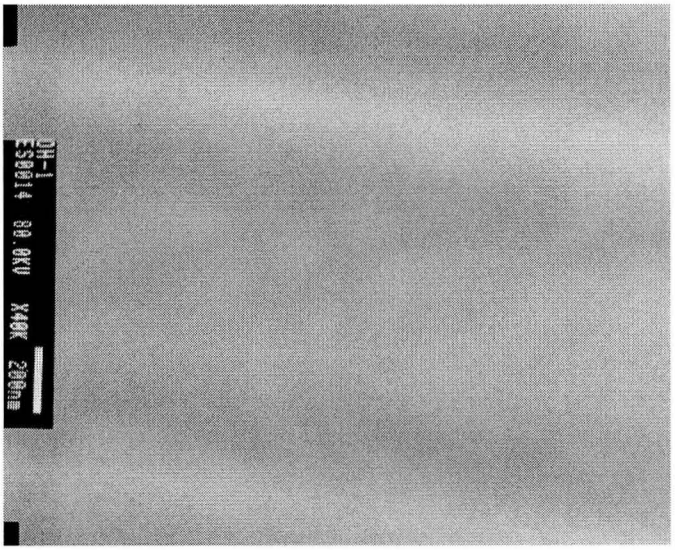

Figure 4.11: TEM image of the PDMS-V control sample. (40,000 x magnification; bar is 200 nm). As expected, only one phase which was PDMS was displayed and very few morphological features could be seen on this image.

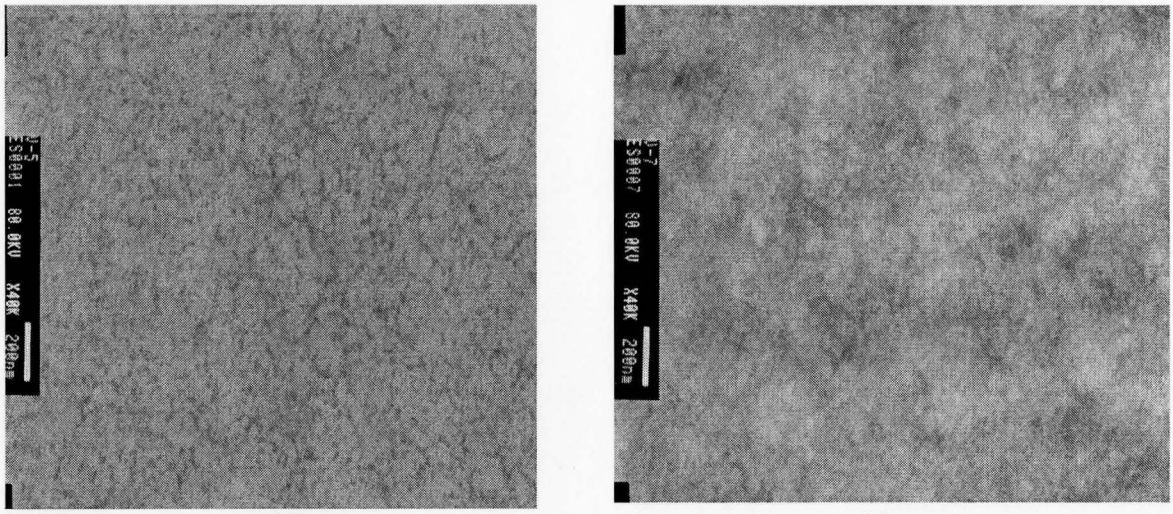

(a) (b)

Figure 4.12 TEM images of PDMS-V IPNs. (a) 41.0% PDMS-V IPN; (b) TEM image of 46.6% PDMS-V IPN. (40,000x magnification; bar is 200 nm). The white areas are thought to represent the PDMS host polymer while the darker areas are through to be the PNIPAAM guest. The PNIPAAM channel width ranged 10 nm to 20 nm in the PDMS-V IPNs. 46.6% IPN with higher content PNIPAAM showed smaller domain size and a little more connective phase than 41.0% PDMS-V IPN.

4.2.3.2 Mechanical Strength of PDMS-V IPNs

The tensile stress and strain were investigated for both dry and more biologically relevant water swollen PDMS-V/PNIPAAM IPN materials. Prior to testing, the wet samples were fully swollen in distilled water for a period of 12 hours. All of the vinyl terminated PDMS / PNIPAAM networks examined showed an increased stress at maximum load relative to the PDMS control in both dry and wet states as shown in Figure 4.13 (a) and (b). As noted in the TEM results, it is likely that the continuity of the PDMS ensured that the strength did not decrease greatly. The introduction of more

PNIPAAM into the network resulted in a higher tensile stress, likely due to the high rigidity of the PNIPAAM and its constraint by the PDMS. Although the tensile stress of wet samples was slightly lower than that of the dry samples, somewhat surprisingly a significant decrease in the mechanical strength did not occur, more likely due to the limited water swelling in PNIPAAM domains.

As shown in Figure 4.14 (a) and (b), the elongation was found to decrease for both the dry and wet samples compared with the PDMS control. In the swollen state, the elongation results were more affected by the water content and the PNIPAAM domains. Surprisingly, the strain of the IPN samples also showed an increasing trend following the introduction of more PNIPAAM into the PDMS matrix in the dry state, likely due to the increase in the strength of the IPNs. The strain at 14% PNIPAAM IPN was similar to that of the PDMS control. The strain, influenced by two properties, elasticity and strength, is more likely the result of the samples breaking due to inadequate strength rather than limitations in the elasticity.

For the wet samples, the trends were not as clear. The presence of more PNIPAAM in the samples results in materials with higher strength, but also decreases the elasticity of the materials. Increasing the amount of PNIPAAM however results in higher water swelling and therefore samples with decreased rigidity. These conflicting factors make prediction of the strain for the PDMS-V / PNIPAAM samples more complex.

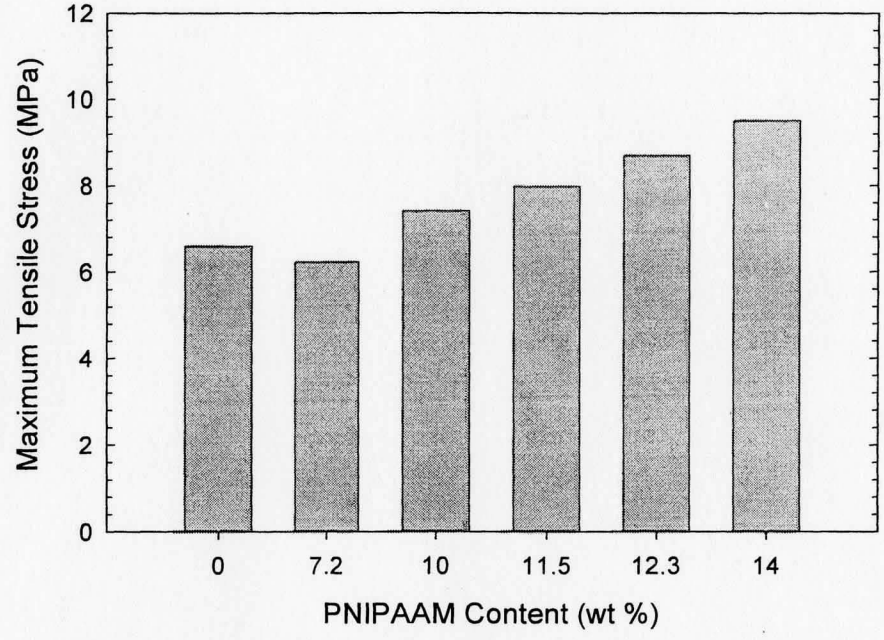

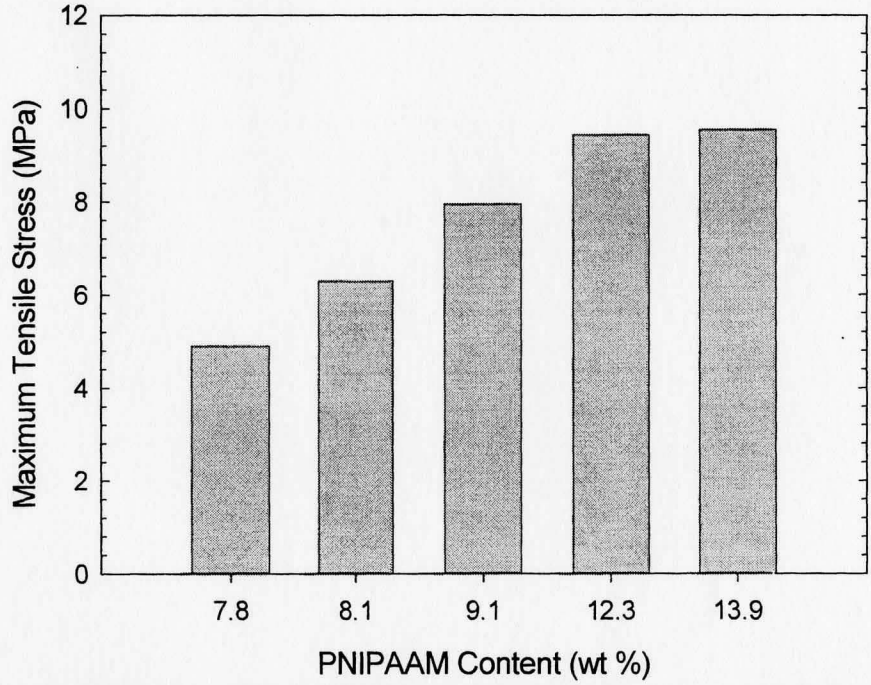

Fig. 4.13: Tensile stress of PDMS-V IPNs: (Top) Tensile stress of PDMS-V IPNs in dry state; (Bottom) Tensile stress of PDMS-V IPNs in wet state. While the PNIPAAM effect on tensile stress were not highly significant in general, the stresses of IPNs in both dry and water swollen state were higher than PDMS control.

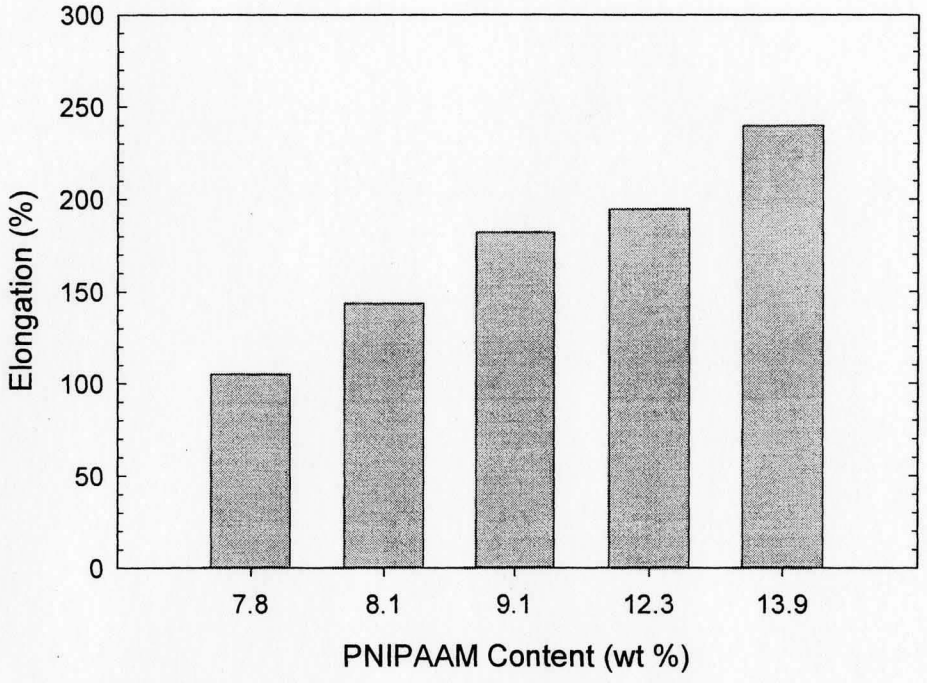

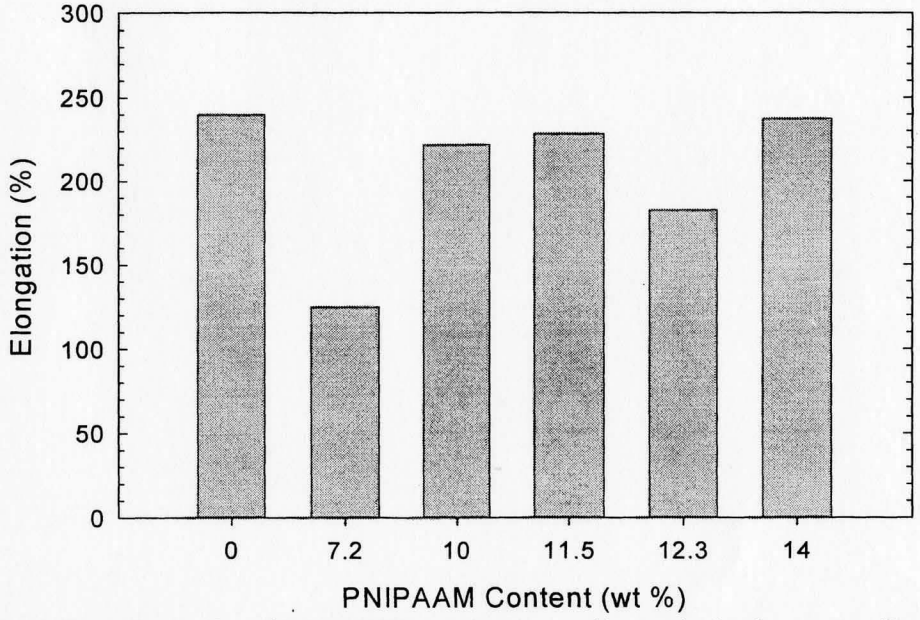

Fig. 4.14: Tensile strain of PDMS IPNs. (Top) tensile strain in dry state; (Bottom) tensile strain in water swollen state. Note a clear increase trend of IPNs with increase of PNIPAAM content in dry state IPNs; For water swollen state of PDMS-V IPNs, the trend was not clear.

4.2.3.3 Equilibrium Water Content of PDMS-V IPNs

To determine the time needed to achieve equilibrium water content, the water uptake as a function of time for the PDMS-V IPN samples was measured. Figure 4.15 shows that the IPN samples with lower PNIPAAM contents required longer to approach equilibrium. However, all of the IPNs reach equilibrium within 10-12 hours. As expected, the IPNs with more PNIPAAM absorb more water. Figure 4.16 illustrates the relationship between water uptake and PNIPAAM content in the IPNs. The highest water uptake that could be achieved by the PDMS-V IPNs was 17.3%. This amount of water was not sufficient to form permeation channels for glucose (Mirejovsky et al., 1993). However, the improvement in the wettability of the polymers improves their potential utility in biomaterials applications (Abbasi et al., 2002).

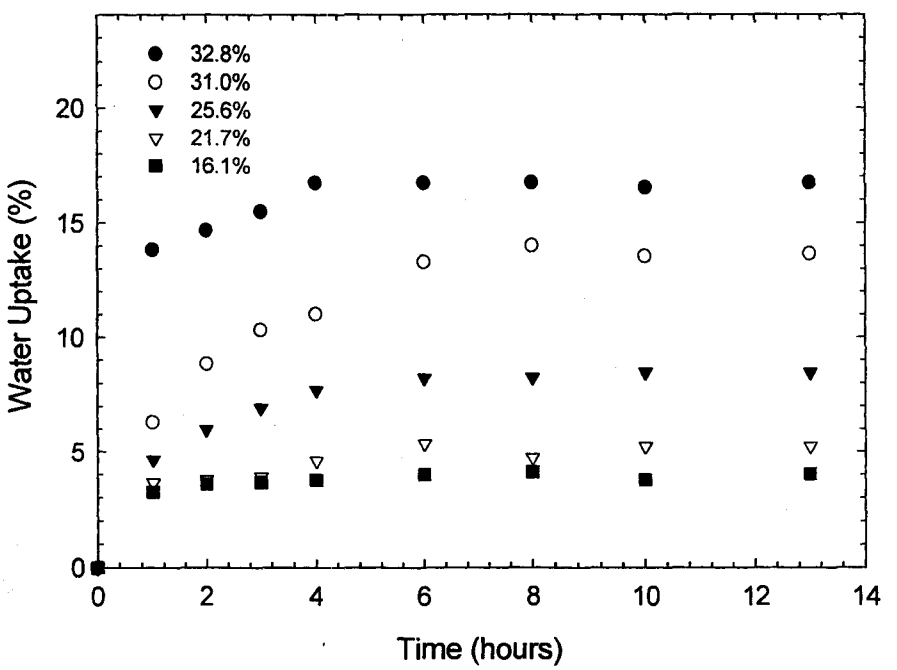

Fig. 4.15: Equilibrium water content of PDMS-V IPNs

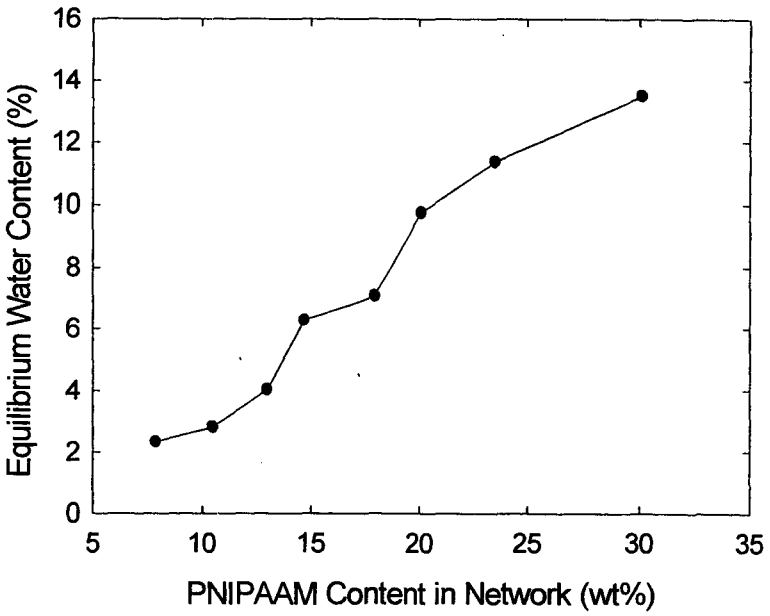

Fig. 4.16: The relationship between water uptake and PNIPAAM% in the IPNs

4.2.4 Surface Characterization

The surface properties of PDMS-V/PNIPAAM IPN and PDMS-V control were studied using several techniques. The wettability of the IPN surfaces was measured using sessile drop water contact angles, the surface composition and elemental information were determined by X-Ray Photoelectron Spectroscopy (XPS) and Atomic Force Microscopy (AFM) was used to investigate the surface morphology and topography. Attenuated Total Reflectance Fourier Transform Infrared Spectroscopy (ATR–FTIR) provided confirmation of the presence of PNIPAAM in the IPNs and provided information about the chemical structure of the IPN surface.

4.2.4.1 Water Contact Angle Measurement

Figure 4.17 shows advancing contact angle data for PDMS-V, PNIPAAM and various IPN surfaces with different amounts PNIPAAM in matrix. There was a clear decrease in advancing contact angle with the introduction of more PNIPAAM in the matrix, indicating increased surface hydrophilicity compared with the PDMS-V control. It is not surprising that that the surface became more hydrophilic despite the fact that the modification was aimed at the bulk, indicating that there was some surface connectivity of the PNIPAAM phase that would be necessary for glucose permeation.

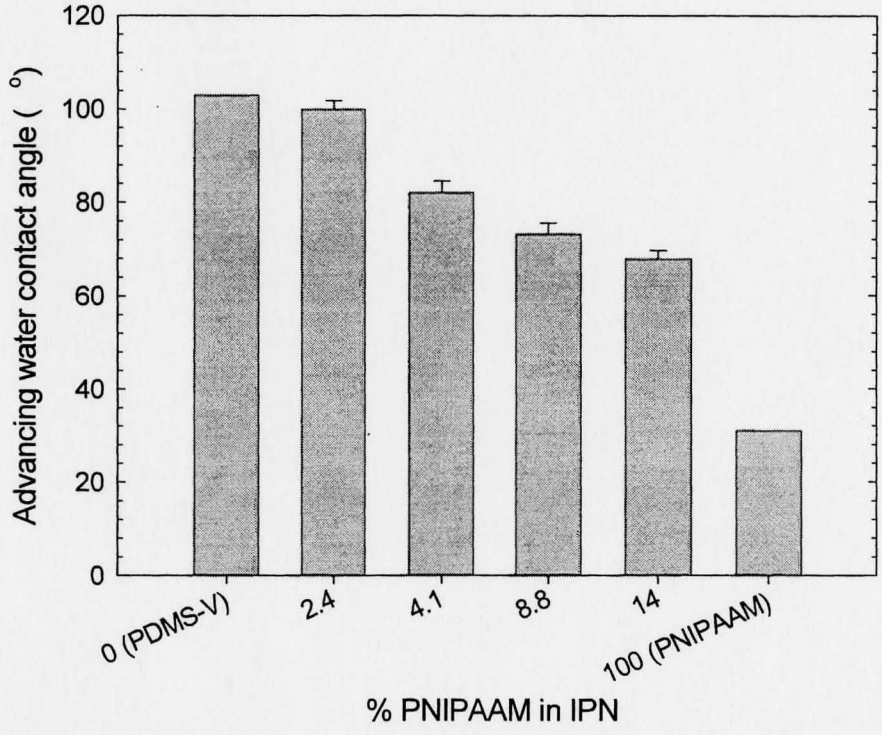

Fig. 4.17: Water contact angles for the PDMS control and PCMS-V IPNs. Contact angles were measured after fully rinsed by THF and dried in 60 °C for 12 hours. Error bars are standard deviations (n=3).

4.2.4.2 X-Ray Photoelectron Spectroscopy

The presence of PNIPAAM on the surfaces of the PDMS-V IPNs was confirmed by XPS. As shown in Table 4.1, the presence of nitrogen on the surface provides evidence for PNIPAAM. Furthermore, a trend was noted in the N1s atomic percentage, decreasing as the PNIPAAM content of the IPN decreased. It is interesting to note that the PNIPAAM on the surfaces may not be at the interface in the hydrophobic XPS environment, as there was generally more N1s found at the less surface sensitive takeoff angle of 90°. Further evidence of the presence of PNIPAAM near the surface was the increase in the C1s signal and decreases in the O1s and Si2p signals. However, it is clear that in the highly hydrophobic environment of the XPS, there is a significant amount of PDMS at the interface and / or increases in surface roughness resulted in shadowing at the 20° takeoff angle.

Table 4.1: XPS results for the PDMS-V IPNs

PNIPAAM (%)	Take off angle (°)	N content (%)	C content (%)	O content (%)	Si content (%)
35.6	90	1.4	54.2	22.9	21.5
	20	0.8	52.2	23.0	24.0
21.9	90	0.3	5.32	23.1	23.3
	20	0.5	54.5	21.3	23.7
19.0	90	0.5	48.6	25.1	25.9
	20	0.6	52.1	23.6	23.6
PDMS	90	0	50	25	25
PNIPAAM	90	12.5	75	12.5	0

4.2.4.3 Attenuated Total Reflectance Fourier Transform Infrared Spectroscopy

Attenuated Total Reflectance Fourier Transform Infrared Spectroscopy (ATR–FTIR) was used to detect both the elemental composition and the presence of chemical functional groups in the near surface layer of PDMS-V/PNIPAAM IPN films. This technique samples the surface to a depth of 1-5 μm, meaning that it is less surface sensitive than XPS. The spectra of the PDMS-V IPNs are shown in Figure 4.18. In the spectra for the IPNs, the four-peak group between 1370 and 1650 cm^{-1} are assigned to PNIPAAM as labeled in the figure. The typical peaks corresponding to PNIPAAM were not as strong as in the FT-IR spectra presented previously. The appearance of a broad peak at 1000-1110cm^{-1} can be identified as corresponding to the Si-O-Si group of PDMS, as discussed previously. However, this peak was a little deformed because it was covered by the absorbance of PNIPAAM at the same wave length range. The peaks attributed to CH_3 were weakened with an increase of PNIPAAM content of the IPNs, as there is less CH_3 in PNIPAAM. While ATR-FTIR signals are not as strong as FTIR signals, these results confirms the XPS results which show that there is less PNIPAAM on the IPN surface than in the bulk IPN.

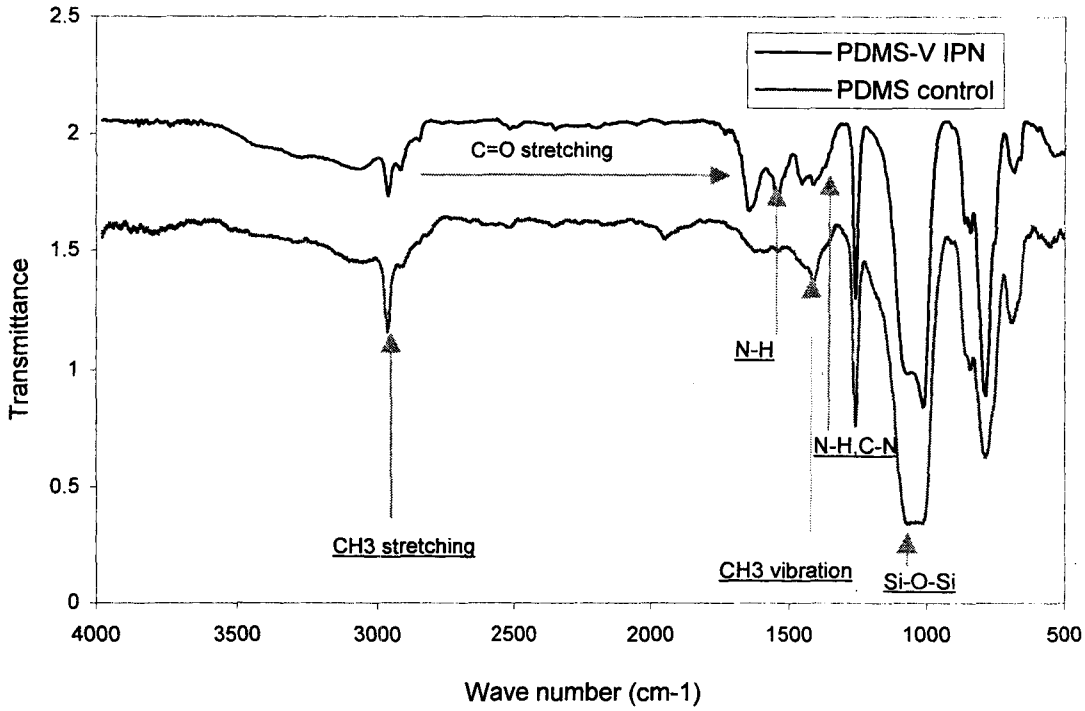

Fig. 4.18: ATRR-FTIR spectra of PDMS-V control and PDMS-V IPN. Comparing with PDMS control, the new peaks corresponded to PNIPAAM at 1370cm(C-N, N-H), 1650cm (C=O), 1540 cm (N-H) etc. confirmed the presence of PNIPAAM at the PDMS-V IPN surface.

4.2.4.4 Atomic Force Microscopy Images of PDMS-V IPNs

The surface morphology of the IPNs and PDMS control was investigated by AFM. Figure 4.19 shows that, while the PDMS-V control surface is very smooth, after the introduction of the PNIPAAM into the PDMS matrix, the surface roughness increased dramatically. Roughness data generated from the AFM images are summarized in Figure 4.20. Z-range, Rms and Ra clearly demonstrate an increasing trend with an increase in the PNIPAAM content of the IPN. This increased surface roughness is thought to result from the presence of PNIPAAM on the IPN membrane surface.

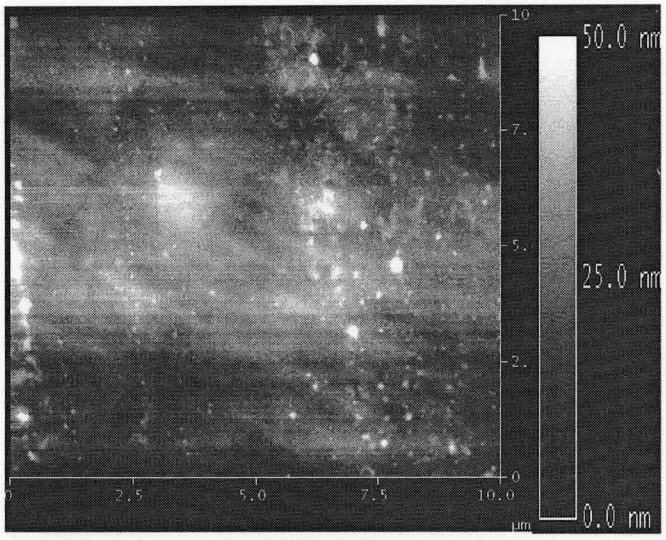

(a) PDMS-V control

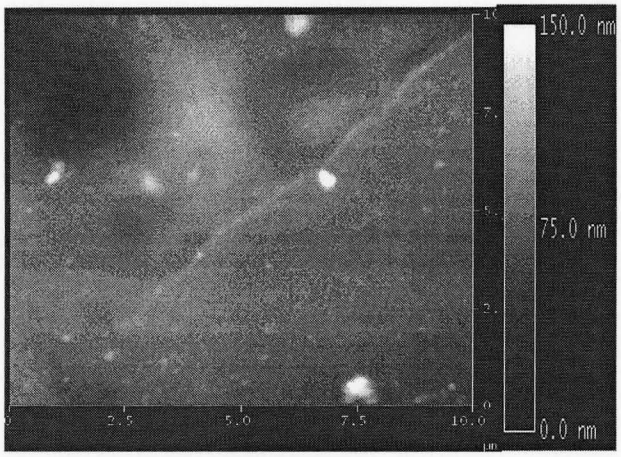

(b) 11.7% IPN

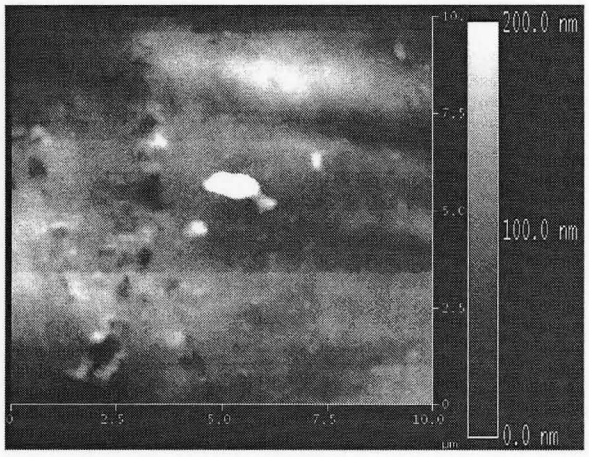

(c) 46.6% IPN

Fig. 4.19: AFM images of PDMS-V control and PDMS-V IPNs. (a) PDMS-V control; (b) 11.7% PNIPAAM PDMS-V IPN and (c) 46.6% PNIPAAM PDMS-V IPN. Images were scanned in contact mode after fully rinsed in THF and dried at 60 °C for 12 hours. PDMS control showed quiet smooth surface. Significant increases in surface roughness were seen after IPN formation, providing evidence of the presence of PNIPAAM on the IPN surface.

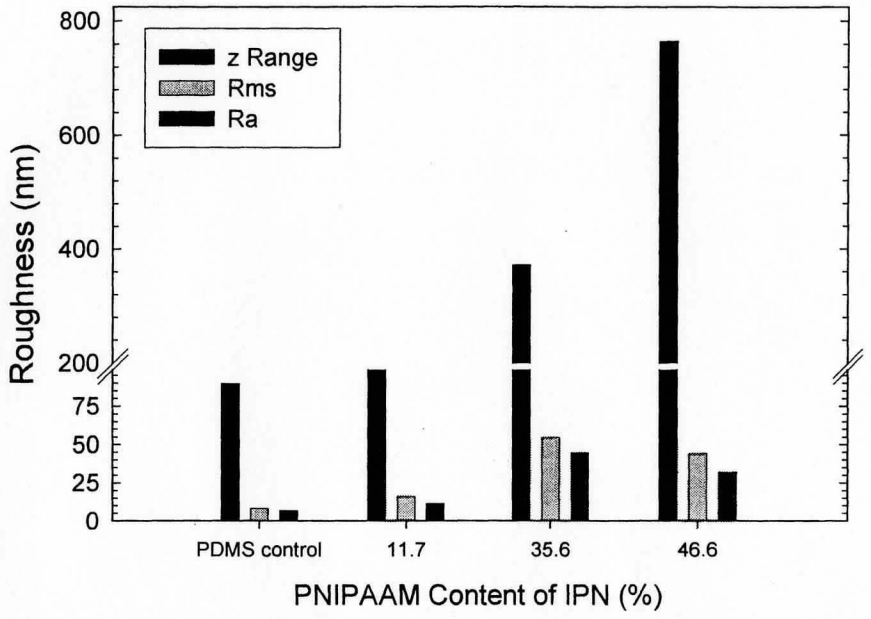

Fig. 4.20: The roughness change with different PNIPAAM% in PDMS-V IPNs. All of the roughness data showed an increased trend with an increase in the PNIPAAM content in IPNs.

4.2.5 Glucose Permeability

The glucose permeability of the PDMS-V / PNIPAAM IPNs was below the sensitivity of the glucose assay. Therefore, the glucose permeability of the membranes was lower than 10^{-10} cm^2/s. This relatively low glucose permeability of PDMS-V IPN membrane was consistent with the low water uptake of the material and the narrow and not very connective PNIPAAM channels as shown by the TEM images. However, glucose release at room temperature from a membrane swollen overnight in a 0.5 mg/mL glucose solution, shown Figure 4.21, demonstrates that these membranes can be used for glucose delivery.

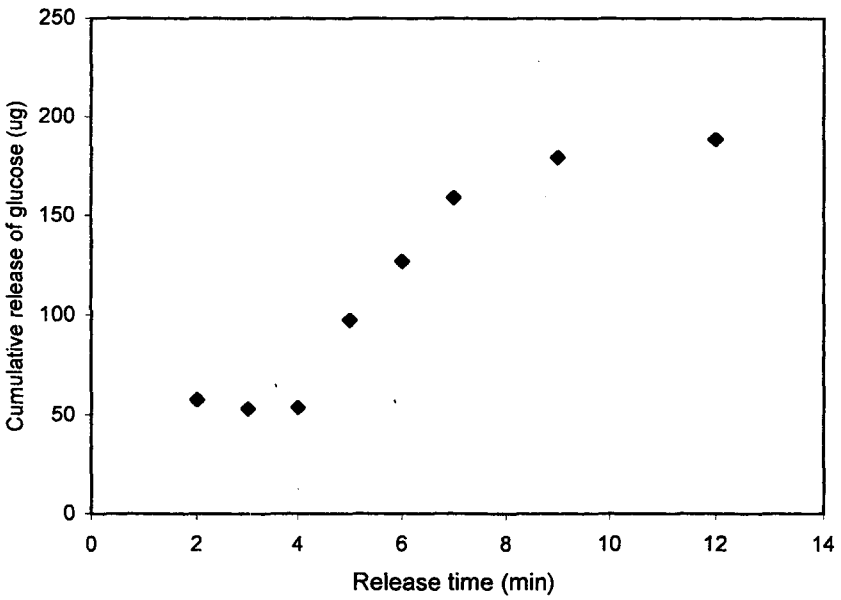

Fig. 4.21: Glucose release profile of 17.5% PDMS-V IPN. Prior to testing, the PDMS-V film was swollen in 0.1 g/ml glucose water solution overnight.

4.2.6 Effect of Temperature on IPNs

4.2.6.1 Equilibrium Water Uptake

Figure 4.22 illustrates the typical profile of the effect of increasing temperature on the equilibrium water content of PNIPAAM and the PDMS-V / PNIPAAM IPNs. While not as dramatic as with pure PNIPAAM, the equilibrium water content of the networks was found to decrease in all cases until reaching the LCST (approximately 32°C). This abrupt change results from the PNIPAAM phase transition induced by changes in the hydrophilic and hydrophobic force balance. While the LCST in PDMS/PNIPAAM IPNs, is not as clear as that for the pure polymer due to the constraints imposed by the PDMS host polymer, the transition remains clear. The equilibrium water content of the various IPNs can be seen to be dependent on the PNIPAAM content of the network and is very stable.

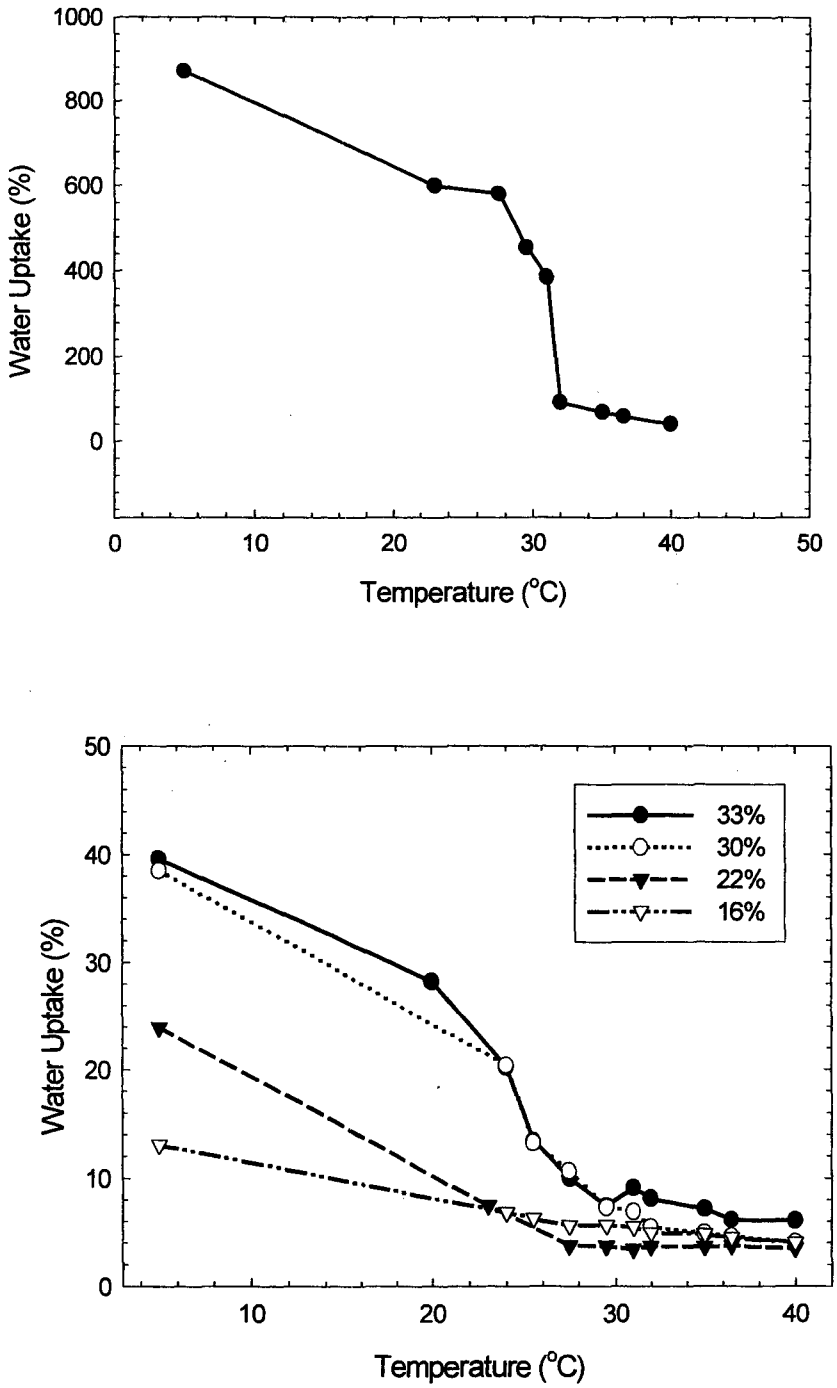

Fig. 4.22: Water uptake of IPN and PNIPAAM control at different temperature for LCST study. Top is PNIPAAM control; Bottom is PDMS-V/PNIPAAM IPNs. Crosslinked PNIPAAM showed an abrupt change in water uptake at 31°C, while the IPNs demonstrated that LCST property remained, but the change was not as dramatic.

4.2.6.2 DSC

Since the LCST phase transition is the result of a thermal change, it can be observed by DSC scanning (Zhang and Peppas, 2000). At the LCST temperature, the structured water in PNIPAAM network phase is dissociated from the system, leading the endothermal peak. From DSC scans of the various IPNs, shown in Figure 4.23, a transition at around 30°C, corresponding to the LCST of the polymers can be seen in 36.8% IPN, similar to the transitions observed in the water swelling studies. Higher PNIPAAM concentrations in the IPN result in more obvious endothermal peaks or transitions. Note that a slight decrease in the LCST of the IPNs compared with the pure PNIPAAM networks, an earlier response to changes in temperature and phase transitions covering a broader temperature range were characteristic of these polymers. This is likely due to the PDMS hydrophobicity disturbance to the LCST of PNIPAAM. It is of interest to note that the LCST changes detected in IPN samples were not as significant in terms of deviation from the LCST of pure PNIPAAM those observed by copolymerization of NIPAAM with other monomers (Yoshioka et al., 1994). This result indicates that the two polymers in the IPN perform more independently, retaining their respective properties to a greater extent than in copolymers.

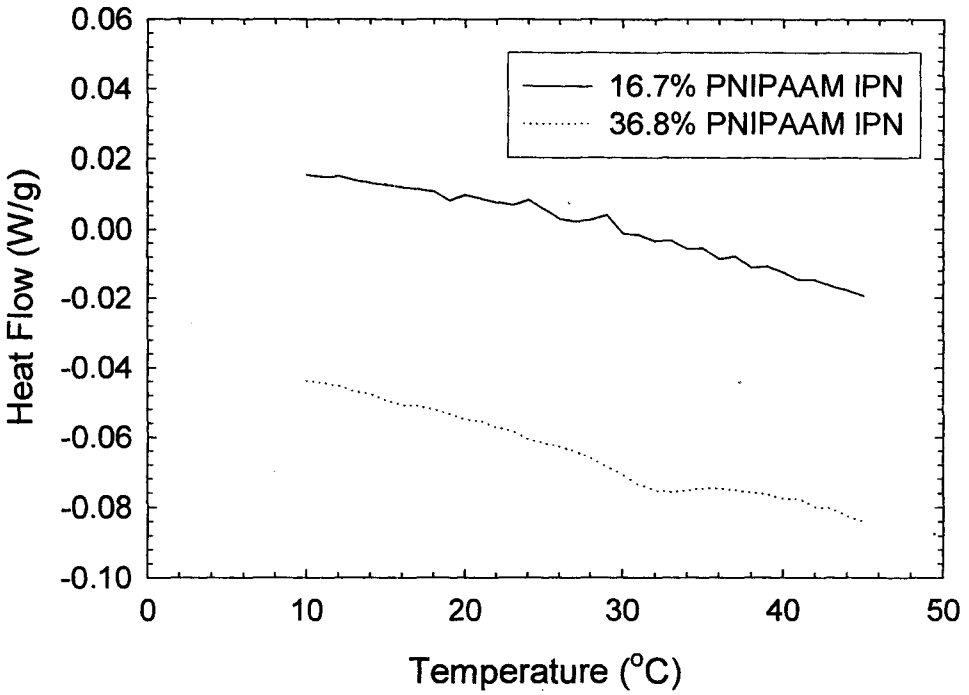

Fig. 4.23: DSC scanning of IPN samples to detect the transition of PDMS-V IPNs indicating the LCST of the IPNs at around 30°C.

4.2.7 Summary for PDMS-V/PNIPAAM IPNs

PDMS-V/PNIPAAM IPN materials with as much as about 50.0 % PNIPAAM were successfully synthesized. FT-IR and DSC results confirmed the formation of the PDMS/PNIPAAM sequential IPNs. TEM images revealed the two phase structure of the IPN material. Incorporation of PNIPAAM into a PDMS host by forming an IPN also resulted in changes in the surface properties of the materials, as confirmed by XPS, AFM, ATR-FTIR, and measurement of advancing and receding water contact angles. Improvements in the wettability suggest that these polymers may be more effective than hydrophobic PDMS in biomaterials applications. The mechanical properties of the network polymers were improved significantly relative to pure PNIPAAM and pure

PDMS in both the wet and dry state. The highest tensile stress of the synthesized IPNs was 9.5 MPa compared with the PDMS-V control at 6.6 MPa. A water uptake of 15% water uptake was observed in the highest PNIPAAM content IPN material.

Despite improvements in the wettibility of these polymers and increased water uptake relative to pure PDMS, glucose permeability of the materials remained low. This is likely due to the density of the PDMS network and the very small size of the PNIPAAM domains as well as the lack of significant connectivity of these domains as observed by TEM. The formation of small domains in these polymers may result from the very high hydrophobicity of the PDMS-V polymers and therefore the lack of interfacial compatibility between the polymers. The PNIPAAM/PDMS networks formed from the PDMS-V cured in solvent were not involved because the PDMS-V curing in solvent needs higher temperature which is difficult to prevent the solvent evaporation and hard to control this procedure.

5. PDMS-OH / PNIPAAM INTERPENETRATING NETWORKS

As summarized in Chapter 4, the dense network structure and hydrophobicity of PDMS-V was thought to result in the lower water uptake and lower glucose permeability of the networks composed of these membranes. Therefore, a cured PDMS-OH film was chosen as the host because it was somewhat less hydrophobic than the PDMS-V. Furthermore, in order to generate looser host polymers, the PDMS-OH prepolymers were cured in the presence of a solvent. This method resulted in the incorporation of more PNIPAAM into the network, greater water swelling and high permeability to glucose.

5.1 Solvent Curing of PDMS-OH

In order to obtain transparent homogeneous films, THF and toluene were found to be superior solvents. Toluene was selected for further experiments as the solvent for PDMS-OH curing since it has a low volatility, minimizing solvent evaporation during the curing process. The PDMS concentration in the toluene was varied from 12.5% to 100% by weight. Curing occurred within 3 – 6 days, with more dilute polymer solutions requiring longer for curing. The hydrophilicity of the surface of the films was increased by curing the films on water. This also allowed for ease of removal of the sample.

5.1.1 Solvent Ratio of PDMS-OH Films

The PDMS-OH films cured in toluene as described above were swollen in 3 different of solvents: toluene, hexane and THF in order to confirm curing in solvent resulting in looser networks and assess which solvent would result in the greatest swelling for the next step of the curing reaction. As shown in Figure 5.1, curing in solvent significantly increased the swelling of the formed film in the organic solvents.

For a PDMS-OH film cast from a 30% polymer solution, the THF swelling ratio was about 400%. Non-solvent curing lowered the swelling ratio to approximately 200%. In comparison, PDMS-V films prepared in a normal manner without the use of solvent had a swelling ratio in THF of 112%. Similar results were obtained with hexane and toluene. These results suggest that the PDMS-OH films, formed from prepolymers of similar molecular weight were much looser networks. This is thought to be the result of a decrease in physical crosslinking or chain entanglement. Curing of PDMS-V curing in solvent required higher temperatures to cause solvent evaporation. Of the three solvents, swelling was found to be highest in THF. Therefore, THF was selected as the solvent for the PNIPAAM reaction as it was believed that this higher solvent uptake would translate into higher amounts of PNIPAAM in the resultant networks.

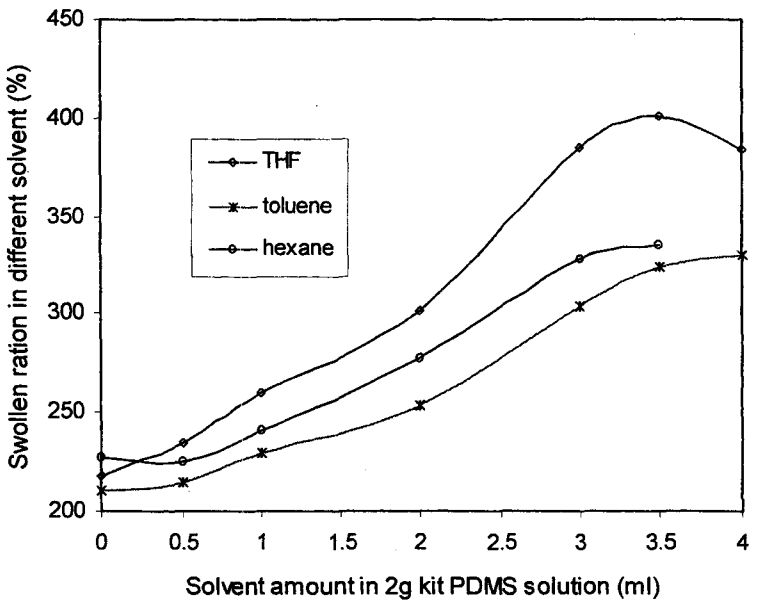

Fig. 5.1: Solvent swelling ratio of PDMS-OH film prepared from different concentration of PDMS prepolymer curing kit in toluene solution. The higher swelling ratio in solvent confirmed the looser network formation by using more diluted PDMS prepolymer solution for curing.

5.1.2 Molecular Weight of PDMS Prepolymer Effect on Swelling Ratio

In addition to curing in solvent, higher molecular weight PDMS prepolymers can result in increased molecular weight between crosslinks, a decreased crosslinking density and therefore a looser polymer network PDMS-OH films were prepared from prepolymers of viscosity 200 and 1800 cst to investigate the effect of prepolymer molecular weight. The results, shown in Table 5.1 showed that as expected, higher molecular weight PDMS prepolymers did result in more open networks as indicated by an increased swelling ratio in THF and toluene. However, the difference was not significant, possibly because at higher Mn the chain entanglement was also intensified, offsetting the effects of the increase in the molecular weight between crosslinks.

Table 5.1: Molecular weight effect on solvent swelling ratio

Viscosity of PDMS (cst)	Mn calculated (Da)	Swelling ratio in THF (%)	Swelling ratio in toluene (%)
1800	33619	377	310
200	11188	301	253

* Samples were cured in room temperature for 24 hrs using solution of 2 g PDMS prepolymer in 2ml toluene. Mn was calculated by using A.J.Barry's relationship between Mn and viscosity of PDMS prepolymers. (See Fig. 2.5 from Gelest Inc. brochure)

5.1.3 Comparison of the Synthesis of PDMS-V and PDMS-OH IPNs

Table 5.2 demonstrates that curing the PDMS-OH films in solvent resulted in IPNs with a higher PNIPAAM content relative to the best PDMS-V films cured in the absence of solvent. Since continuous PNIPAAM phases are necessary for glucose permeation, higher PNIPAAM contents are expected to result in better facilitation of

glucose transport. It is clear from the water uptake and the glucose permeation results that more continuous PNIPAAM phases were formed in these membranes as expected.

Table 5.2: Comparison of vinyl and hydroxyl terminated PDMS IPN

PDMS	PDMS oligomer concentration	Weight increase (%)	Water uptake (%)	Permeability (cm^2/s)
Vinyl terminated	100%	46	13.6	0.6×10^{-10}
OH terminated	30%	51	30.7	2.1×10^{-9}

*Sample preparation conditions: viscosity of PDMS prepolymers: 2000cst; 312 nm UV lamp; NIPAAM monomer solution swelling time: 8 hrs; initiation time: 14 hrs; distance to UV lamp: 2cm; NIPAAM solution concentration: 35%.

5.1.4 PDMS Prepolymer Concentration and Swelling Time Effects on IPN Formation

As shown in Table 5.3, the swelling time of the PDMS host films in the NIPAAM monomer solution had a significant effect on the IPN formation. At a constant concentration of NIPAAM, increasing the swelling time from 5 to 9 hours as shown resulted in an IPN containing significantly more PNIPAAM. However, the water uptakes of the samples were similar, and the network formed from the shorter NIPAAM swelling time actually showed a slightly higher level of water swelling. This result suggests that it takes more than 5 hours for complete swelling of the PDMS host in the NIPAAM monomer solution. Interestingly, decreasing the concentration of PDMS prepolymers during the host film curing procedure seemed to result in the incorporation of more PNIPAAM in the resultant networks likely because of the looser PDMS host network formed.

Table 5.3: Curing concentration and swelling time effects on IPN synthesis

PDMS curing kit concentration (%)	Swelling time (hrs)	PNIPAAM (%)	Water uptake (%)
10	5	32.8	30.2
13	5	25.0	28.0
13	9	50.0	23.6
35	9	38.6	29.7

*IPN preparation conditions: 40%NIPAAM reaction solution; Degassing for 30 mins; 312 UV lamp initiation for 12 hrs; Distance to UV lamp was 2cm.

Furthermore, Figure 5.2 illustrates the effect of solvent amount during the PDMS curing on the PNIPAAM content of the resultant IPNs. As the amount of solvent in the film preparation was increased, for films prepared under similar conditions, the PNIPAAM content of the film increased. PDMS concentrations of between 25 and 40% by weight were found to be optimum. With lower amounts of PDMS in the film cure however, the amount of PNIPAAM in the resultant IPN decreases. This is thought to be due to the decreased interpenetration of the polymer chains when higher amounts of solvent were present. With solvent fractions of greater than 40%, the PNIPAAM amount introduced to the host was found to decrease since the denser host networks formed limit the volume available to accommodate PNIPAAM. Interestingly, water uptake of the samples generally paralleled the PNIPAAM content results. However, the network prepared using the PDMS sample cured with the most solvent (13% PDMS) had a very high swelling ratio despite having a relatively low PNIPAAM content as determined by weight increase indicating that even though less PNIPAAM is present in the sample, it is connected to the surface, providing an effective diffusion path for glucose or other small molecules.

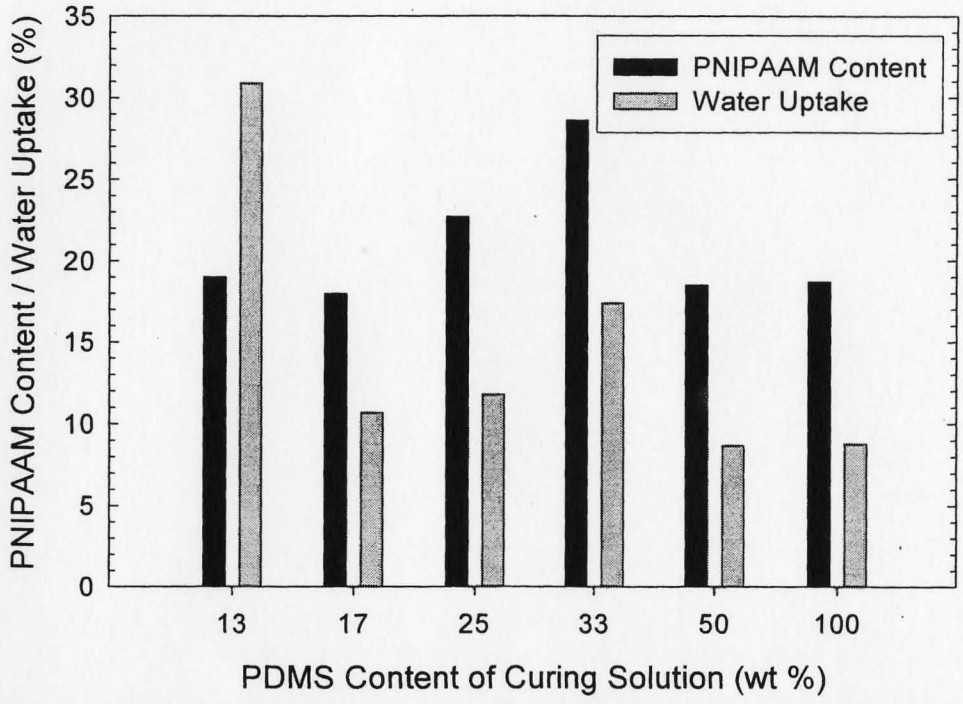

Fig. 5.2: Effect of solvent content in PDMS curing solution on the PNIPAAM content of the resultant IPN and on the water uptake of the IPN. All of the IPNs were synthesized under the same conditions with the excection of the PDMS curing solution concentration. Note the parallel trend of PNIPAAM content and water up take in general. However, the PDMS control cured in 87% solvent (13%) showed a similar PNIPAAM content, but had highest swelling ratio based on its IPN weight, likely due to much looser PDMS network formed in this case.

5.1.5 Crosslinker Effect on PNIPAAM% in IPNs

As with the PDMS-V IPNs, bifunctional BisAAM was used as crosslinker for PNIPAAM in these network polymers. However, in this case, the crosslinker was found to play a more important role in network formation as summarized in Figure 5.3. Between 0 to 2.0% (mol) crosslinker, increasing the amount of crosslinker during the NIPAAM polymerization stage increased the amount of PNIPAAM in the resultant IPN. Crosslinker amounts greater than 2% crosslinker were not examined since it was believed

that high crosslinking densities in the PNIPAAM would decrease the water uptake of the resultant IPNs. It is thought the crosslinker was important for creating the interpenetration of the networks and for forming a gel like PNIPAAM phase in the case of the PDMS-OH based IPNs. The dense PDMS-V host polymers on the other hand were able to contain the hydrogel even at very low crosslinking densities. For the case when no exogenous crosslinker was added, a semi-IPN was formed. The water uptake of this network was dramatically lower than that of the other polymers, likely because the connectivity of the PNIPAAM with the surface was very limited.

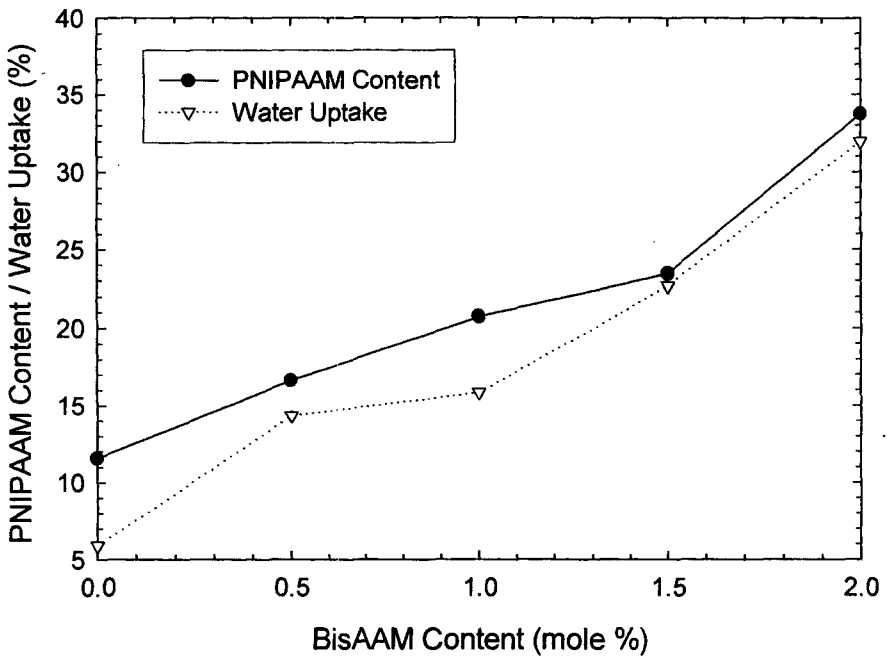

Fig. 5.3: Crosslinker content effect on PNIPAAM% and water uptake of IPNs. All samples were prepared by PDMS host network cured from 13% prepolymer solution and 35% NIPAAM monomer concentration with 10 hour PDMS film swelling time; The distance to 312 nm UV lamp was 1.5 cm. It can be seen that crosslinker content had significant influence on PNIPAAM content and water uptake of IPNs.

5.2 Confirmation of PDMS-OH/PNIPAAM IPNs

Similar to the PDMS-V/PNIPAAM IPNs, FT-IR and DSC were used to confirm IPN formation and the presence of the PNIPAAM in the host polymer. FT-IR was used to detect the PNIPAAM in the IPN by tracing the typical IR transmittance peaks assigned to PNIPAAM. The presence of the Tg of PNIPAAM was confirmed by DSC.

5.2.1 FT-IR

FT-IR spectra of PDMS-OH IPNs showed similar results to the PDMS-V IPN as shown in Figure 5.4. Both the typical peaks associated with PDMS at 1000-1110 cm^{-1} and the fingerprint peaks at 1370 cm^{-1}, 1450 cm^{-1}, 1540 cm^{-1}, 1640 cm^{-1} corresponding to PNIPAAM appeared in the spectra. The CH_3 stretching at 2970 cm^{-1} showed a slight weakening with high PNIPAAM content in the IPN. Similar to the PDMS-V networks, the PNIPAAM peaks increased in intensity with increasing amounts of the polymer in the network as determined by measuring changes in the weight. These peaks confirmed that the composite material contained both polymers as expected and that the trends in the weight measurement accurately predicted the amounts of PNIPAAM in the network polymers.

5.2.2 DSC

As shown in Figure 5.5, DSC scans of the PDMS-OH/PNIPAAM IPN samples in the range 75-225°C clearly showed the Tg of PNIPAAM. As expected, the pure PDMS-OH polymers did not show any transition in the range examined as the Tg of PDMS has

been reported to be approximately –114 °C. Similar to the PDMS-V IPNs, there was no obvious Tg shift dependence on the content of PNIPAAM in the IPNs, again likely due to limited phase mixing of PDMS and PNIPAAM domains even at boundary between the two polymers. However samples with higher PNIPAAM contents showed clearer transitions. Differences between the transition temperatures measured for networks with different PNIPAAM content were likely the result of changes in the heat capacity of the samples with the introduction of greater amounts of PNIPAAM in the polymers.

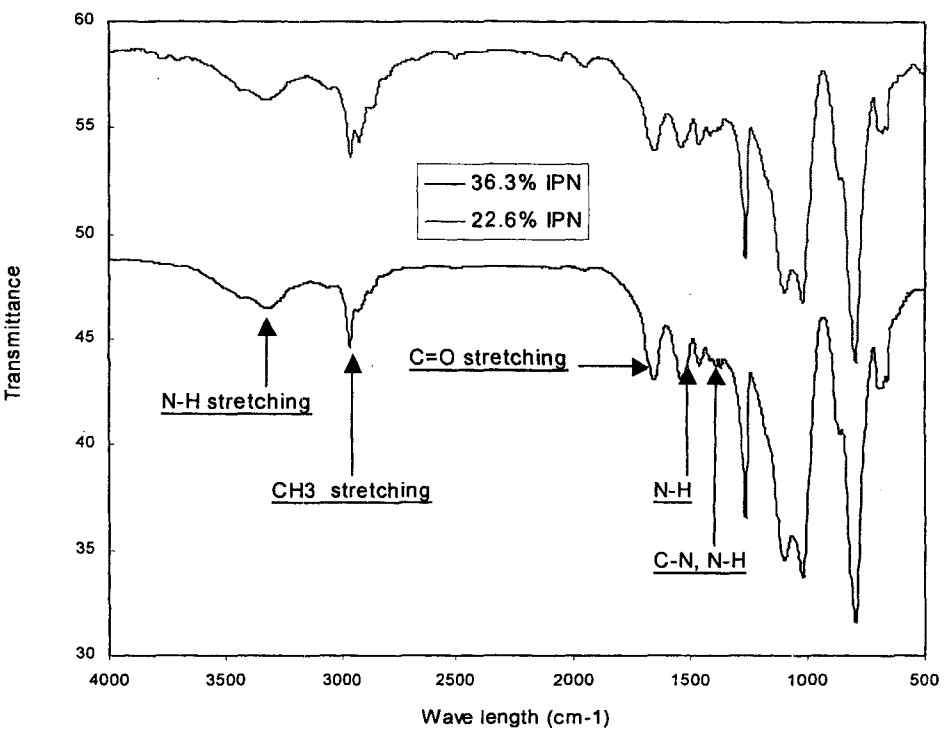

Fig. 5.4: FT-IR spectra of PDMS-OH/PNIPAAM IPNs. Note that peaks corresponding to C-N, N-H and C=O bonds in PNIPAAM clearly appear in the IPN as shown on the figure.

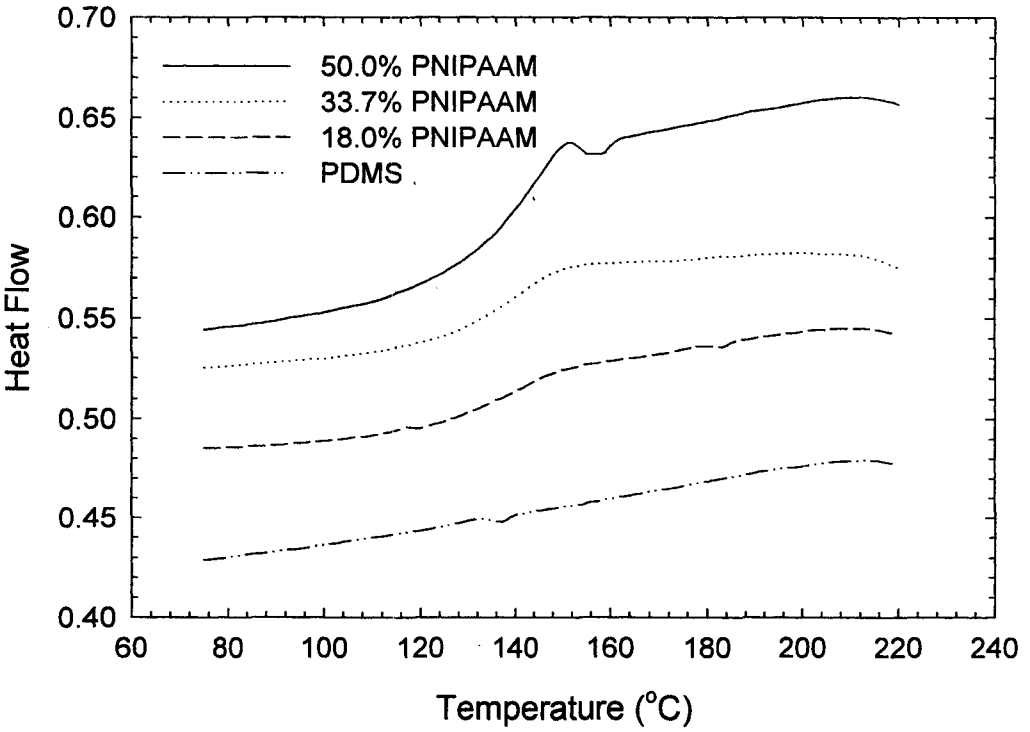

Fig. 5.5: DSC result of PDMS-OH IPN for Tg determination. The scans were performed at a heating rate 15°C/min temperature. The IPN spectra clearly showed the glass transition of PNIPAAM at 140 °C indicating the introduction of it to PDMS host.

5.3 Morphological Characterization and Bulk Characterization

5.3.1 SEM and TEM

To investigate the micro-structure and phase information of PDMS-OH IPNs, SEM and TEM were used. An SEM cross-section image of PDMS-OH/PNIPAAM IPN is shown in Figure 5.6. While two continuous phases can be visualized in this image, the resolution of SEM is not adequate to obtain satisfactory micro-structural information about the polymers. TEM images of the materials, as shown in Figures 5.7 (a) and (b) provided additional information about the morphology of the polymer samples. Based on the image of PDMS control shown in Figure 4.11 and the relative amount of PNIPAAM and PDMS in samples, the white areas were identified as the PDMS domains, while the darker areas were thought to be PNIPAAM. As the PNIPAAM content of the IPN was increased, the domain size was found to decrease, but the connectivity of the PNIPAAM in the samples increased. Generally, it has been reported that higher concentrations of monomer and higher conversions are necessary to achieve the interpenetration of two network and dual continuous phases (Sperling, 1997). In the current study, the concentration of NIPAAM, at 40%, was quite low. Regardless, the TEM images clearly show that two continuous phases were formed. This is thought to be due to the role of the solvent during the formation of the PDMS host polymer films, since similar continuity was not found with the PDMS-V network polymers. This dual continuous phase structure provided interpenetrating polymer network formation and resulted in water diffusion channels as expected. Furthermore, the continuity of the PDMS phase in these polymers, in addition to providing structure, provides a channel for

oxygen permeation. The morphology was more open and more connective than PDMS-V IPNs, with PNIPAAM domains on the order of 20-50nm, significantly larger than 10-20 nm channels present in the PDMS-V IPNs.

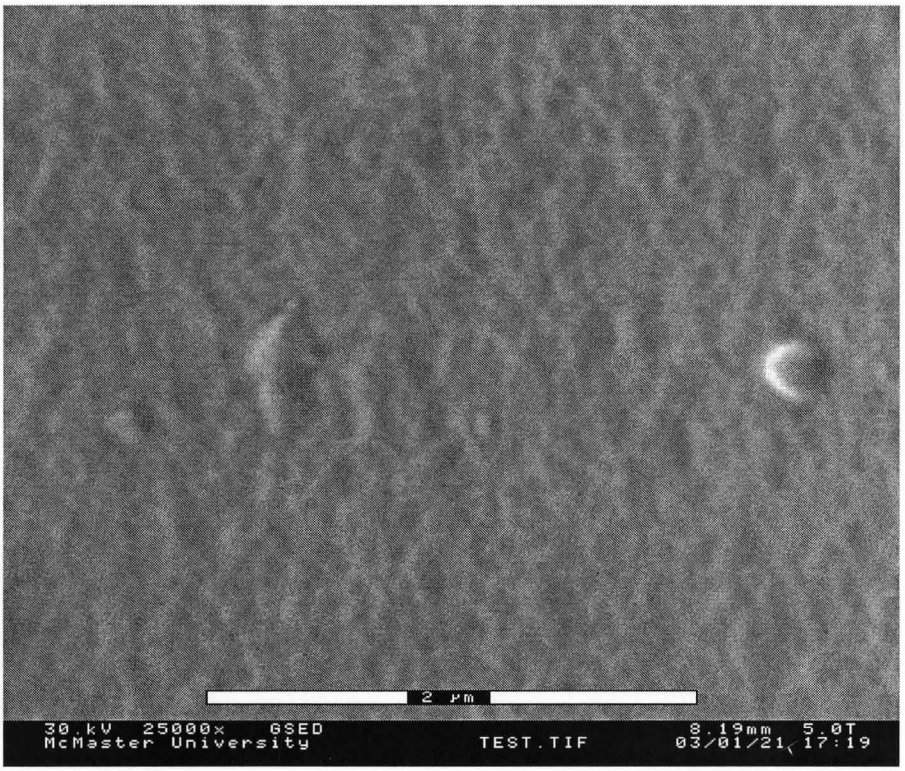

Fig. 5.6: SEM image of a PDMS-OH IPN. The PDMS-OH IPN was cross-sectioned by fracture of the frozen sample in liquid nitrogen and was spurred using gold. Magnification:25,000×, Bar: 2 μ m. Two continuous phases of PDMS and PNIPAAM are shown, although resolution is not adequate to obtain significant morphological information

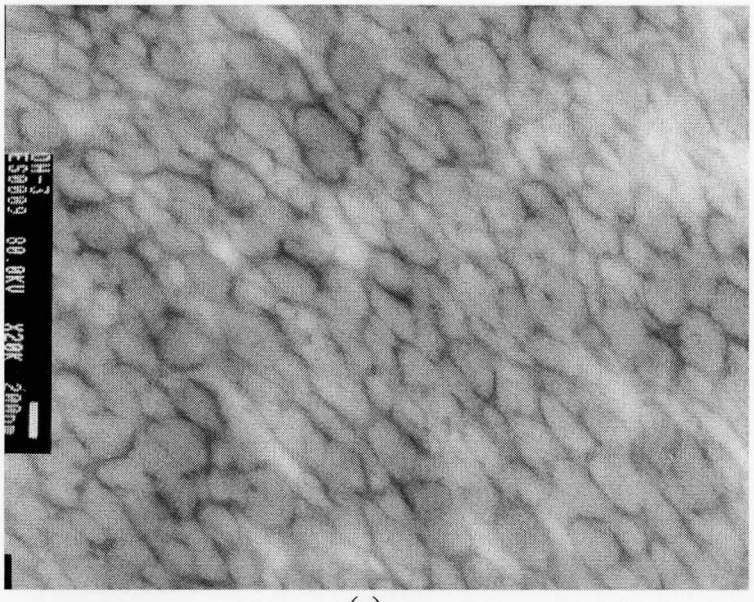

(a)

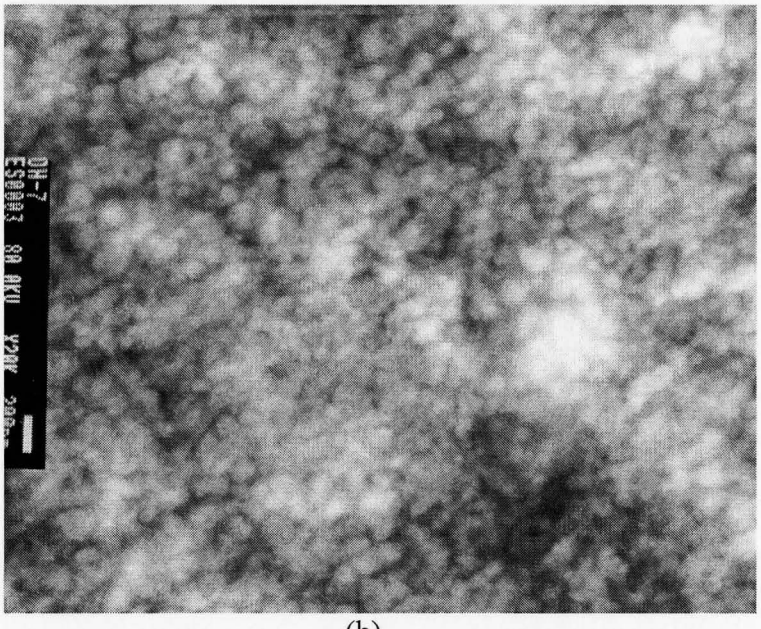

(b)

Fig. 5.7: TEM images of PDMS-OH IPNs. (a) 24.5% IPN; (b) 37.4% IPN. The images were 100 nm thick cross-sections of PDMS-OH IPNs (80 kv; 20,000×). Bar: 200 nm. The white area is identified as PDMS, while the dark area is thought to be the PNIPAAM domains. Dual connective phases of the two polymers were clearly visualized in these images. The 37.4% IPN had more PNIPAAM, with greater connectivity.

The skin layer phenomenon was observed in TEM images taken from areas close to the edge of film as shown in Figure 5.8. A PNIPAAM composition gradient from the top surface to the bulk was detected on the samples. The PNIPAAM domain size and connectivity gradually increased with the distance from the interface. The skin layer approximately 2 μm thick for a 1.2 mmthick, 50.9% PNIPAAM IPN and 400nm thick for 0.8 mm, 36.3% PNIPAAM IPN. A similar gradient structure in sequential IPNs was also found in PMAA/PNIPAAM (Zhang and Peppas, 2002) and PDMS/PMAA (Turner and Cheng, 2000) IPNs, and was believed to result from monomer evaporation during IPN formation. In the current study, skin layer formation was thought to be induced by solvent evaporation during the PDMS curing phase. Evaporation of the toluene, particularly at the solution and air interface would result in the formation of a denser polymer. This dense layer would swell significantly less in the NIPAAM monomer solution resulting in the observed composition and morphology in the surface layer. These skin layers may lower permeability to water or glucose. TEM images suggested that thicker film had thicker skin layers for an unknown reason. Zhang and Peppas (2002) reported that the skin layer in PMMA/PNIPAAM IPNs represented 2~3% of the total thickness of the samples. In comparison, PDMS-V IPN showed a more uniform distribution between the bulk and surface.

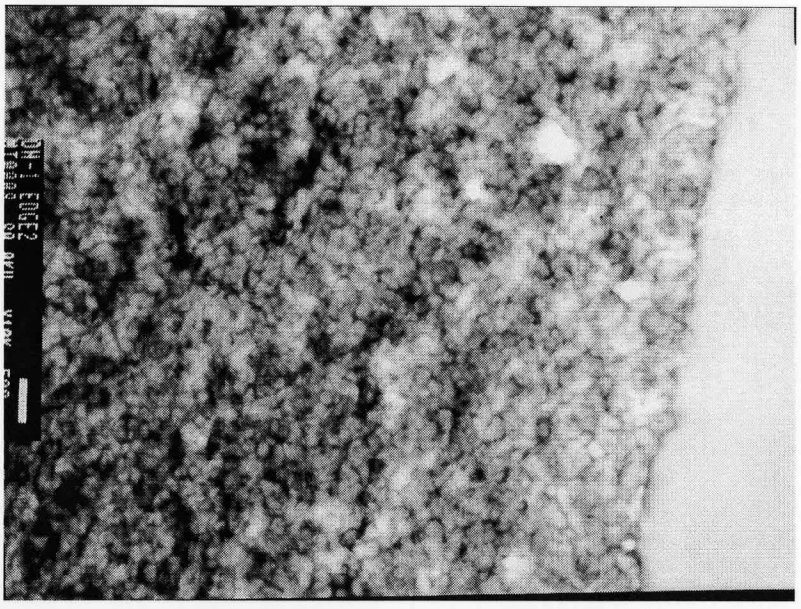

Fig. 5.8(a):

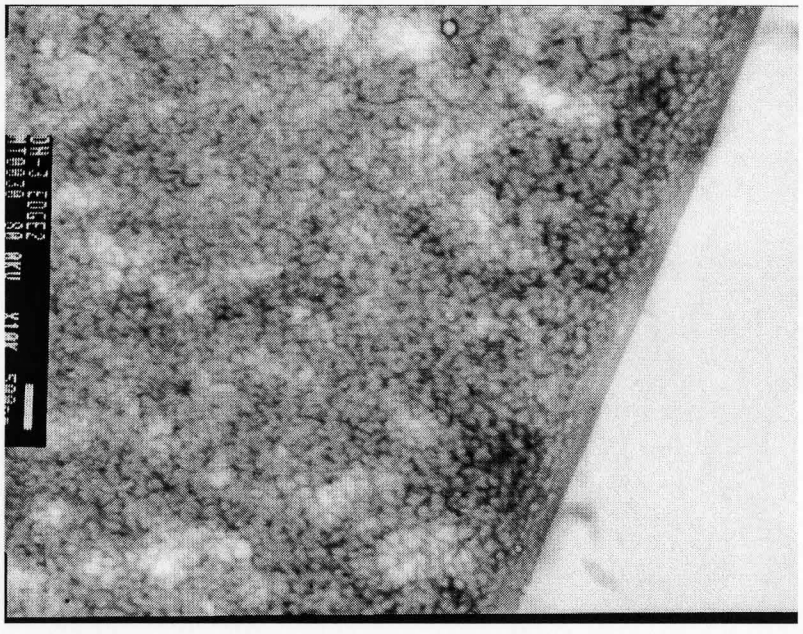

Fig.5.8 (b)

Fig. 5.8: Skin layer phenomenon of the IPNs. (a) PDMS-OH IPN (50.9% PNIPAAM; thickness: 1.2 mm); (b) PDMS-OH IPN (36.3% PNIPAAM, Thickness: 0.8 mm). The bars indicate a length of 500 nm (80kv, 10,000×). Skin layers were clearly observed.

5.3.2 Equilibrium Water Content: Equilibrium Time and Water Uptake

It is believed that the water swollen channels form the basis for glucose permeation through the IPN materials. Higher water uptake was expected for the PDMS-OH IPNs since weight change measurements suggested that there was a higher PNIPAAM content in these polymers and TEM results demonstrated that the PDMS-OH IPNs cast from solvent formed more connective PNIPAAM domains in the networks. The equilibrium water content data summarized in Figure 5.9 indicate that the water uptake of the various films increased with increasing PNIPAAM content, reaching 42% at 31% PNIPAAM IPN membrane PDMS-V IPNs containing similar amounts of PNIPAAM had an equilibrium water content of only 15%. Furthermore, the networks with higher PNIPAAM contents also required less time to reach equilibrium as shown. On average, the PDMS-OH networks required approximately 40 hours to equilibrate in water, significantly shorter than the time required by the PDMS-V networks. It is thought that PDMS-OH is more moisture sensitive and during water swelling process, curing reaction may have occurred influencing the water uptake time.

5.3.3 Mechanical Properties

The mechanical properties of the composite films in the wet state, summarized in Figures 5.10 (a) and (b), were found to be significantly improved relative to PDMS-OH controls as expected. Increases in the stress at maximum load with increasing PNIPAAM content were also found in these polymers, particularly at 25-30% PNIPAAM which has optimal glucose permeability. The effect of the incorporation of solvent during the curing

process on the mechanical properties of the control PDMS films is also shown. Control 1 represents a PDMS-OH film cured in the absence of solvent; control 2 is a PDMS-OH film cured in the presence of 85%(wt) solvent. This same film was used for the preparation of the IPNs in this study. The tensile strength of the hydroxyl terminated PDMS control was approximately an order of magnitude lower than that measured for the vinyl control polymer. Furthermore, curing the PDMS in the presence of solvent decreased the mechanical strength by an additional factor of approximately 3, likely due to the increase in the molecular weight between crosslinks in these polymers. The tensile strains of the two controls were not greatly different. However, significant increases in mechanical strength did occur with the incorporation of even small amounts of PNIPAAM into the polymer networks.

Furthermore, somewhat surprisingly, the mechanical properties of these polymers in the swollen state were only 10-20% lower than the polymers in the dry state. It is clear from these results that the continuous PDMS phase maintained the strength of the polymers when wet. Since the water uptake of the networks is likely primarily in the PNIPAAM phase, it can be determined that the water uptake of the PNIPAAM in the network is between 80 and 100%. Pure PNIPAAM polymers can take up as much as 700% water, significantly impacting the mechanical strength. The improved tensile strain of these polymers demonstrates that the PNIPAAM is not as rigid in the dry state as expected. Dry state measurements, shown in Figures 5.11 a) and b) show similar trends Composites with the highest PNIPAAM contents exhibited significantly increased strain relative to PDMS controls.

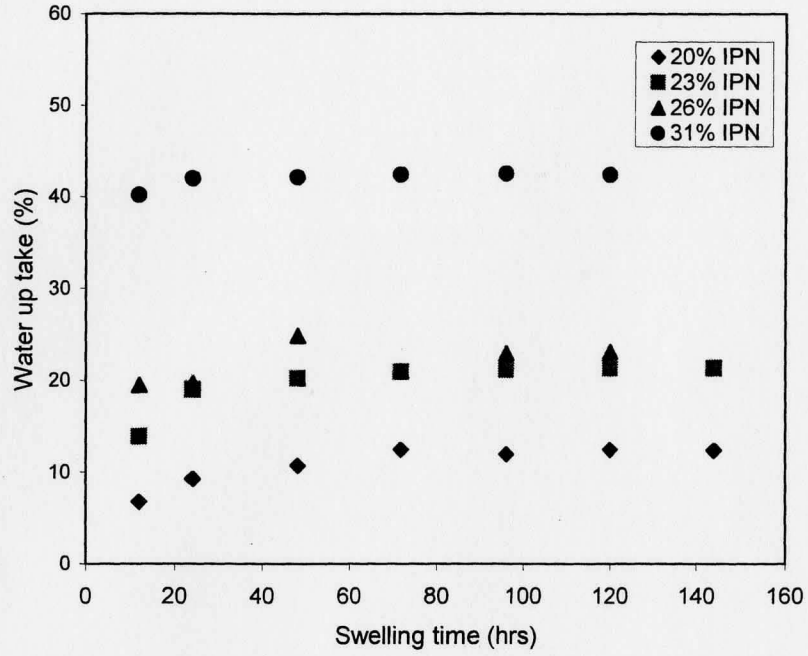

Fig. 5.9: Water equilibrium time of PDMS-OH IPNs. The plots indicated that 40 hours are long enough for all PDMS-V IPNs with different PNIPAAM content to reach equilibrium water swollen state in general.

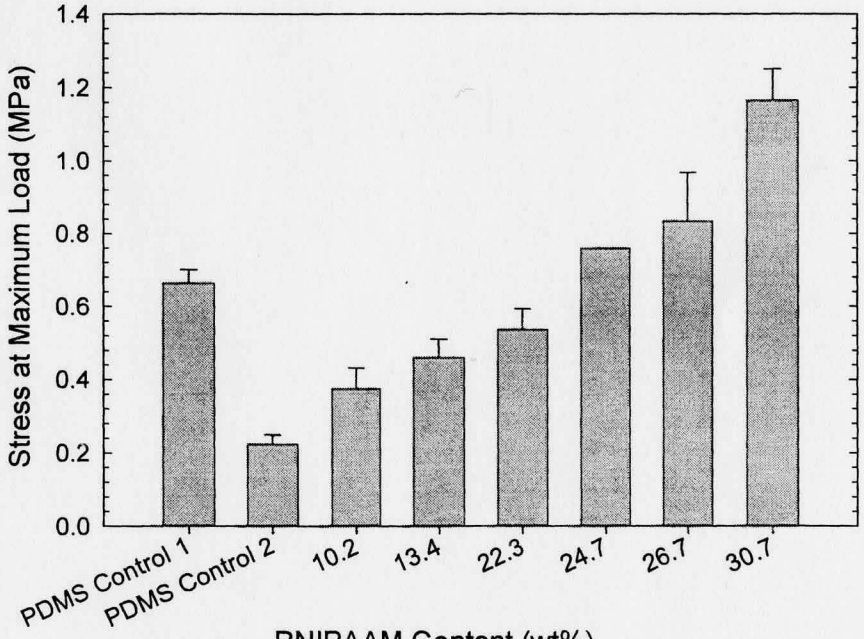

Fig. 5.10 (a)

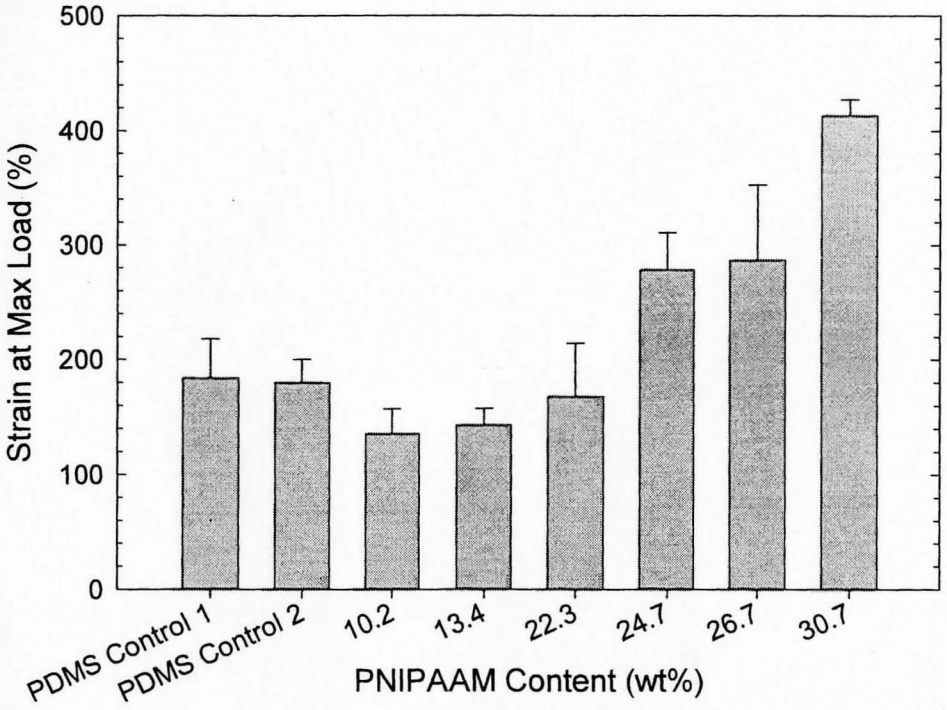

Fig.5.10 (b)

Fig. 5.10: (a)Tensile stress of PDMS-OH IPNs in wet state; (b)Tensile strain of PDMS-OH IPNs in wet state. The tensile strength was measured at 50 mm/min cross-head speed. The error bars represent standard deviations (n=3). Before testing, all samples were fully swollen in deionized water for 12 hours. Control 1 was PDMS-OH film cured in normal procedure and control 2 was the PDMS-OH film cured incorporating with 85% toluene which was same as the PDMS used for IPN synthesis in this study. Note the increase trend of stress and strain with increase of PNIPAAM content in IPNs.

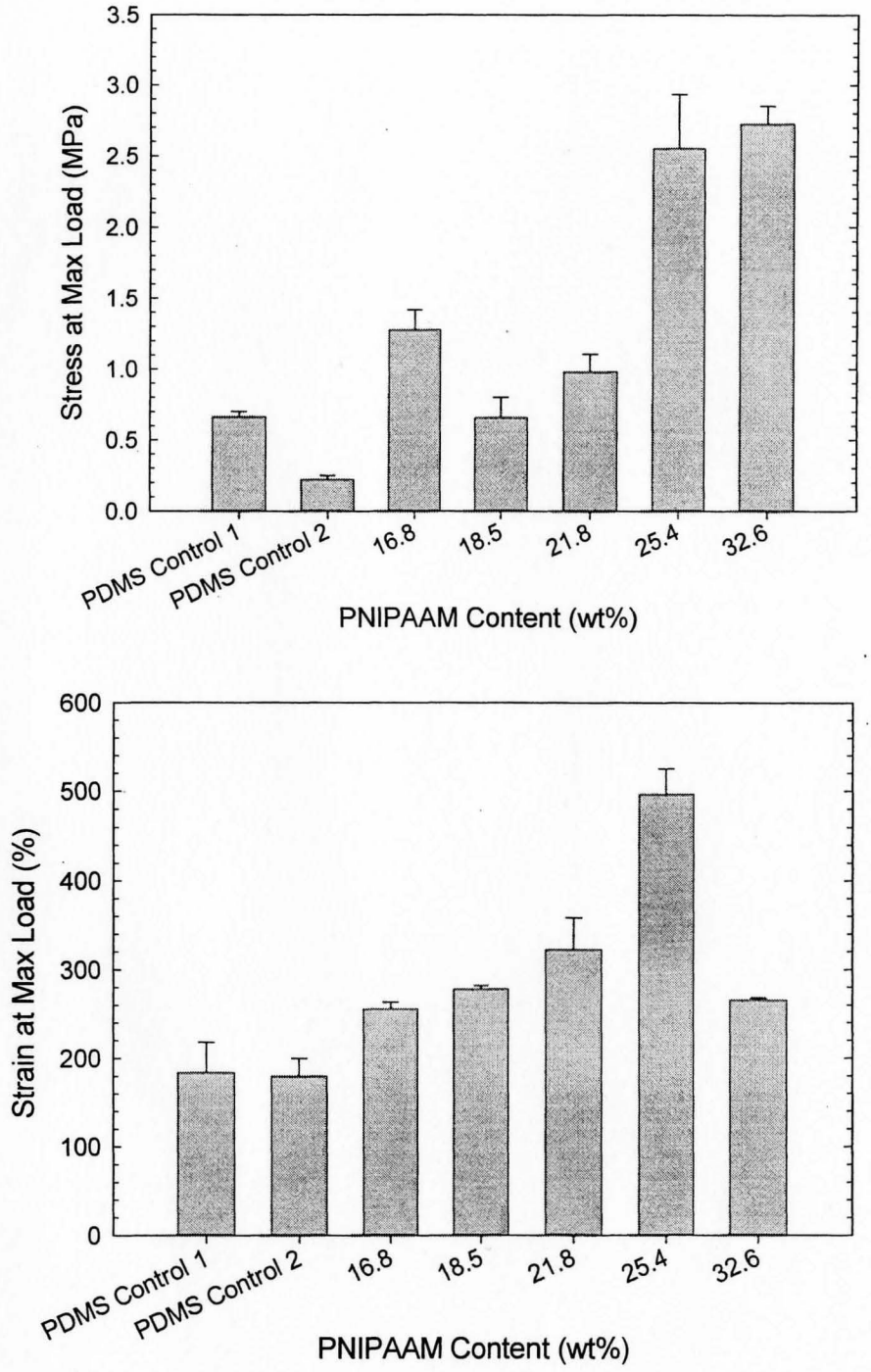

Fig. 5.11: (a) The tensile stress of PDMS-OH IPNs in dry state . (b) The tensile strain of PDMS-OH IPNs in dry state. Before test, all the samples were dried at 60 °C for 12 hours. The other test conditions were same as the test in wet state. Highly significant improvement of both strain and stress were observed comparing to control 1 and control 2 in general.

5.4 Surface Characterization

Not surprisingly, the presence of the PNIPAAM in the PDMS host films also causes changes to the surface properties of the films. These property changes were characterized by various methods including sessile drop water contact angles, XPS and ATR-FTIR as well as AFM.

5.4.1 Water Contact Angle Measurement

Figure 5.12 summarizes the advancing and receding sessile drop water contact angle data for both control and PDMS-OH IPN film surfaces. The results clearly demonstrate that the presence of the PNIPAAM affects the surface of the polymer network films. Contact angles of all IPN film surfaces were decreased relative to PDMS-OH surface indicating improvement of surface wettability. However, there were no apparent trends, either as a function of the PNIPAAM content of the membranes or as a function of the water uptake. This result is not surprising since IPN formation is primarily a bulk modification technique and while some surface modification would be expected, the incorporation of larger amounts of PNIPAAM is more likely to occur within the host polymer. Furthermore, the domain sizes of the PNIPAAM in these networks is significantly smaller than the size of the water drops used and therefore the information is likely more indicative of the global hydrophilicity / hydrophobicity of these surfaces. The relatively large error bars and significant hysteresis suggests that the surfaces are not uniform and are likely quite rough (Adamson, 1990). It is of interest that the water contact angles measured on the membrane surface exposed to water during the

preparation phase were 5° to 10° lower than those measured on the membrane surface exposed to air. This may result from the evaporation of monomer at the interface or more likely the preferential partitioning of the hydrophilic NIPAAM monomer to the water interface.

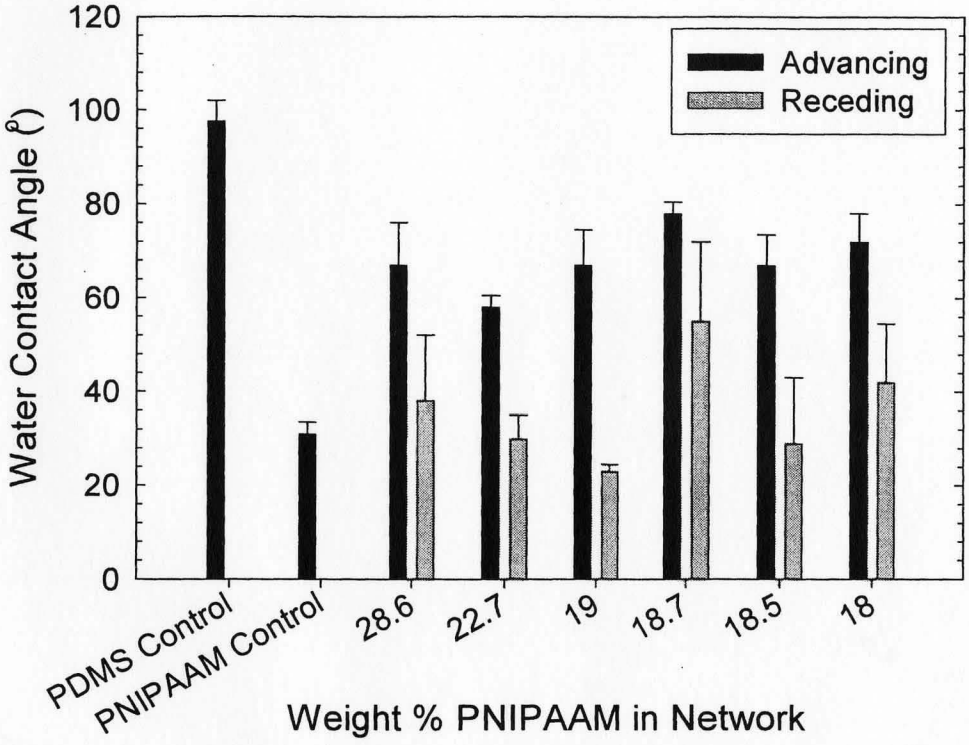

Fig. 5.12: Contact angle measurement of PDMS-OH IPN films. Error bars are standard deviations (n=3). The plots show that the water contact angles for all of the IPNs were lower than PDMS control indicating the improvement of wettibility.

5.4.2 XPS Results

The presence of PNIPAAM on the PDMS-OH IPN was confirmed by XPS analysis. The low resolution spectra of the PDMS-OH control and an IPN containing 19.5% PNIPAAM are shown in Figure 5.13 and 5.14. The presence of an N1s signal in

the spectra is indicative of the presence of PNIPAAM on the surface. Atomic compositions, summarized in Table 5.4 show that the ratio of C: O: Si, roughly 2:1:1 is as expected based on the theoretical atomic composition as shown in Figure 4.1. The trace nitrogen found in PDMS control is thought to be contamination or signal noise. Theoretically PNIPAAM contains carbon, nitrogen and oxygen in a 6:1:1 ratio (C:N:O). Therefore, the presence of PNIPAAM at the surface would result in an increase in the C1s signal, the appearance of a significant N1s signal and a decrease in the Si2p signal. As expected, there was a significant N1s signal on the IPN surfaces that was not present on the control. Furthermore, an increase in the C1s signal and decreases in the O1s and Si2p signals were noted on these samples.

However, a comparison of the N1s signal at a takeoff angle of 90° relative to that at a more surface sensitive 20° suggests that there was less PNIPAAM at the surface than slightly below the surface. This may be due to surface enrichment of the PDMS at the interface in the highly hydrophobic XPS environment. As expected from the water contact angle results, the surface compositions of air and water exposed sides of the film were different particularly at a takeoff angle of 20°. The surface exposed to water during preparation had higher N1s and C1s contents and lower Si2p contents than the corresponding surface exposed to air.

Table 5.4: Comparison of PDMS and IPN Film Low Resolution XPS Data

Element	Atom (%)					
	PDMS control		IPN—Water Exposed Surface		IPN—Air Exposed Surface	
	20°	90°	20°	90°	20°	90°
C1s	50.3	40.9	54.9	53.8	54.0	52.7
Si2p	23.5	22.0	19.5	19.5	20.7	20.4
O1s	25.6	27.8	23.9	24.3	24.7	24.9
N1s	0.6	0.8	1.7	2.4	0.6	2.0

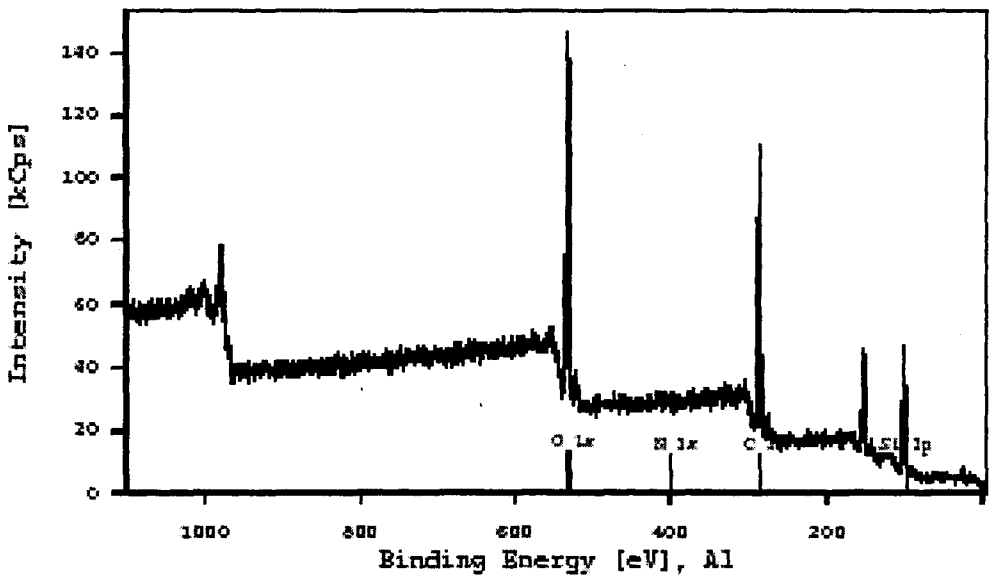

Fig. 5.13 (a)

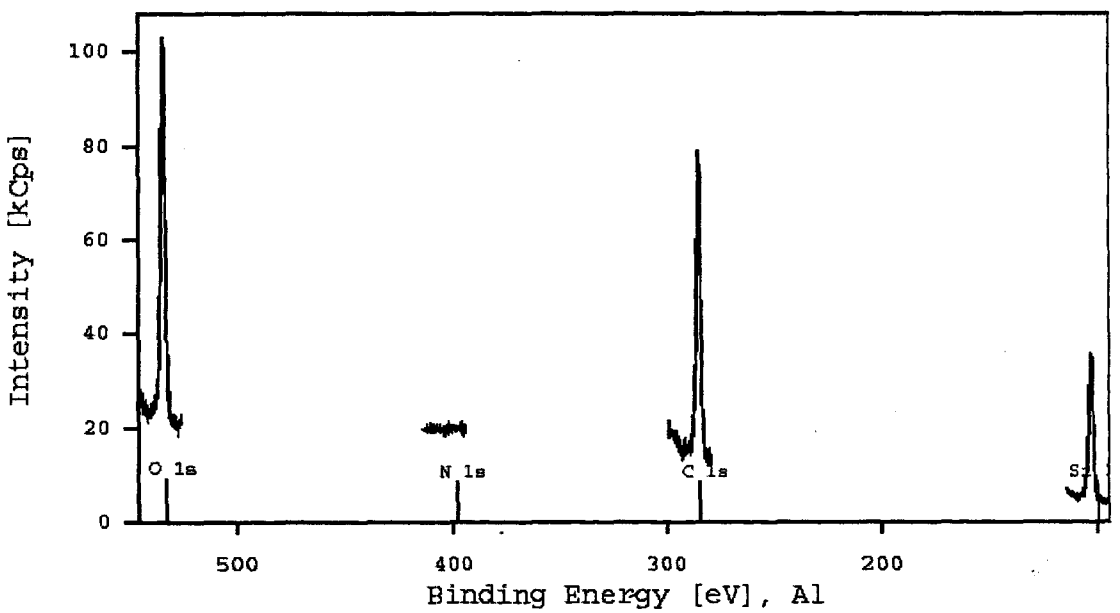

Fig. 5.13 (b):

Fig. 5.13: XPS spectrum of PDMS control. (a) 90° take off angle; (b) 20° take off angle

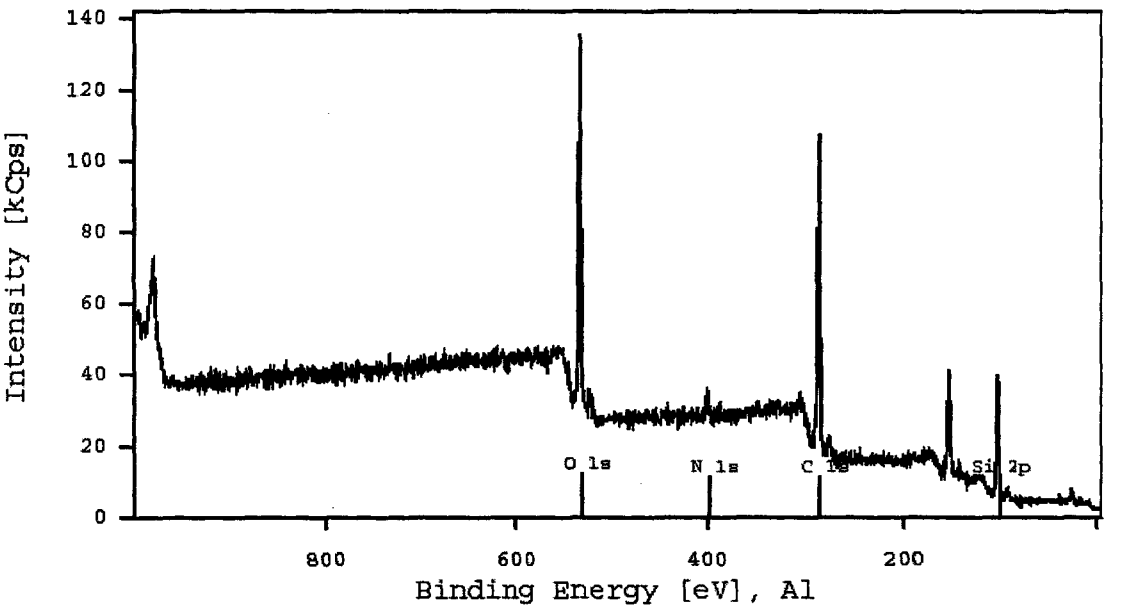

Fig. 5.14 (a):

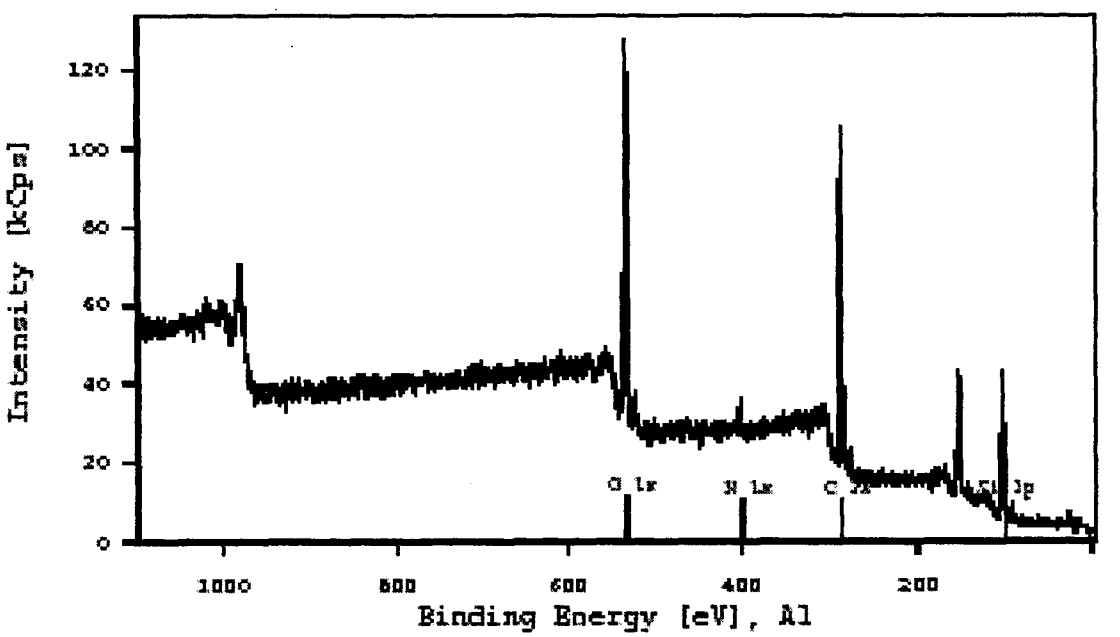

Fig. 5.14 (b):

Fig. 5.14: XPS spectrum of PDMS-OH IPN. (a): side to air, 90° take off angle; (b): side to water, 90° take off angle

5.4.3 AFM Images

The surface morphology of a PDMS-OH IPN was investigated by AFM. The atomic force microscopy images of PDMS-OH control and PDMS-OH IPN samples with different PNIPAAM contents are shown in Figure 5.15. The relatively smooth PDMS control becomes considerably rougher following network formation. This is thought to result from the presence of PNIPAAM on the surfaces of these membranes.

Roughness analysis of the membranes is shown in Figure 5.16. With an increase in the PNIPAAM content in the IPNs, there was an increase in all three of the roughness parameters shown. Furthermore, compared to the PDMS-V IPNs, the roughness of these surfaces was considerably greater. While a number of factors could contribute to this increase, it is believed that it is partly the result of the presence of greater amounts of PNIPAAM at the interface in PDMS-OH IPN.

AFM results obtained for the two sides of the membranes are shown in Figure 5.17 and Table 5.5. Consistent with the water contact angle and XPS results, there was a difference in roughness between the water and air exposed sides of the membrane. As expected, the water exposed side to water presents a much rougher appearance which is thought to be the result of the presence of more PNIPAAM domains at the interface.

Phase mode images of the PDMS-OH IPN are shown in Figure 5.18. Consistent with the tapping mode AFM images, there are significant differences between the height and phase images of the PNIPAAM containing IPN, indicating the presence of the two phases at the interface.

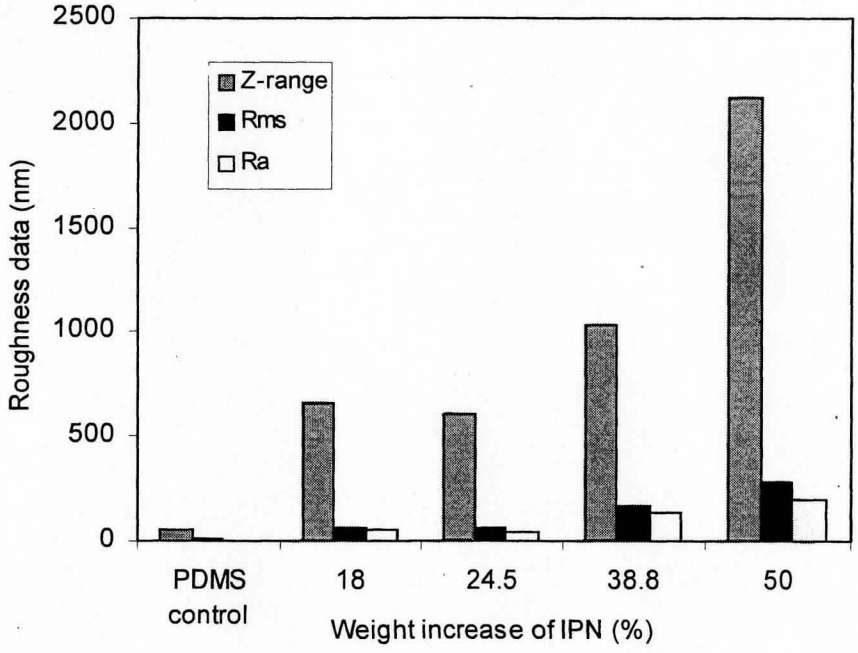

Fig. 5.16: Roughness analysis of PDMS-OH IPN AFM images.

Table 5.5:Roughness comparison of two sides of 24.5% IPN

Side	Z-range (nm)	Rms (nm)	Ra (nm)
To air	611.61	63.13	43.58
To water	2743.11	395.17	309.65

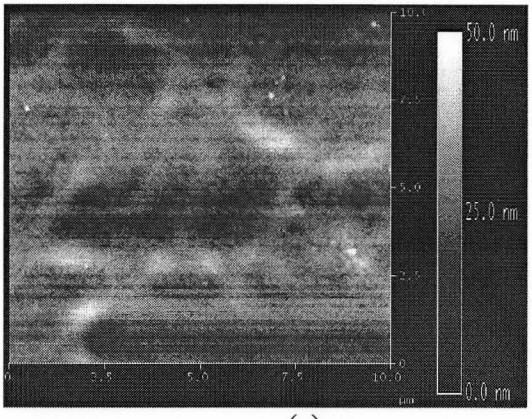

(a)

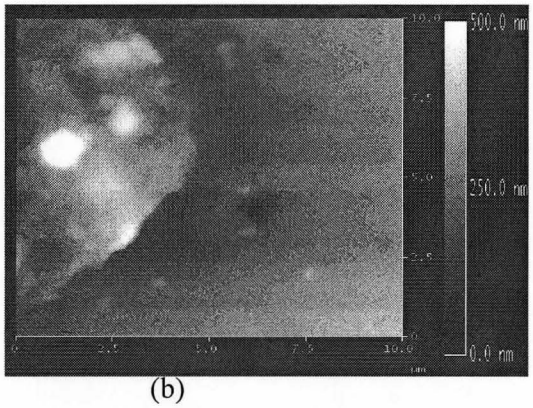

(b)

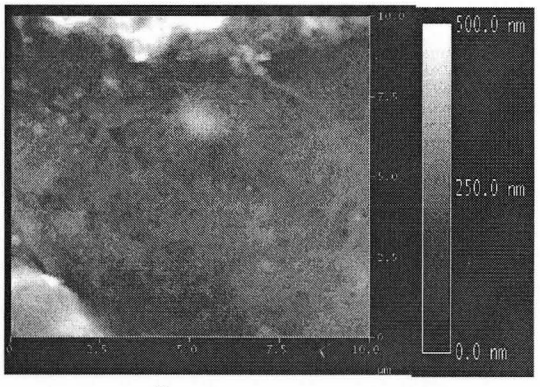

©

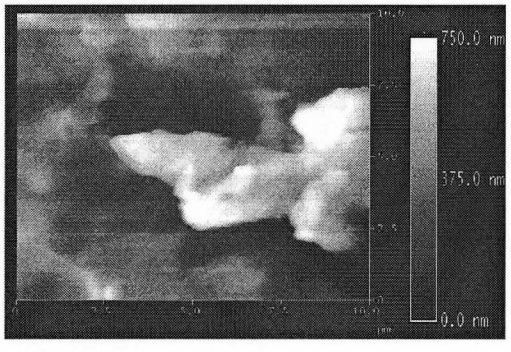

(d)

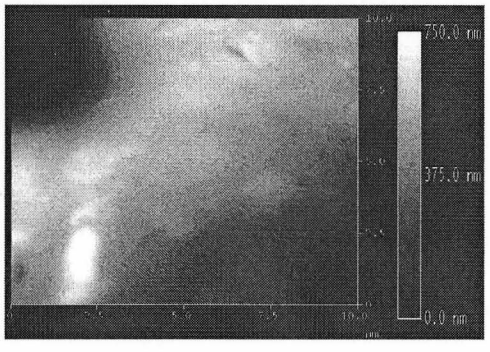

(e)

Fig. 5.15: AFM contact mode images PDMS control and PDMS-OH IPNs. (a) PDMS-OH control; (b) 18.0% PDMS-OH IPN; (c) 24.5% PDMS-OH IPN; (d) 38.8% PDMS-OH IPN; (e) 50.0% PDMS-OH IPN

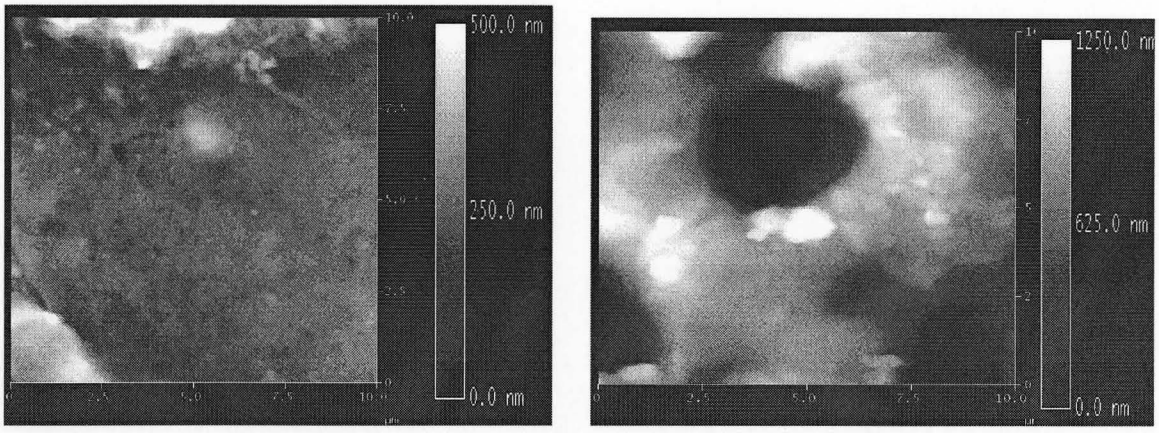

Side A Side B

Fig. 5.17: AFM contact mode images of the two sides of PDMS-OH IPNs. (a) The side to air when PDMS film was cured; (b) The side to water.

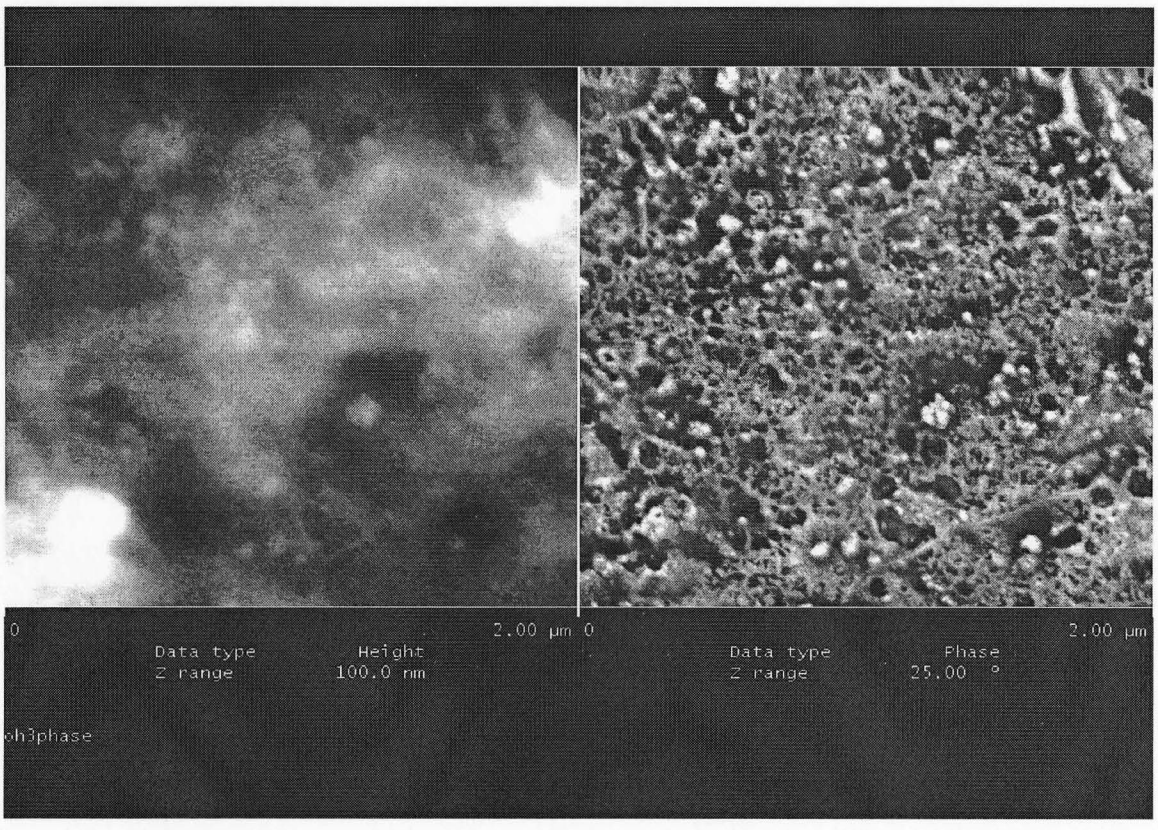

Fig. 5.18: AFM phase image of 24.5% PDMS-OH IPN. (a) height image; (b) phase image

5.4.4 ATR-FTIR Result

ATR-FTIR spectra of PDMS-OH IPNs obtained, shown in Figure 5.19, were similar to that of PDMS-V IPNs. As described in section 4.2.4.3, the peak group between 1370 cm^{-1} and 1650 cm^{-1} assigned to PNIPAAM, particularly the peak at 1640 cm^{-1} associated with C=O stretching vibration, appeared in IPN spectrum suggesting that PNIPAAM is present at the surface layer. However, since the element and bond information provided by ATR-FTIR is from 1~5μm to the surface, the XPS results provide a more accurate picture of the interface. The FTIR data combined with the XPS result which have surface sensitivity to 0~25nm can be used to provide an elemental depth profile (Ratner, 1996).

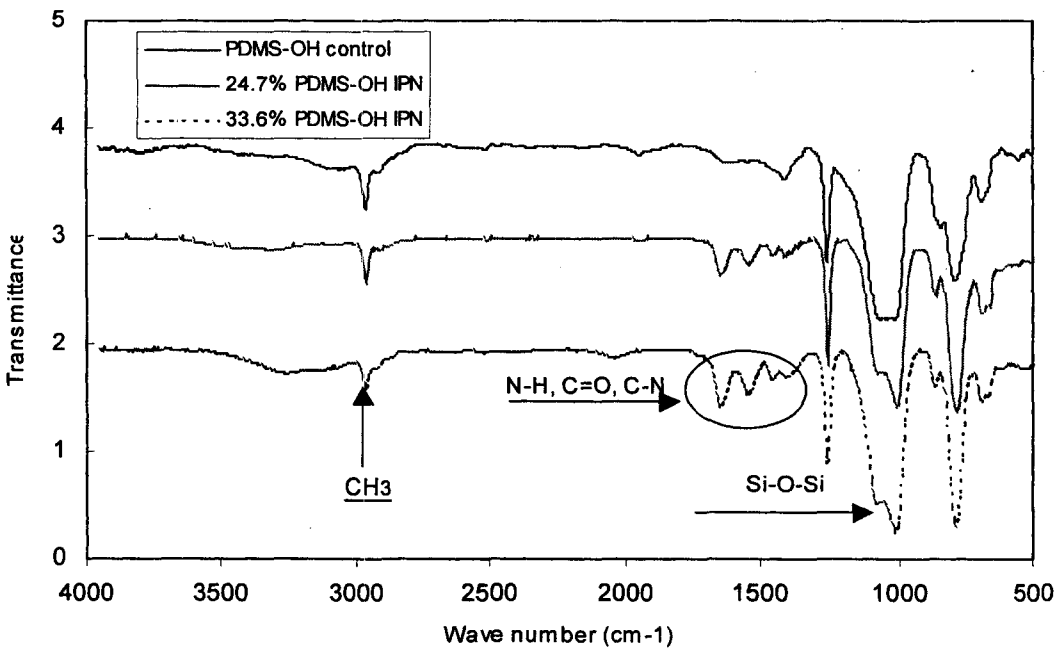

Fig. 5.19: ATR-FTIR spectra of PDMS-OH IPNs. (Resolution is 8 and scan number is 16) The spectra show peaks which corresponding adsorbance by the bonds in PNIPAAM as marked in the figure.

5.5 Glucose Permeability of PDMS-OH IPNs

Glucose permeation results for the various networks are summarized in Table 5.6. While PDMS is essentially glucose insoluble, depending on the fabrication method and the PNIPAAM content, it was possible to synthesize networks with significant glucose permeability, comparable to that of the native cornea. Glucose permeability of the networks is expected to depend on a number of factors including the presence of PNIPAAM at the surface, the connectivity of the PNIPAAM phase in the host PDMS polymer and the size of the PNIPAAM domains. While the amount of PNIPAAM in the polymer network does affect some of these parameters, it cannot be used as the only measure of glucose permeability. Vinyl terminated PDMS / PNIPAAM polymer networks containing as much as 45% PNIPAAM could be formed using the methods described. However, these networks showed limited water uptake and remained virtually impermeable to glucose. TEM results clearly shown that the host PDMS-V IPNs in this case has a much tighter structure and that the domain size of the PNIPAAM in the resulting networks is significantly smaller, resulting in glucose impermeability. Similarly, networks of limited glucose permeability were fabricated using PDMS-OH as the host and cured in the absence of solvent.

When the PDMS-OH was cured in the presence of the solvent, resulting in the formation of a more open network and therefore larger PNIPAAM domains, permeabilities on the order of 10^{-7} cm^2/s were achievable. These results compare with

that for the native cornea which is estimated based on literature results to be between 10^{-6} and 10^{-7} cm^2/s (McCarry et al., 1990). However, again it should be noted that neither the PNIPAAM content of the polymer nor the water uptake could be used to predict the glucose permeability. While the very low glucose permeability was unexpected for the membranes containing 50% + PNIPAAM, it seems likely that the surface and or bulk connectivity of these membranes is not adequate for significant transport of glucose through the membranes. Furthermore, from the data in Table 5.6 and with all other variables held constant, it was found thickness strongly influences the glucose permeability. In all cases, membranes with a thickness greater than 1 mm were found to have significantly decreased permeability. This is thought to be caused by the formation of a thicker skin layer when a thicker PDMS host is used. TEM images in Figure 5.8 provided the skin layer evidence clearly. In all cases, the membranes, as cast, were significant thicker than would be required for the intended artificial cornea application. Under optimal conditions, IPN films with permeabilities of 10^{-7} cm^2/s to 10^{-8} cm^2/s can be prepared. However, there is a significant deviation noted in the final measured permeability of membranes prepared in a similar fashion. This is likely the result of the complicated and multi-step nature of the fabrication process. Important determinants of the permeability of the networks include the amount of solvent present during the curing phase for the PDMS host, as well as the thickness of the membrane.

Table 5.6: Glucose Permeation Results of Various IPN Films

PDMS Host	Solvent Used in PDMS Cure (wt%)	PNIPAAM Content in IPN (wt%)	Water Uptake of IPN (%)	Thickness (mm)	Permeability (cm^2/s)
PDMS-vinyl	0	0	0		~0
PDMS-vinyl	0	45.5			~0
PDMS-OH	0	28.1	21.2		~0
PDMS-OH	66.7	50.9	30.7		2.52×10^{-12}
PDMS-OH	87.5	21.8	30.9		0.63×10^{-7}
PDMS-OH	87.5	25.7	29.5	0.8	1.42×10^{-9}
PDMS-OH	87.5	27.8	34.6	1.8	~0
PDMS-OH	87.5	34.2	40.5	0.6	0.71×10^{-7}
PDMS-OH	85.0	33.8	35.0	0.6	2.12×10^{-9}
PDMS-OH	87.5	29.2	34.7	0.3	0.71×10^{-8}
PDMS-OH	87.5	21.8	30.9	0.3	0.63×10^{-7}
PDMS-OH	82.4	32.4	23.4	0.3	0.14×10^{-7}
PDMS-OH	66.7	50.9	30.7	1.2	2.52×10^{-12}
PDMS-OH	0	28.1	21.2	0.6	~0

5.6 Temperature Effect on PDMS-OH IPN Properties

The effect of changing the temperature around the PNIPAAM LCST and its effect on the water uptake of the networks and on their glucose permeability was performed. Differential scanning calorimetry was used to determine the phase transition temperatures.

5.6.1 Effect of Temperature on Equilibrium Water Content

The change in the water uptake of the PDMS-OH IPNs with increasing temperature is shown in Figure 5.20. The profile is very similar to that noted for the PDMS-V IPNs as expected. However, the range of phase transitions noted with the PDMS-OH IPNs is broader, but the change at the transition temperature is more abrupt.

The LCST of the IPNs is much broader than for pure PNIPAAM. With increasing PNIPAAM content, the LCST phenomenon becomes more obvious and as expected the 50% PNIPAAM IPN demonstrated the sharpest temperature response. Furthermore, a PDMS-OH semi IPN showed almost no thermal response.

The LCST of PNIPAAM containing polymers is caused by the hydrophobic and hydrophilic balance of PNIPAAM polymer chains. In the PDMS-OH/PNIPAAM IPNs, due to interpenetration and the presence of smaller domains, the interaction between PDMS and PNIPAAM networks is stronger. The hydrophobic PDMS will interact with the hydrophobic regions of PNIPAAM chains, resulting in LCST behavior at lower temperatures than in the pure PNIPAAM polymers. The decrease in water uptake decrease of the IPNs was influenced by 3 factors: water interaction, PDMS elasticity and interaction between PDMS and PNIPAAM. As the temperature is increased, changes in the PDMS/PNIPAAM water swollen networks alters these complex interactions resulting in decreased water interaction and dissociation.

5.6.2 Different Scanning Calorimetry for Determination of Tc

Consistent with water uptake results, the DSC spectra, depicted in Figure 5.21, show a transition at about 28°C, slightly lower than that noted for pure PNIPAAM. Compared with PNIPAAM homopolymers, the temperature response begins earlier, with a broader transition. However, as the PNIPAAM content of the IPNs is increased, the peaks become sharper. As with the PDMS-V IPNs, there was no significant shift in temperature as a function of the PNIPAAM content.

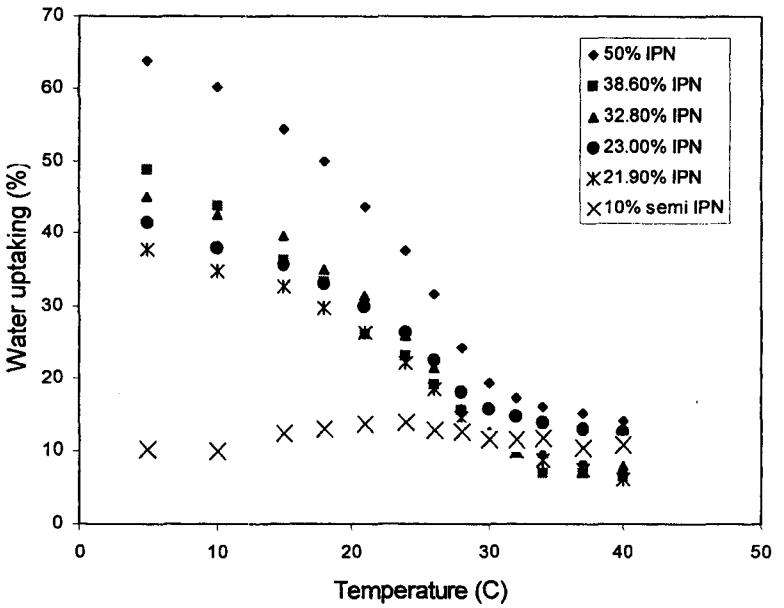

Fig. 5.20: EWC of PDMS-OH IPNs at different temperature. All swelling was performed in deionized water for 12 hours at different temperatures. It can be seen that LCST phenomenon still remained in the IPNs, with more PNIPAAM in IPNs resulting in more obvious water swelling ratio change at phase transition temperature.

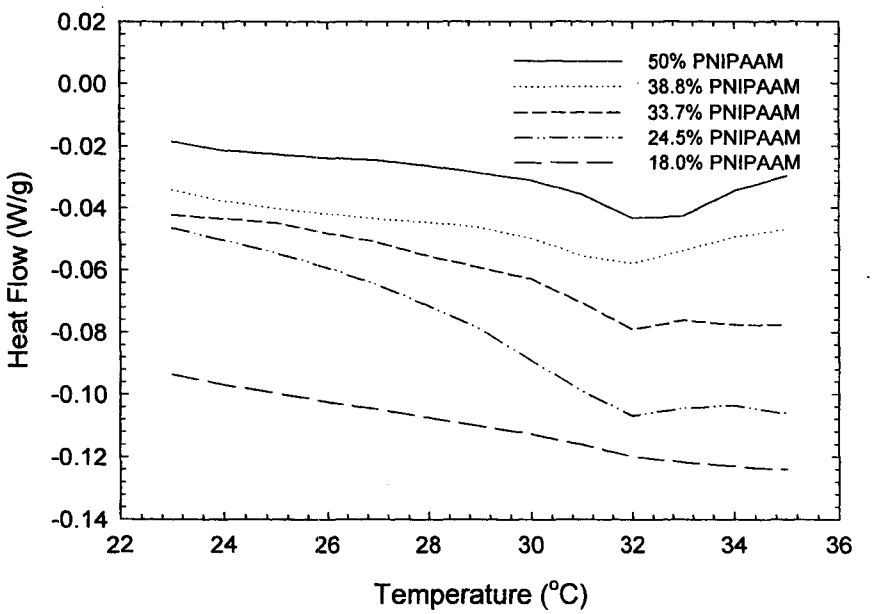

Fig. 5.21: DSC result of LCST determination for PDMS-OH IPNs. Spectra were scanned at 1°C/min ramp rate with 30 cc/min N_2 purge. Before testing, all samples were fully swollen in water at 5° C. Note the clear phase transition at about 32 ° C, but the heat capacity change started very early.

5.6.3 Effect of Temperature on Glucose Permeation

The effect of temperature on the glucose permeability of the networks was also examined. Permeation cells were placed into a controlled temperature water bath. As shown in Figure 5.22, there was an abrupt change of glucose permeability at 27°C. As the temperature was increased above this point, permeability continued to decrease. This result provides additional evidence that the glucose transport in these membranes is determined by the size and nature of the PNIPAAM phase. However it is interesting to note that that a measurable glucose permeability remains in these polymers. Furthermore, it appears that at higher temperatures, particularly above the LCST, the glucose permeability is less dependent on the PNIPAAM content of the polymers.

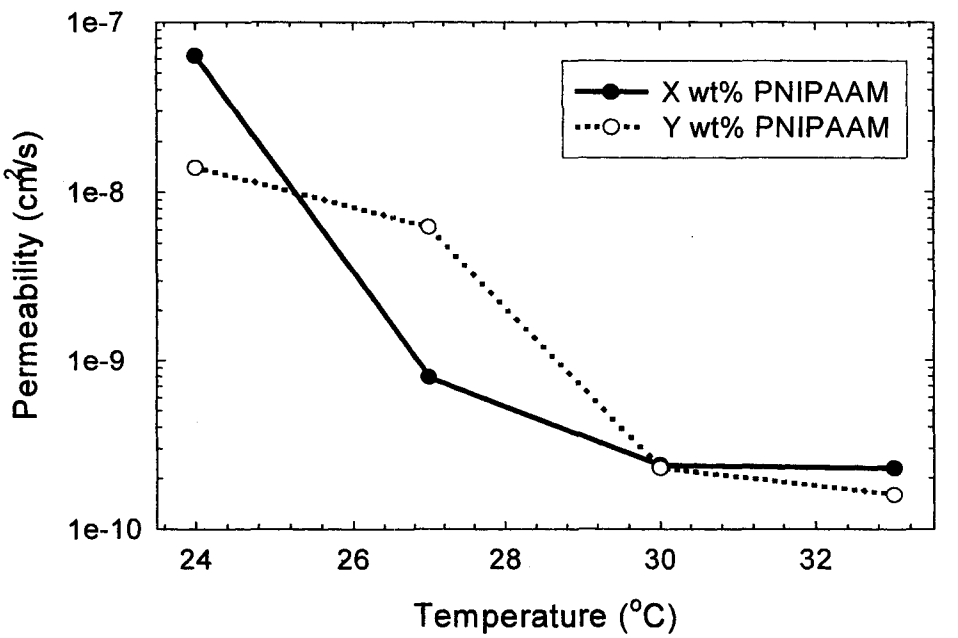

Fig. 5.22: LCST effect on glucose permeability coefficients of PDMS-OH IPNs x=21.8% PNIPAAM content and 30.9 % water uptake; Y=32.4% PNIPAAM% and 23.4% water uptake

5.7 Summary for PDMS-vinyl/PNIPAAM IPN

PDMS-OH IPNs were prepared. Curing the PDMS-OH films in the presence of solvent resulted in a more open PDMS host and higher levels of PNIPAAM in the resultant networks. This PNIPAAM was found to have a domain size that was suitable for significant water uptake and for glucose permeation on the order of 10^{-7} cm^2/s, that similar to that observed in the native cornea. The composition of network was confirmed by FT-IR and DSC analysis. FT-IR results clearly showed the presence of peaks associated with both polymers. The differential scanning calorimetry measurements showed that the network polymers had thermal transitions appropriate for PNIPAAM. IPN formation also resulted in changes to the surface. XPS results were consistent with the presence of PNIPAAM at the surface of these polymers. Less surface sensitive R-IR results showed fingerprint peaks for PNIPAAM, demonstrating that PNIPAAM was present at the surface. The AFM images revealed a topography change caused by PNIPAAM. Furthermore, the surface of the film exposed to water during network formation showed significantly more PNIPAAM in all measurements. TEM images illustrated that continuous PNIPAAM channels were formed. Interestingly, the network polymers were significantly stronger in both the wet and dry states than unmodified PDMS control polymers. The LCST phenomenon of pure PNIPAAM still remained in the IPN materials and was more obvious than for the PDMS-V IPN.

6. CONCLUSIONS AND RECOMMENDATIONS

6.1 Conclusions

- Novel PDMS/PNIPAAM composite polymer networks were successfully prepared using the interpenetrating polymer network method to improve glucose permeability of PDMS. Three kinds of PDMS/PNIPAAM composite polymer network materials were prepared. While Semi-IPNs showed a slight wettability improvement, mechanical strength decreased. This material was not suitable for further study due to its low water uptake and mechanical strength. The PDMS-V/PNIPAAM IPNs had improved water uptake and increased tensile stress and strain and may therefore be useful in biomaterials applications. A PDMS-OH/PNIPAAM IPN was successfully synthesized with reasonable physical properties and a glucose permeability of $10^{-7}cm^2/s$ which comparable to the native cornea.
- FT-IR, DSC and weight increase results confirmed the presence of PNIPAAM in the IPNs. The FI-IR spectra of the IPNs showed peaks that could be assigned to PDMS and PNIPAAM respectively. DSC results of the new networks showed the glass transition of PNIPAAM.
- The polymerization kinetics of PDMS/PNIPAAM IPN were studied and the reaction conditions relative to the properties were optimized. It was found that 12.5% PDMS oligomer in solvent produced the best PDMS-OH host polymer. NIPAAM polymer conditions for optimal membrane synthesis included 9 hours swelling in a 35% (wt) NIPAAM solution, and 12 hours polymerization time. In

this case, an IPN with a PNIPAAM content of approximately 35% IPN with a permeability of approximately 10^{-7} cm^2/s was synthesized. Contact angle measurements showed an increase in the hydrophilicity for both PDMS-V and PDMS-OH IPNs compared to the PDMS control surface. This was particularly true for the PDMS-OH IPNs. Nitrogen was observed in the XPS spectra of the IPNs and IR adsorption of acrylamide group in ATR-FTIR spectra of the IPNs provided evidence of the presence of PNIPAAM on the surfaces. The topography of the IPN surfaces were investigated by AFM and the images showed rougher surface morphology thought to be caused by PNIPAAM on the surfaces.Water uptakes of up to 40% for PDMS-OH IPN and 15% for PDMS-V IPNs were measured. This result agreed well with the glucose permeability of the IPNs. TEM images demonstrated the dual continuous phases of PDMS and PNIPAAM in IPNs which provided the basis for glucose and oxygen permeation through the membranes. Significant improvements to the mechanical properties of networks were observed. There were clear increases in the measured tensile stress and strain as the PNIPAAM content of the IPNs increased, particularly with IPNs containing 25-35% PNIPAAM. The mechanical stress at maximum load was approximately 2 MPa for PDMS-OH IPN and 9 MPa for PDMS-V IPNs. Glucose permeability, water uptake response with LCST temperature and DSC detection of Tc phase transition suggested the LCST phenomenon of pure PNIPAAM still remained in the IPNs. This could lead to potential application as a drug delivery system.

6.2 Recommendations for Future Study

1. To fulfill the specific applications which require LCST response at physiologically relevant temperature, adjustment of the LCST can be achieved by in situ copolymerization of the NIPAAM with the other more hydrophilic monomers such ethyl glycol or acryl amide. For cases in which an LCST response is not desired, copolymerization with other polymers or replacement of PNIPAAM in the IPN system could be used.
2. To obtain higher glucose permeability of PDMS based material, commercially available PEO-PDMS-PEO tri-block copolymers should be examined, allowing for the introduction of functional end groups for further curing.
3. Surface wettability of the IPNs may be improved by surface grafting with various hydrophilic moieties.
4. Since the PDMS/PNIPAAM IPN material has a potential application in drug delivery, drug loading and drug release studies would be of interest.
5. Biocompatibility of the materials should be investigated including measurement of protein adsorption to the materials and assessment of interactions with cells.

REFERENCES

Abbasi F., Mirzadeh H. and Katbab A.A., Review: modification of polysiloxane polymers for biomedical applications, Polymer International, 50: 1279-1287, 2001

Abbasi F., Mirzadeh H., and Katbab A.A., Comparison of viscoelastic properties of polydimethyl siloxane / poly (2-hydroxyethyl methacrylate) IPN's with their physical blends, Journal of Applied Polymer Science, 86: 3480-3485, 2002

Abbasi F., Mirzadeh H., and Katbab A.A., Sequential interpenetrating polymer networks of poly (2-hydroxyethyl methacrylate) and polydimethylsiloxane. J Applied Polymer Science, 85: 1825-1831, (2002)

Adamson A.W., The Solid-Liquid Interface — Contact Angle in Physical Chemistry of Surfaces, Fifth Edition, A Wiley – Interscience Publication, p379, 1990

An J. H. and Sperling L.H., in Cross-Linker Polymer: Chemistry, Properties, and Ionomers, Utracki, L. A. Eds, ACS Symposium Series 395, American Chemical Society, 1989

Arkles B., Look what you can make out of silicones, Chemtech, 13: 542-555, 1983

Aucoin L., Griffith C. M., Pleizier G., Deslandes Y., Sheardown H., Interactions of corneal epithelial cells and surfaces modified with cell adhesion peptide combinations, Journal of Biomaterials Science: Polymer Edition, 13(4): 447-462, 2002

Bae You Han, Okano Teruo, Kim Sung Wan, Temperature dependence of swelling of crosslinked poly(N,N-alkyl substituted acrylamides) in water, Journal of Polymer Science Physics, 28: 923-936, 1990

Baker, John P., Siegel, Ronald S., Enzyme-mediated oscillatory drug release through hydrogel membranes, Materials Research Society Symposium Proceedings, 394(Polymers in Medicine and Pharmacy): 119-30, 1995

Belanger M. and Marois Y., Hemocompatibility, biocompatibility, inflammatory and in vivo studies of primary reference materials low-density polyethylene and polydimethylsiloxane: a review, Journal of Biomedical Material Research, 58: 467-477, 2001

Belanger MC., Marois Y, Roy R., Mehri Y., Wagner E., Zhang Z., King MW, Yang M.C., Guidoin R., Selection of a polyurethane implantable artificial heart: blood compatiblity and biocompatibility studies, Artificial Organs, 24: 879-888, 2000

Binder K. and Frisch H.L., Phase stability of weakly crosslinked interpenetrating polymer networks, Journal of Chem. Phys., 81: 2126-2136, 1984

Boileau S., Bouteiller L., Khalifa R.B., Liang Y., Teyssie D., Polycarbonate-polysiloxane based interpenetrating networks, Polymer Preprints, 39(1): 457-458, 1998

Borsig E. and Fiedlerova A., Structure and properties of an interpenetrating polymer network-like system consisting of polystyrene-polyethylene: Synthesis, elastomeric and thermoanalytical characterization, Polymer, 34(22): 4785-4792, 1993

Brazel C.S. and Peppas N.A., Transport in hydrophilic polymer gels: Applications in controlled release, Macromolecules, 28: 8016, 1995

Burczak K, Fujisato T, Hatada M, Ikada Y, Protein permeation through poly(vinyl alcohol) hydrogel membranes. Biomaterials, 15(3): 231-8, 1994

Burczak K, Rosiak J., Polymeric materials for biomedical purposes obtained by radiation methods. V. hybrid artificial pancreas (abstract), Polmery W Med Ycynie, 24(1-2): 45-55, 1994

Chandy T. and Sharma C. P., Glucose-responsive insulin release from poly(vinyl alcohol)-blended polyacrylamide membranes containing glucose oxidase, Journal of Applied Polymer Science, 46: 1159-1167, 1992

Chang Patricia Chuen-Thuen, Lee Shyh-Dar, Hsiue Ging-Ho, Heterobifunctional Membranes by Plasma Induced Graft Polymerization as an Artificial Organ for Penetration Keratoprosthesis, Journal of Biomedical Materials Research, 39(3): 380-389, 1998

Chen JP, Chu DH, Sun YM, Immobilization of α-amylase to temperature-responsive polymers by single or multiple point attachments, Journal of Chemical Technology Biotechnology, 69: 421-428, 1997

Chiang W. Y. and Chang D. M., Preparation and characterization of polyurethanes/allyl novolac resin simultaneous interpenetrating network, European Polymer Journal, 31(8): 709-714, 1995

Chirila T. V., Crawford G.J., Constable I.J., Russo A.V., Australian Patent No. 650,156, 1994a

Chirila T. V., Crawford G.J., Constable I.J., Russo A.V., U.S. Patent No. 5,300,116, 1994b

Chirila T. V., Crawford G.J., Constable I.J., Russo A.V., U.S. Patent No. 5,458,819, 1995

Chirila T. V., Hicks C.R., Dalton P.D., Vijayasekaran S., Lou X., Hong Y., Clarton A.B., Ziegelarr B.W., Fitton J. E., Platten S., Crawford G.J., Constable I.J., Artificial cornea, Prog. Polym. Sci., 23: 447-473, 1998

Chirila T. V., Vijayasekaran S., Horne R., Chen Y. C., Dalton P. D., Constable I. J., Crawford G. J., Interpenetrating polymer network (IPN) as a permanent joint between the elements of a new type of artificial cornea, Journal of Biomaterials Research, 28(6), 745-753, 1994c

Dohlman C.H., Physiology of The Cornea, in The cornea ---Scientific Foundations and Clinical Practice, Ed., Gilbert Smolin et al. p3,1983

Donatelli A. A., Sperling L. H., Thomas D. A., A semiempirical derivation of phase domain size in interpenetrating polymer networks, Journal of Applied Polymer Science, 21: 1189-1197, 1977

Donatelli A. A., Sperling L. H., Thomas D. A., Interpenetrating polymer networks based on SBR/PS: 2. Influence of synthetic detail and morphology on mechanical behavior, Macromecule, 9: 676-680, 1976

Dumbleton K., Noninflammatory silicone hydrogel contact lens complications, Eye Contact Lens, 29(1): 186-189, 2003

Eeckman F., Moes A.J., Amighi K., Evaluation of a new controlled-drug delivery concept based on the use thermoresponsive polymers, International Journal of Pharmaceutics, 241: 113-125, 2002

Ertel S.I., Ranter B.D., Kaul A., Schway MB, Horbeet T. A., In vivo study of the intrinsic toxicity of synthetic surfaces to cells, Journal of Biomedical Material Research, 28: 667-675,1994

Falcetta J.J., Friends G. D., Niu G.C., Ger Offen Pat: 2-518-904-1975, 1975

Feil H., Bae Y. H., Feijen J., Kim S.W., Effect of comonomer hydrophilicity and ionization on the lower critical solution temperature of N-isopropylacrylamide copolymers, Macromolecules, 26(10): 2496-2500, 1993

Frisch K. C. and Klempner D., Recent Advance in Interpenetrating Polymer Network, Polymer Engineering and Science, vol.22, No. 17, pp1143-1152, 1982

Gelest Inc., Brochure of PDMS

Grulke E.A., Solubility Parameter Values in Polymer Handbook, eds. J. Brandrup et al, A wiley – interscience Publication, 1999

Guilherme M.R., Toledo E.A., Rubira A.F., Muniz E.C., Water affinity and permeability in membranes of alginate-Ca^{2+} containing poly(n-isopropylacrylamide), Journal of Membrane Science, 210: 129-136, 2002

Guyton A.C., Hall J. E., Ed., Textbook of Medical Physiology, 9th Ed, Philadelphia: W.B. Saunders, p583, 1996

Haaf F., Breuer H., Echte A., Schmitt B. J., Stabenow J., Kunststofflab G., Structure and properties of rubber reinforced thermoplastics, Journal of Scientific & Industrial Research, 40(10): 659-79, 1981

Heim P., Wrotechi M. A., Gaillard P., High impact cast sheets of poly(methyl methacrylate) with low level of polyurethane, Polymer, 34(8): 1654-1660, 1993

Hiroshi Inomata, Shuichi Goto, and Shozaburo Saito, Phase transition of N-substituted acrylamide gels, Macromolecules, 23:4887-4888, 1990

Hoch G., Anuj C., Radke C. J., Permeability and diffusivity for water transport through hydrogen membranes, Journal of Membrane Science, 214(2): 199-209, 2003

Hoffman A. S., Hydrogels for biomedical applications, Advanced Drug Delivery Review, 54: 3-12, 2002

Hoffman A.S., Affrassiabi A., Dong L.C., Thermally reversible hydrogels: Delivery and selective removal of substances from aqueous solution, Journal of Controlled Release, 4: 213-222, 1986

Honda T., Cockrell J. V., Kito Y., Gibson W. H., Akutsu T., Refinement in application of total artificial heart, with improvement in survival and histopathological findings, Journal of Thoracic and Cardiovascular Surgery, 70(2): 214-222, 1975

Honda T., Kito Y., Gibson W. H., Nemoto T., Cockrell J. V., Akutsu T., One 25 day survivor with total artificial heart, Journal of Thoracic and Cardiovascular Surgery, 69(1): 92-101, 1975

Hsiue G. H., Chang R.W., Wang C.H., Lee S.H., Development of in situ thermosensitive drug vehicles for glaucoma therapy, Biomaterials, 24: 2423-2430, 2003

Hsiue G. H., Hsu S.H., Yang C.C., Lee S.H., Yand I.K., Preparation of controlled release ophthalmic drops, for glaucoma therapy using thermosensitive poly(N-isopropylacrylamid), Biomaterials, 23: 457-462, 2002

Hsiue G. H., Lee S. D., Wang C. C., Shiue M. H. Chang P. C., pHEMA-modified silicone rubber film towards improving rabbit corneal epithelial cell attachment and growth, Biomaterials, 14(8): 591-597, 1993a

Hsiue Ging Ho, Lee Shyh Dar, Wang Chee Chan, Chang Patricia Chuen-Tsuei, The effect of plasma-induced graft copolymerization of on silicone rubber towards improving corneal epithelial cells growth, Journal of Biomaterials Science, Polymer Edition, 5(3): 205-220, 1993b

Ito Yoshihiro, Chen Guoping, Guan Yanqing, Imanishi Yukio, Patterned immobilization of thermoresponsive polymer, Langmuir, 13(10): 2756-2759, 1997

Jan K. and Luca F., Phase Structure Coarsening in Polymer Blends: Predicted Effects of the Phase Duality Interval on Selected Physical Properties, Macromolecular Materials and Engineering, 283: 41-47, 2000

Jeong B., Kim S.W., Bae Y.H., Thermosensitive sol-gel reversible hydrogels, Advanced Drug Delivery Review, 54: 37-51, 2002

Kanazawa Hideko, Kashiwase Yuki, Yamamoto Kazuo, Matsushima Yoshikazu, Kikuchi Akihiko, Sakurai Yasuhisa, Okano Teruo, Temperature-responsive liquid chromatography. 2. Effects of hydrophobic groups in N-Isopropylacrylamide copolymer-modified silica, Analytical Chemistry, 69(5): 823-830, 1997

Kazunori Yamada, Tadanori Sato, Shigeaki Tatekawa, Mitsuo Hirata, Membrane properties of polyethylene films photografted with hydrophilic monomers, Polymer Gels and Networks, 2(3-4): 323-31, 1994

Kazunori Yamada, Toyokichi Ebihara, Takeshi Gondo; Koichi Sakasegawa, Hirata Mitsuo, Membrane properties of porous and expanded poly(tetrafluoroethylene) films grafted with hydrophilic monomers and their permeation behavior, Journal of Applied Polymer Science, 61(11): 1899-1912, 1996

Kim I.S., Jeong Y.I., Cho C.S., Kim S.H., Thermo-responsive self-assembled plymeric micelles for drug delivery in vitro, International Journal of Pharmaceutics, 205: 165-172, 2000

Kim S. Y., Cho S.M., Lee Y.M., Kim S.J., Thermo- and pH-responsive behavior of graft copolymer and blend based on chitosan and N-isopropylacrylamide, Journal of Applied Polymer Science, 78: 1381-1391, 2000

Kim S. J., Shin Mi Seon, Synthesis and characteristics of interpenetrating polymer network hydrogels based on silicone and poly(vinyl alcohol), (Abstract), Key Engineering Materials, 198-199 (Functional Biomaterials): 301-307, 2001

Kim So. Yeon., Kanamori Toshiyuki, Shinbo Toshio, Preparation of thermal-responsive poly(propylene) membranes gragted with N-isopropylacrylamide by plasma induced polymerization and their water permeation, Journal of Applied Polymer Science, 84: 1168-1177, 2002

Klein A.J., Interpenetrating polymer networks, Advanced Materials & Processes, 7: 25-31, 1986

Klempner D., Interpenetrating Polymer Networks, American Chemical Society 239, Washington, DC, 1994

Klyce S.D., Structure and Function of the Cornea, in The Cornea, Herberte. Kaufman et al., Ed., Butterworth-Heinemann Publication, p3 , 1998

Knodo A., Kaneko T., Higashitani K., Development and application of thermosensitive immunomicrospheres for antibody purification, Biotech Bioeng, 44: 1-6, 1994

Kono K., Kawakami K., Morimoto K., Takagisshi, T., Effect of hydrophobic units on the PH-responsive release property of polyelectrolyte complex capsules, Journal of Applied Polymer Science, 72:1763-1773, 1999

Kwon O. H., Kikuchi M., Yamato M., Sakurai Y.S., Okano T., Rapid cell sheet detachment from poly(N-isopropylacrylamide)-grafted porous cell culture membranes, Journal of Biomedical Materials Research, 50: 82-89, 2002

Lai Y., Surface wettable silicone hydrogels for prosthetics, WO: 9 323 774, PCT Int. Appl., 1993

Lai Y.C., Valint P.L. Jr. Control of properties of silicone hydrogels by using a pair of hydrophilic monomers, J Applied Polymer Science, 61: 2051-2058, 1996

Lee D.S., Jung D.S., Kim T.H. and Kim S.C., Gas transport in polyurethane-polystyrene interpenetrating polymer network membranes: Effect of crosslinked state and annealing, Journal of Membrane Science, 75: 15-27, 1992

Lee D.S., Kang W.K., An J.K. and Kim S.C.,Gas transport in polyurethane-polystyrene interpenetrating polymer network membranes: Effect of synthesis temperature and molecular structure variation, Journal of Membrane Science, 60: 233-252, 1991

Lee Shyh-Dar, Hsiue Ging-Ho, Kao Chen-Yu, Chang Patricia Chuen-Tsuei, Artificial cornea: surface modification of silicone rubber membrane by graft polymerization of pHEMA via glow discharge, Biomaterials, 17(6): 587-595, 1996

Legeais J. M., Renard G., Parel J. M., Savoldelli M., Pouliquen Y., Keratoprosthesis with biocolonizable microporous fluorocarbon haptic. Preliminary results in a 24-patient study. Archives of Ophthalmology, 113(6): 757-763, 1995

Legeais J. M., Rossi C., Renard G., Salvoldelli M., D'Hermies F., Pouliquen Y. J., A new fluorocarbon for keratoprosthesis, Cornea, 11(6): 538-545, 1992

Leoncio G., Characterization of biomaterials with NMR, Materials Research Society Symposium Proceedings, 217: 49-54, 1991

Li J., Zhai M., Yi M., Gao H., Ha H., Radiation graftign of thermo-sensitive poly(N-isopropylacrylamide) onto silicone rubber, Radiation Physics and Chemistry, 55:173-178, 1999

Liang L., Feng X., Peurrung L., Viswanathan V., Temperature-sensitive membranes prepared by UV photopolymerization of N-isopropylacrylamide on a surface of porous hydrophilic polypropylene membranes. Journal of Membrane Science 162(1-2): 235-246, 1999

Liang L., Feng X., Perrung L., Viswanathan V., Temperature-sensitive membranes prepared by UV photopolymerization of N-isopropylacrylamide on a surface of porous hydrophilid poly propylene membranes, Journal of Membrane Science, 162: 235-246, 1999

Liang L.,Rieke P.C., Liu J., Fryxell G. E., Young J. S., Engelhrd M. H., and Alford K. L., Surfaces with reversible hydrophilic/hydrophobic characteristics on cross-linked poly(N-isopropylacrylamide) hydrogels, Langmuir, 16: 8016-8023, 2000

Ling G.N., Hydration of macromlecules. In Water and Aqueous Solutions, Ed. T.A. Horne, J. Wiley, New York, p663-700, 1972

Ling G.N., Solute exclusion by polymer and protein dominated water: correlation with results of nuclear magnetic resonance (NMR) and calorimetric studies and their significance for understanding of the physical state of water in living cells, Scanning Microscopy, 2: 871-884, 1988

Liou Feng Jyh, Wang Yng Jiin, Preparation and characterization of crosslinked and heat-treated PVA-MA films, Journal of Applied Polymer Science, 59(9): 1395-403, 1995

Lipatov Y. S., Peculiarities of self-organization in the production of interpentrating polymer networks, JMS- Review Macromolcule Chem. Phys.. C30(2): 209-232, 1990

Lopez-Alemany A., Compan V., and Refojo M.F., Porous structure of PurevisionTM versus Focus® Night and DayTM and conventional hydrogel contact lenses. Journal of Biomedical Material Research (Appl Biomaterial), 63: 319-325, 2002

Louai A., Sarazin D., Pollet G., FrancoisJ., Moreaux F., Effect of additives on solution properties of ethylene oxide-propylene oxide statistical copolymers, Polymer, 32(4): 713-720, 1991

Lowe T. L., Benhaddou M., Tenhu H., Partially fluorinated thermally responsive latices of linear and crosslinked copolymers, Journal of Polymer Science B: Polymer Physics, 36: 2141-2152, 1998

Mark J.E., Synthesis and characterization of polymer networks made from poly(ethylene oxide) and polysiloxane, Macromolecular Chemistry, 4: 266-268, 1990

Maudgal P.C., Ed., Herpetic Eye Diseases, Dr. W. Junk Publishers, 1985

McCarey B.E., Schinidt F.H., Modeling glucose distribution in the cornea ,Current Eye Research, 9: 1025-1038, 1990

Merrett K, Cornelius R. M., McClung W. G., Unsworth L. D., Sheardown H., Surface analysis methods for characterizing polymeric biomaterials, Journal of Biomaterials Science, Polymer Edition, 13(6): 593-621, 2002

Merrett K., Griffith C. M., Dub M. A., Sheardown H., Interactions of corneal cells with TGF-b2 modified poly(dimethyl siloxane) surfaces, Journal of Biomedical Material Research (Accepted for publication)

Mester, U., Stein, H. J., Meier, J., Studies on the permeability of hydrogel plastics (PHEMA) to different substances of corneal metabolism, Albrecht von Graefes Archiv fuer Klinische und Experimentelle Ophthalmologie, 1978

Mirejovsky D., Patel A.S., Young G., Water properties of hydrogel contact lens materials: a possible predictive model for corneal desiccation staining, Biomaterials, 14 (14): 1080-1088, 1993

Miyata T., Higuchi J. I., Okuno H., Uragami T., Preparation of Poly(dimethylsiloxane) /Polystyrene Interpenetrating Polymer Network Membrane and Permeation of Ethanol Solution through the Membrane by Pervaporation, Journal of Applied Polymer Science, 61(8): 1315-1324, 1996

Montalvo J., U. S. Patent 3 869 354, 1975

Mueller K. F. and Heiber S. J., Gradient –IPN-Modified hydrogel beads: Their synthesis by diffusion-polycondensation and function as controlled drug delivery dgents, Journal of Applied Polymer Science, 27: 4043-46, 1982

Muniz E.C. and Geuskens G., Influence of temperature on the permeability of poly acrylamide hydrogels and semi-IPNs with poly(N-isopropylacrylamide), Journal of Membrane Science, 172: 287-293, 2000

Muratore L. M., Synthesis and properties of oxygen permeable hydrogel based on copolymers of Dimethylacrylamide and Fluorosulfonamide methacrylates. Journal of Materials Chemistry, 10(4): 859-865, 2000

Nelson M., U. S. Patent 3 020 260,1962

Nonaka Takamasa, Hashimoto Keisuke, Kurihara Seiji, Preparation of thermosensitive cellophane-graft-N-isopropylacrylamide copolymer membranes and permeation of solutes through the membranes, Journal of Applied Polymer Science, 66(2): 209-216, 1997

Okano Teruo, Kikuchi Akihiko, Sakurai Yasuhisa, Takei Yoshiyuki, Ogata Naoya, Temperature-responsive poly(N-isopropylacrylamide) as a modulator for alteration of hydrophilic/hydrophobic surface properties to control activation/inactivation of platelets, Journal of Controlled Release, 36(1-2): 125-33, 1995

Otake K., Inomata H., Konno M., Saito S., Thermal Analysis of the Volume Phase Transition with N-isopropylacrylamide Gels, Macromolecule, 23: 283-288, 1990

Panda A., Manohar S.B., Sabharwal S., Bhardwaj Y.K., Synthesis and swelling characteristics of poly(N-isopropylacrylamide) temperature sensitive hydrogels crosslinked by electron beam irradiation, Radiation Physics and Chemistry, 58: 101-110, 2000

Pandit S. B. and Nadkarni V. M., Sequential interconnected interpenetrating polymer networks of polyurethane and polystyrene: Synthesis and chemical structure elucidation, Macromolecules, 27: 4583-4594, 1994

Park T. and Hoffman A. S., Immobilization and characterization of β-galactosidase in thermally reversible hydrogel beads, Journal of Biomedical Material Research, 24: 21-38, 1990

Peng T. and Cheng Y., Temperature-responsive permeability of porous PNIPAAM-g-PE membranes, Journal of Applied Polymer Science, 70: 2133-2142, 1998

Pu H., Ding Z., Ma Z., Preparation, characterization, and properties of EVA preirradiation grafted NIPAAM, Journal of Applied Polymer Science, 62: 1529-1535, 1996

Ree M., Shin T.J., Kim S.I., Woo S.H., Yoon D.Y., High-temperature polyimide comppsites prepared from soluble polymeric and crosslinkable oligomeric precursors: Phase demixing and properties, Polymer, 39(12), 2521-2529, 1998

Renard Gilles, Cetinel Berin, Legeais Jean-Marc, Savoldelli Michele, Durand Jacques, Pouliquen Yves, Incorporation of a fluorocarbon polymer implanted at the posterior surface of the rabbit cornea, Journal of Biomedical Materials Research, 31(2): 193-199, 1996

Ricardo G. Sousa et al., Glass Transition and Thermal Stability of Poly(N-isopropylacrylamide) Gels and Some of Their Copolymer with acrylamide Polymer Degradation and Stability, Vol. 61, pp275-281, 1998

Robert C., Diseases of the Cornea, Ed., Arfta, 3 Ed. Mosby Year Book, 1993

Ruckenstein E. and Liang L., Poly(acrylic acid)-poly(vinyl alcohol) semi- and interpenetrating polymer network pervaporation membranes, Journal of Applied Polymer Science, 62: 973-987, 1996

Ruedemann A.D.Jr, Silicone keratoprosthesis, Transactions of the American Ophthalmological Society, 72: 329-359, 1974

Schild H. G. and Tirrell D. A., Interaction of poly(N-isopropylacrylamid) with sodium n-alkyl sulfates in aqueous solution, Langmuir, 7: 665-671, 1991

Schild H. G. and Tirrell D. A., poly(N-isopropylacrylamid): Experiment, theory and application, Progress Polymer Science, 17: 163-249, 1992

Schild H.G., Tirrell, D. A., Sodium 2-(N-dodecylamino) naphthalene-6-sulfonate as a probe of polymer-surfactant interaction, Langmuir, 6(11): 1676-1679, 1990

Schulz J. T., Tompkins R. G., Burke J. F., Artificial skin, Annual Review of Medicine, 51: 231-244, 2000

Sevastianov V.I., Tseytlina EA, Volkov AV, Shumakov VI, Importance of adsorption-desorption processes of plasma proteins in biomaterial hemocompatibility, Trans, Am Soc Artif Intern Organs, 30: 713-731, 1984

Shapiro L. and Cohen S., Novel alginate sponges for cell culture and transplantation, Biomaterials, 18: 583-590, 1997

Shin Mi-Seon, Kim Sun I., Kim In Young, Kim Nam Gyun; Song Chul Gyu, Kim Seon Jeong, Characterization of hydrogels based on chitosan and copolymer of poly(dimethylsiloxane) and poly(vinyl alcohol), Journal of Applied Polymer Science, 84(14): 2591-2596, 2002

Shin Y., Liu J., Chang J.H., Exarhos G.J., Sustained drug release on temperature-responsive poly(N-isopropylacrylamide)-intergrated hydroxyapatite, Chem. Commun., 1718-1719, 2002

Shtanko N. I., Kabanov V.Ya., Apel P. Yu., Yoshida M., Vilenskii A.I., Preparation of permeability-controlled of "smart" polymers, Journal of Membrane Science, 179: 155-161, 2000

Sperling L. H., Interpenetrating Polymer Networks and Related Materias, Plenum, New York, 1981

Sperling L. H., Interpenetrating Polymer Networks: An Overview, P 6, in Interpenetrating Polymer Networks, American Chemical Society, Klempner D., Ed., 1994

Sperling L. H., Polymeric Multicomponent Materials- An Introduction, A Wiley-Interscience Publication, 1997

Sperling L.H., Multicomponent Polymer Materials, Paul D.R. , Sperling L. H. Eds., Advances in Chemistry 211, American Chemical Society, 1986

Stayton PS, Shimoboji T., Long C., Chikoti A., Chen G., Harris JM, Hoffman AS, Control of protein-ligand recognition using a stimuli-responsive polymer, Nature, 378: 472-474, 1995

Stile Ranee A., Burghardt Wesley R., Healy Kevin E., Synthesis and characterization of injectable poly(N-isopropylacrylamide)-based hydrogels that support tissue formation in vitro, Macromolecules, 32(22): 7370-7379, 1999

Sun Y., Chen J., Chu D, Preparation and characterization of α-amylase-immobilized thermal-responsive composite hydrogel membranes, Journal of Biomedical Material Research, 45: 125-132, 1999

Suzuki K., Yumura T., Tanaka Y., Akashi M., Thermo-responsive release from interpenetrating porous silica- poly(N-isopropylacrylamide)hybrid gels, Journal of Controlled Release, 75: 183-189, 2001

Tanaka K., Takahashi K., Kanada M., US Patent: 4 139 692, 1979

Tenhu H. and Vaahtera K., Phase seperation in polystyrene crosslinker with samples of poly(dimethyl siloxane) of various chain length, Europian Polymer Journal, 27(7): 717-722, 1991

Trinkaus-Randall V, Banwatt R, Capecchi J, Leibowitz H M, Franzblau C, In vivo fibroplasia of a porous polymer in the cornea, Investigative Ophthalmology andVisual Science, 32(13): 3245-3251, 1991

Turner J. S. and Cheng Y.-L., Preparation of PDMS-PMAA interpenetrating polymer network membranes using the monomer immersion method, Macromolecules, *33*(10): 3714–3718, 2000

Vasheghani-Farahani Ebrahim, Cooper D.G., Vera J.H., Weber M.E., Concentration of large biomolecules with hydrogels, Chemical Engineering Science, 47(1): 31-40, 1992

Wang M., Qiang J., Fang Y., Hu D., Cui Y., Fu X., Preparation and properties of chitosan-poly(N-isopropylacrylamide) semi-IPN hydrogels, Journal of Polymer Science: Part A: Polymer Chemistry, 38: 474-481, 2000

Winnik F. M., Ottaviani M. F., Bossmann S. H., Garcia-Garibay M., and Turro N. J., Consolvency of poly(N-isopropylacrylamide) in mixed water-methanol solutions: a look at spin-labeled polymers, Macromolecules, 25: 6007-6017, 1992

Wu J., Sassi A. P., Blanch H. W., Prausnitz J. M., To predict partitioning of proteins between a temp.- and pH-sensitive hydrogel and its surrounding, Polymer, 36: 857, 1996.

Xie R. Z., Sweeney D. F., Griesser H. J., Tout S., Cheng H. Y., Steele J. G., A thin glycoprotein coating of a synthetic lenticule does not cause nutritional deficiency of the anterior cornea, Current Eye Research, 18(5): 335-341, 1999

Yeo J. K., Sperling L. H., Thomas D. A., Theoretical prediction of domain sizes in IPN's (interpenetrating polymer networks) and related materials, Polymer, 24: 307-313, 1983

Yoo K.M., Yong K.S., Effect of polymer complex formation on the cloud-point of poly(N-isopropylacrylamide)in the poly(NIPAAM-co-acrylic acid): polyelectrolyte comples between poly(acrylic acid)and poly (allylamine), Polymer, 38(11): 2759-2765,1997

Yoo K.M., Yong K.S., Young M.L., Cho C.S., Effect of polymer complex formation on the cloud-point of poly(N-isopropylacrylamide)in the poly(NIPAAM-co-acrylic acid): polyelectrolyte comples between poly(acrylic acid)and poly (L-lysine), Polymer, 39(16): 3703-3708, 1998

Yoshioka H, Mikami M., Mori Y., Preparation of poly(N-isopropylacrylamide)-b-poly(ethylene glycol) and calorimetric analysis of its aqueous solution, J.M.S.-Pure Appl. Chem., A31(1): 109-112, 1994

Zhang J. and Peppas N. A., Morphology of poly(methacrylic acid)/poly(N-isopropylacrylamide) interpentrating polymer networks, Journal of Biomaterial Science Polymer Education, 13(5): 511-525, 2002

Zhang J. and Peppas N. A., Synthesis and characterization of pH- and temperature-sensitive poly(methactylic acid)/poly(N-isopropylacrylamide) interpenetrating polymeric networks, Macromolecules, 33: 102-107, 2000

Zhang X. and Zhou R, Preparation of fast responsive, temperature-sensitive poly(*N*-isopropylacrylamide) hydrogel,Macromolar Chemistry Physics, 200: 2602, 1999

Zhang X. and Zhou R., A novel method to prepare a fast responsive, thermosensitive poly(*N*-isopropylacrylamide) hydrogel, Macromolar Rapid Communications, 4: 229, 1999

Zhang X., and Zhou R.., Dynamic properties of temperature-sensitive poly(N-isopropylacrylamide) gel cross-linker through siloxane linkage, Langmuir, 12: 12-16, 2001

Zhou R. and Li W., Preparation and characterization of macroporous poly(N-propylacrylamide) hydrogels for the controlled release of proteins, Journal of Polymer Chemistry, 41: 152-159, 2003

Zhou W. J., Hsieh Y.L., Kurth M.J., Krochta J.M., Synthesis of novel lactose-based hydrogels, Polymer Preprints, 39(2): 120-121, 1998

Appendix A: Reagents and Solvents

Name of Chemicals	Description	Manufacture
Vinyl PDMS kit Sylgard 184	5000cst	Dow Corning Corporation
Hydroxy terminated PDMS	2000cst	Aldrich *
Tetraethyl orthosilicate(TEOS)	Crosslinker	Aldrich *
Tin(2)2-ethylhexanote	Catalyst	Aldrich *
N-isopropylacrylamide	97% purity	Aldrich *
N,N-methylene bisacrylamide (BisAAm)	Crosslinker 99%	Aldrich *
Xanthone	Initiator, 97%	Aldrich *
2,2-aobisisobutyronitrile (AIBN)	Initiator, 98%	Aldrich *
Ethylene glycol dimethylacrylate (EGDMA)	Crosslinker, 98%	Aldrich *
Poly(N-isopropylacryamide)	Mw=180.000 Da	Aldrich *
D-glucose	ACS reagent grade	Aldrich *
Glucose assay kit	20ml Kit	Sigma-Aldrich Co.#
Toluene	Class 1B, 99.9 %	Fisher Scientific Co.
Tetrahydrofruan(THF)	HPLC grade,99.9%	Caledon Laboratories Ltd.
Hexane	Reagent grade, 98.5%	Caledon Laboratories Ltd.

* Aldrich Chemical Company, Inc., Milwaukee, WI, USA

Sigma-Aldrich Co. St. Louis, Mo, USA

Appendix B: Glucose Assay Kit—Principle and Procedure

1. Principle of Glucose Assay Testing

The GAHK-20 Glucose assay kit is a quantitative, enzymatic tool for determination of glucose concentration. Its principle is based on the following reactions

$$Glucose + ATP \xrightarrow{Hexokinase} Glucose-6-Phosphate + ADP$$

$$Glucose-6-Phosphate + NAD \xrightarrow[Dehydrogenase]{gludose-6-Phosphate} 6-Phosphoguconate + NADH$$

equations:

Glucose assay kit GAHK20 contains 1.5 mM NAD, 1.0 mM ATP, 1.0 U/ml hexokinase and Glucose –6-phosphate dehydrogenase. When glucose contacts with this assay kit, it is phosphorylated by adenosine triphosphate (ATP) in the reaction catalyzed by hexokinase. The product of this first step, glucose-6-phosphate, is then oxidized to 6-phosphogluconate and NADH by NAD in the presence of glucose-6-phosphate dehydrogenase. The resultant NADH can be measured by UV spectroscopy at a wavelength of 340 nm and is directly proportional to glucose concentration.

2.Procedure for Glucose Concentration Determination using the Glucose Assay Kit

The tubes were prepared according to Table 1 as directed by the manufacturer (Sigma Chemical Co., St. Louis MO). After incubation for 15 minutes at 20-35°C, the absorbance at 340 nm was analyzed using a Beckman DU-640 spectrophotometer. The concentration of glucose was calculated using Equation B-1.

Table C1: Tube preparation for glucose assay analysis

Tube	Glucose Assay Reagent (ml)	Sample Volume (ul)	Volume of Deionized Water (ml)
Sample Blank	----	Same as for Test	1.0
Reagent Blank	1.0	----	Same as Sample Volume for Test
Test	1.0	10~200	----

$$\text{mg Glucose/ml} = \frac{(A)(TV)(F)(0.029)}{(SV)} \qquad (Equation\ B-1)$$

$$A_{totalblank} = A_{sampleblank} + A_{reagentblank}$$

$$A = A_{test} - A_{totalblank}$$

TV= total assay volume (ml)

SV= sample volume (ml)

F= dilution factor from sample preparation

Appendix C: Derivation of Permeation Coefficient Equation

The mass balance of solute between the two cells:

$$\frac{VdC_t}{dt} = -\frac{PA}{D}(C_0 - 2C_t)$$

P: permeability coefficient (cm^2/s)

V: solution or water volume in each cell (ml)

D: thickness of the membrane (cm)

A: permeate area of the membrane (cm^2)

C0: initial solute concentration in donor cell (μg/ml)

Ct: the solute concentration in receiver cell at time t (μg/ml)

t: permeate time (s)

$$\frac{VdC_t}{dt} = -\frac{PA}{D}(C_0 - 2C_t) \quad \Rightarrow \quad \int_0^{Ct} \frac{dC_t}{C_0 - 2C_t} = -\int_0^t \frac{PA}{DV} dt$$

$$\Rightarrow -\frac{1}{2}\int_0^{C_t} \frac{dC_t}{(C_0 - 2C_t)} = \int_0^t \frac{PA}{VD} t \quad \Rightarrow -\frac{1}{2}\ln(C_0 - 2C_t)\Big|_0^{C_t} = -\frac{PA}{VD}t$$

$$\Rightarrow -\frac{1}{2}\left[\ln(C_0 - 2C_t) - \ln C_0\right] = -\frac{PA}{VD}t \quad \Rightarrow -\ln\frac{C_0 - 2C_t}{C_0} = -\frac{2PA}{VD}t$$

$$\Rightarrow \quad \ln(1 - 2C_t/C_0) = \frac{2 \times P \times A}{V \times D}t \quad \Rightarrow k = \frac{2 \times P \times A}{V \times D} \qquad (Equation C-1)$$

Appendix D: Example of Permeation Coefficient Calculation

Glucose Permeate Test for IPN Sample 1# -2 of 021303

IPN weight increasing: 34.2% water up taking: 40.5%

Reagent reading: 0.0752 A Solution volume: 5 ml; Permeation area: 0.64 cm^2

TableD-1: data processing of glucose permeation testing

sample No.	V of removed (ul)	t(s)	D factor	sam. V ul	UV reading	RG reading	ΔA	C of calcu. Mg/ml	glu. Amount of cal. ug	glucose removed ug	Glu. Accum. ug	Ct (ug/ml)	ln
1	500	1800	1	200	0.0763	0.0627	0.0136	0.0023	11.8	1.1	11.8	2.3	4.74E-05
2	500	5400	1	200	0.2396	0.0627	0.1769	0.0307	153.9	15.3	155.1	31.0	0.000621
3	500	12600	1	100	0.58	0.0684	0.5116	0.1632	816.0	81.6	832.6	166.5	0.003336
4	500	19800	1	100	0.9555	0.0684	0.8871	0.2829	1414.9	141.4	1513.168	302.6	0.006071
5	500	31800	1	50	1.0565	0.0716	0.9848	0.5997	2998.9	299.8	3238.6	647.7	0.013039
6	500	43200	1	25	1.0071	0.0734	0.9337	1.1102	5551.05	555.105	6090.6	1218.1	0.024664
7	500	91800	1	25	1.1655	0.0734	1.0921	1.2985	6492.738	649.2	7587.4	1517.4	0.03082
8	500	106200	1	25	1.3211	0.0734	1.2477	1.4835	7417.78	741.7	9161.738	1832.3	0.037335
9	500	189000	5	50	0.9959	0.0716	0.9242	2.8144	14072.18	1407.2	16557.9	3311.5	0.068527
10	500	257400	5	50	1.3069	0.0716	1.2352	3.7614	18807.15	1880.7	22700.1	4540.0	0.095191
11	500	347400	5	50	1.5494	0.0716	1.4777	4.4998	22499.22	2249.9	28272.8	5654.5	0.120014
12	500	520200	5	25	1.1696	0.0734	1.0962	6.5171	32585.56	3258.5	40609.1	8121.8	0.177258

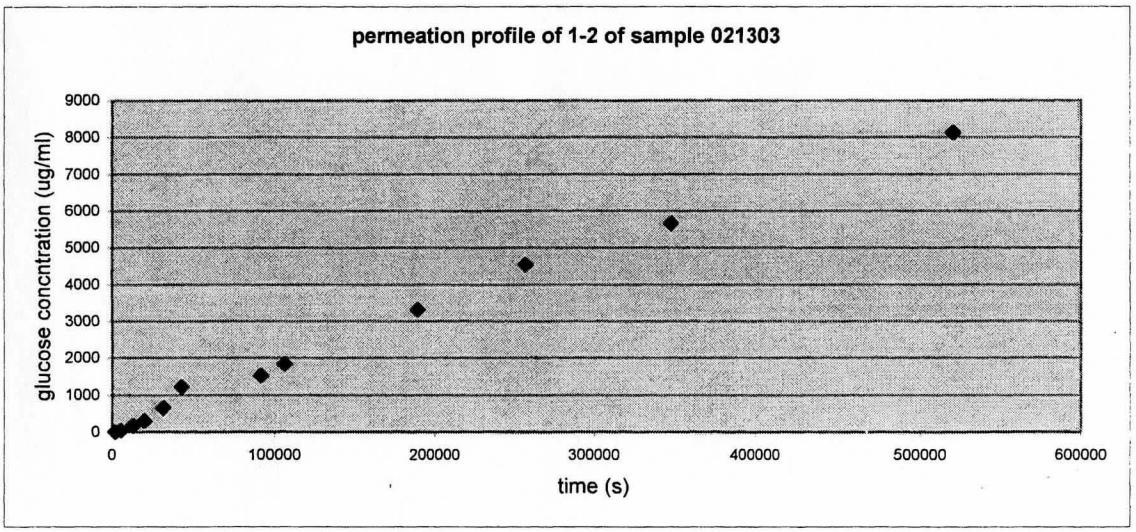

Figure D-1: Permeation profile of sample 021303

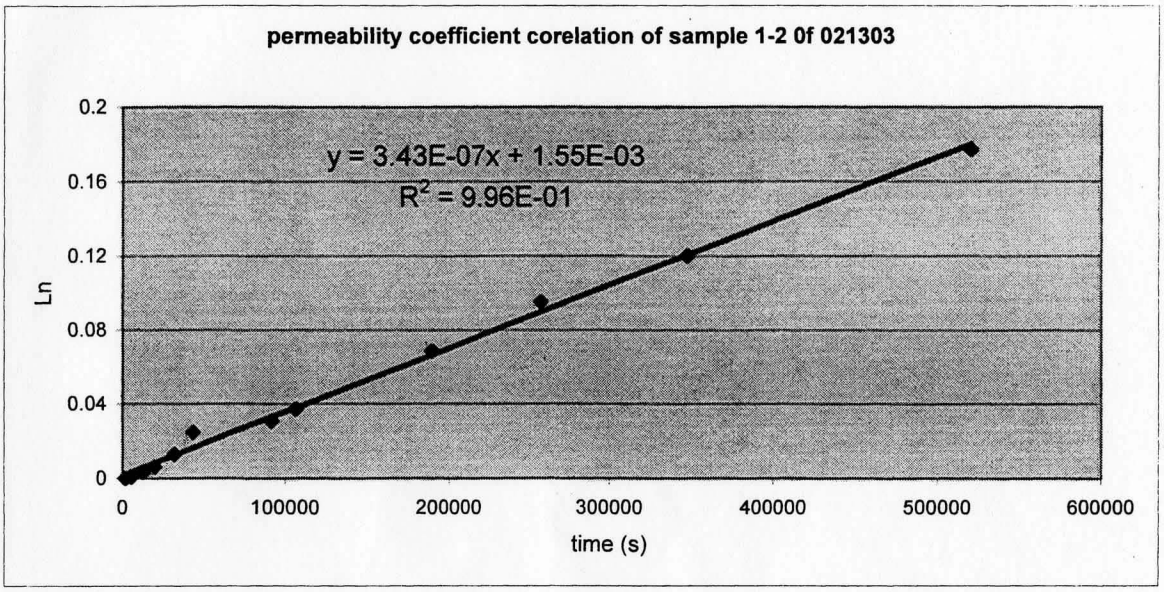

FigureD-2: permeability coefficient correlation of sample 1-2 0f 021303

Permeability Coefficient Calculation:

Solution volume of each cell: V=5 (cm^3)

Thickness of membrane: d=0.06 (cm)

Permeation area of membrane: A=0.45 x 0.45 x 3.14=0.636 (cm^2)

Slope of plot in figure D-2: K=$3.43x10^{-7}$

Based on Equation B-1:

$$K = \frac{2 \times P \times A}{V \times d} \quad \Rightarrow P = \frac{K \times V \times d}{2 \times A}$$

$$So: Permeability\,Coefficient \quad P = \frac{(3.43 \times 10^{-7}) \times 5 \times 0.06}{2 \times 0.636} = 0.71 \times 10^{-7} (cm^2 / s)$$